



Universitat Autònoma de Barcelona

ADVERTIMENT. L'accés als continguts d'aquesta tesi queda condicionat a l'acceptació de les condicions d'ús establertes per la següent llicència Creative Commons:  http://cat.creativecommons.org/?page_id=184

ADVERTENCIA. El acceso a los contenidos de esta tesis queda condicionado a la aceptación de las condiciones de uso establecidas por la siguiente licencia Creative Commons:  <http://es.creativecommons.org/blog/licencias/>

WARNING. The access to the contents of this doctoral thesis it is limited to the acceptance of the use conditions set by the following Creative Commons license:  <https://creativecommons.org/licenses/?lang=en>



**Universitat Autònoma
de Barcelona**

**The functional response of Mediterranean mountain
ecosystems to herbivore pressure**

Miguel Ibáñez Álvarez

Supervisors:

Dr. Jordi Bartolomé Filella

Dra. Elena Baraza Ruiz

Dr. Emmanuel Serrano Ferron

Universitat Autònoma de Barcelona
Departament de Ciència Animal i dels Aliments

June 2022

Table of Contents

Table of Contents **i**

List of tables **iv**

List of figures **vii**

Acknowledgements..... **xii**

Abstract..... **1**

1. General introduction..... **6**

 Shifts in livestock management and landscape use in a global warming scenario 7

 Herbivory in the Mediterranean mountains 10

 Herbivores and the ecosystem services associated with the soil..... 12

 Remote sensing for monitoring the effects of herbivores 13

 UAVs and herbivory monitoring 16

 References 18

2. Objectives..... **30**

3. Chapter 1 Ungulates alter plant cover without consistent effect on soil ecosystem functioning **33**

 Abstract 34

 1. Introduction 35

 2. Materials and methods 39

 3. Results 46

 4. Discussion 50

 5. Conclusions 53

 6. References 54

4. Chapter 2 Satellite-Based Monitoring of Primary Production in a Medi-terranean Islet Post Black Rat Eradication..... **66**

 Abstract 67

 1. Introduction 68

 2. Materials and methods 71

 3. Results 84

 4. Discussion 87

 5. Conclusion 92

 6. References 93

5.	Chapter 3 Remote mapping of foodscapes using sUAS and a low cost BG-NIR sensor	109
	Abstract	110
	1. Introduction	111
	2. Materials and methods	115
	3. Results	125
	4. Discussion	135
	5. Conclusion	139
	6. References	140
6.	General discussion.....	149
	References	154
7.	Conclusions	160
8.	Supplementary material	162
	Supplementary material chapter 1.....	163
	Supplementary material chapter 2.....	167
	Supplementary material chapter 3.....	182

List of tables

Table 1. 1. Ecosystem goods and services in the major functional groups of terrestrial ecosystems according to Rodà et al., 2003.....	6
Table 1. 2. Main features of major sensors used to assess terrestrial ecosystems. Useful imagery can be obtained by combining the spectral bands of different spectral ranges (VIS = visible; NIR= Near- Infrared; SWIR = Short Wave Infrared; TIR = Thermal Infrared). To provide higher spatial resolution for multispectral images some sensor include a panchromatic band (PAN)	15
Table 3. 1. Study site characteristics in Majorca Mountains: type of habitat, soil texture classification, mean elevation, annual mean temperature, Net Primary Production (NPP). The Time of exclusion indicates the approximate years of ungulates exclusion establishment until the data collection, and Design indicates the number of fenced areas with respect to the number of plots inside each fenced area.	38
Table 3. 2. Ungulate exclusion effects on the percentage of bare soil, total vegetation cover and percentage of cover with multiple different species (complexity) as analysed by a mixed general lineal model GLMM.....	47
Table 3. 3. Statistical results of the overall effects of ungulate exclusion over the response variables analysed by multi-level meta-analytic models. In the first column, a global increase on the studied variable was indicated by ↑ whereas a decrease was indicated by ↓. The p-value of the fitted model is outlined in bold when the effect is statistically significant. LnRR (95% CI) indicates the effect size of the ungulate exclusion and is also shown as a percentage of response (inverse transformation of the logarithm) to facilitate interpretation. N° indicates the number of pair plot comparisons. The test of heterogeneity Q-test shows significant variation between all effect sizes when p-value < 0.005. The variance is distributed across the sampling variance (<i>ILevel 12</i>), variance within plots (<i>ILevel 22</i>), and between site/plot (<i>ILevel 32</i>)	48
Table 4. 1. Timing and NDVI magnitudes of breaks in the trend component of Sa Dragonera (treatment zone) and Mallorca (control zone) time series. The left and right limits of the breakpoint dates indicate a 95% confidence interval of date estimation. 1 = Timing indicated by year and month. Data format: Year (Month). 2: Difference between the NDVI value at the end of a linear model and the intercept of the next one. 3: Linear regression parameters of segments after the breakpoints date, where the intercept represents the starting NDVI, and the slope represents the greening (+) or browning (-) ratio of the vegetation. The parameters of the starting segment are omitted in this table.....	86
Table 5. 1. Species and number of individuals (n) sampled in NGRPTB Iberian ibex enclosure. species are grouped by families and given a code to simplify the interpretation of the consequent analysis. Plant life-forms agree with Raunkier´s classification (1934).....	118

- Table 5. 2.** Image processing information for each flight executed in NGRPTB ibex enclosure. The table includes final resolution (ppcm, pixel per centimetre) of the image, surface recorded by the image, number of ground control points (GCP), calibration error (mean RMS error), and number of recorded images and number of images used to create the model..... 120
- Table 5. 3.** Plant species classification from random forest models using digital values of the three bands recorded by a BG-NIR camera (NIR, Blue and Green). Data collected using a sUAS flying in July (2018) and March (2019) in the Iberian Ibex (*Capra pyrenaica*) enclosure in the NGRPTB. Images were recorded at two heights (30 and 60 m) and different resolutions (3.5, 5, 10 and 30 cm pixel size). OOB error is the classification error according to the random forest algorithm. Test error is the error obtained when comparing algorithm prediction results with test data not included in the model development. We performed two kinds of classification: for the most abundant plants in the enclosure (n=19, All species), and for plants preferred by Ibexes (Diet). In the Diet group, plants have been grouped in 4 types namely: *Cistus albidus*, *Erica multiflora*, Fagaceae (*Quercus coccifera* and *Q. ilex*) and Graminoids (e.g., *Brachypodium phoenicoides*, *B. retusum* and other graminoids). 130
- Table MS 3. 1.** Effect of the continuous covariates (elevation, NPP, temperature, and soil texture), and the categorical covariate habitat on the effect size $\ln(RR)$ of ungulate exclusion on soil characteristics, soil microbial activities (measured as AWCD) and functional diversity (measured as a H considering observations of by Biolog EcoPlates™) and organic material Stabilization factor (S) and Decomposed rate (k) (measured with the “Tea Bag index” method). The p-value associated with the test of moderators QM indicates statistical significance at $\alpha = 0.95$ NPP Net Primary Productivity, texture corresponds to the first PC of a PCA made with all percentages of the soil texture classes. 163

List of figures

- Figure 1. 1.** Forest encroachment process due to the cessation of rural activities for 65 years in a Mediterranean mountain area Esporles, Serra de Tramuntana, Mallorca Island, Spain. The upper aerial scene was taken in 1956, while the lower satellite scene was in 2021. The abandoned agricultural areas on the right side have been replaced by an Aleppo pine (*Pinus halepensis*) forest. The orography is better appreciated in the old scene due to the lower holm oak forest (*Quercus ilex*) density. Oak has a finer-grained green colour than pines. 9
- Figure 1. 2.** Examples of the impact of browsing on the morphology of different plants in the Finca La Victoria, a mountainous area of the Island of Mallorca, Spain. The upper image (A) shows the short term effect of feral goat (*Capra hircus*) browsing (to the right of the fence) on the Mediterranean vegetation. The lower images show intensely browsed trees such as wild olive (*Olea europaea*, B), and Aleppo pine (*Pinus halepensis* together with well-developed grass *Ampelodesmos mauritanica*, a species very tolerant to herbivory, C)..... 11
- Figure 3. 1.** The first slot indicates the geographical location of the study sites. The rest of the slots show photographic details of the habitats for the fenced study sites. A (Na Burguesa) and E (La Victoria) represent scrubland. The forest areas are related to the letters B (Sobremunt), C (Son Moragues) and D (Binifaldó)..... 39
- Figure 3. 2.** Forest plot of the effect of the herbivory on four key response variables (Bulk density, AWCD, organic matter and soil organic nitrogen content). In each plot, the names on the left identify the individual plots in each of the five study areas. The boxes represent the $\ln(RR)$ of the individual studies, and the horizontal lines their 95% confidence intervals. The size of the boxes expresses the weight (see methods) of each study in the total effect, which is represented by a diamond. Response rates less than zero (vertical dotted line) indicate a negative effect of ungulate exclusion, while values greater than zero indicate a positive effect. If the diamond does not cross the zero line, the overall effect is significant. For a full list of comparisons see Table 3.3 or Table MS 3.1. 49
- Figure 4. 1.** Damage caused by the black rat (*Rattus rattus*) in 2010 in Sa Dragonera Islet. (Top left) Wild olive tree (*Olea europaea* var. *sylvestris*) with damaged bark. (Top right) Damage in a perennial herb (*Urginea maritima*). (Bottom right) Damage in a pinecone (*Pinus halepensis*). Author of the photos: Martí Mayol (Director of the Sa Dragonera Natural Park at the time of the deratization campaign). 74
- Figure 4. 2.** Temporal distribution of Landsat Collection 1 Surface Reflectance (SR) imagery. More images were used (when available) where clouds obstructed data collection or where SLC off-data error in Landsat 7 was detected over study zones. 76

List of figures

Figure 4. 3. Workflow of spatial criteria to select fifty-four $30 \times 30\text{m}^2$ plots (29 in the treatment zone and 25 in the control zone represented by pink dots in Figure 4) to compare NDVI time series..... 78

Figure 4. 4. Map showing locations of selected sampling plots (pink dots) to create the NDVI time series for both treatments. On the left are the sampling plots of Dragonera Islet (the treatment zone), and on the right those of Mallorca Island (the control zone). High-resolution aerial orthophotos ($15 \times 15\text{cm}$) show two examples of the $30 \times 30\text{m}$ sampling plots of both treatments. Spatial reference map in the bottom right corner. 79

Figure 4. 5. Monthly NDVI time series showing the average NDVI of the sampling plots for each zone. The coloured lines (Red = Sa Dragonera; Blue = Mallorca Island, i.e., control zone) represent the trend throughout the study period, with a LOESS smoothing and standard deviation shown with the corresponding colours. The black lines represent the real data for each treatment (Solid = Sa Dragonera; Dotted= control zone), in which the seasonal variation can be observed. The dashed vertical line dates the rodent eradication campaign (February 2011). 80

Figure 4. 6. The STL decomposition of the monthly NDVI time series of Sa Dragonera and control zone (Mallorca Island) into the seasonal, trend, and remainder components. In each plot, NDVI units are plotted against time. The seasonal component is estimated by taking the mean of all seasonal sub-series (e.g., for a monthly time series the first sub-series contains the January values). The sum of the seasonal, trend, and remainder components equals the data series. The solid bars on the right-hand side of the plots act as a reference to show the same data range and aid comparison. 82

Figure 4. 7. Decomposed NDVI data (Y_t) into seasonal (S_t), trend (T_t) and remainder (et) components for NDVI time series between 1999 and 2020 for both treatment zone (A), and control zone (B), using the breaks for additive seasonal and trend (BFAST) method. The dotted vertical line shows when the rodent eradication campaign took place (February 2011). The dashed lines in T_t represent the timing of each significant NDVI change ($p < 0.05$) in the trend component, together with its 95% confidence intervals (horizontal red bars). Ordinal numbers are used to name the breakpoints. Vertical axis units are absolute NDVI values. The slope coefficient (β) and p-value is shown for each fitted trend segment. Coloured slots represent Hydrological Drought Index (HDI) between March 1999 and December 2019 [95] which describes the water resources state from more to less abundant for: normality (green), pre-alert (yellow), alert (orange), and emergency (red). 85

Figure 5. 1. The study area is placed in the National Game Reserve “Ports de Tortosa i Besit” (NGRPTB) in Catalonia, northeast Spain ($40^\circ 46' 08''$ N, $0^\circ 20' 04''$ E, 450m.a.s.l.) marked in the upper inset. The yellow line marks the Iberian Ibex enclosure. The white area indicates the flight area. (For interpretation of the references to colour in this figure legend, the reader is referred to the web version of this article.) 116

- Figure 5. 2.** Field sampling in the Iberian Ibex enclosure in the NGRPTB. Up to 20 individuals of the most representative species of the area were marked with a dGPS. In sets present the species most consumed by Iberian ibex in the enclosure. 118
- Figure 5. 3.** A) Monthly variation of mean NDVI values recorded in the Iberian Ibex enclosure, in the NGRPTB. Mean NDVI values corresponding to the 2014–18 period. Clear seasonal pattern evident with peak primary production in winter and minimum in summer. The asterisk indicates statistically significant differences between march and June NDVI (red bars). B) Variation of mean Blue-NDVI in the plants recorded in the Ibex enclosure in March and June calculated from the images obtained by a BG-NIR camera. All species have statistical differences (t-test) except for those marked with asterisks. *Brachypodium retusum* (BR), *Helianthemum marifolium* (H), and *Pinus pinaster* (PP). All plant species abbreviations are depicted in Table 5. 2. (For interpretation of the references to colour in this figure legend, the reader is referred to the web version of this article). 126
- Figure 5. 4.** Diet composition assessed by a faecal micro-histological analysis of 10 faecal samples collected in the Ibex enclosure in December 2019. Bars represent the mean of the proportion of each plant species in our faecal samples. ONLW(Other Non-LegumeWood species), EM (*Erica multiflora*), G (*Brachypodium phoenicoides*, *B. retusum* and other graminoids), ONLF (Other Non-Legume Forb species), L-A (Labiatae-Asteraceae), QI (*Quercus ilex*), CA (*Cistus albidus*), TV (*Thymus vulgaris*), PL (*Pistacia lentiscus*), HH (*Hedera helix*), CM (*Crataegusmonogyna*), RU (*Rubus ulmifolius*), RO (*Rosmarinus officinalis*), GS (*Genista scorpius*), Sasp (*Smilax aspera*), L (Laminaceae), Dsp (Dorycnium sp.), A (Asteraceae), BS (*Buxus sempervirens*), I–O (Iridaceae- Orchidaceae), PA (*Phillyrea angustifolia*), Psp (Pinus sp.), Csp (Carex sp.), Ssp (Satureja sp.), Rsp (Rosa sp.). 129
- Figure 5. 5.** Mean scores from the first PCA dimension performed with NIR, Green and Blue band recordings on 19 plant species sampled in the NGRPTB vegetation study. All plant species abbreviations are depicted in Table 5.2. (For interpretation of the references to colour in this figure legend, the reader is referred to the web version of this article.)..... 133
- Figure 5. 6.** Mean scores from the first PCA dimension performed with NIR, Green and Blue band recordings on 5 plant categories consumed by Iberian ibexes in the NGRPTB. ‘C’: *Cistus albidus*; ‘G’: *Brachypodium phoenicoides*, *B. retusum*, and other grass-like plants as Graminoids. ‘L’: *Rosmarinus officinalis* and *Thymus vulgaris* as the family Labiatae; ‘E’: *Erica multiflora*; ‘F’: *Quercus* spp. as the family Fagaceae. (For interpretation of the references to colour in this figure legend, the reader is referred to the web version of this article.) 134

- Figure 5. 7.** Food scape map overlaid with the infrared false-colour orthomosaic of the study area. Predicted categories are based on RFMI with an OOB error of 18.4%. A pie chart illustrates the proportion of the 6 dietary categories: ‘F’: *Quercus* spp. as the family Fagaceae; ‘L’: *Rosmarinus officinalis* and *Thymus vulgaris* as the family Labiatae; ‘E’: *Erica multiflora*; ‘C’: *Cistus albidus*; ‘G’: *Brachypodium phoenicoides*, *B. retusum*, and other grass-like plants as Graminoids. ‘Others’ category includes plants without dietary interest, bare soil and rock. 135
- Figure SM 3. 1.** Forest plot of the effect of the herbivory on additional response variables (Litter, Electrical Conductivity, Organic Carbon, pH, C/N, H⁺, S, k). In each plot, the names on the left identify the individual plots in each of the five study areas. The boxes represent the Ln(RR) of the individual studies, and the horizontal lines are their 95% confidence intervals. The size of the boxes expresses the weight (see methods) of each study in the total effect, which is represented by a diamond. Response rates less than zero (vertical dotted line) indicate a negative exclusion effect, while values greater than zero indicate a positive effect. If the diamond does not cross the zero line, the overall effect is significant..... 165
- Figure SM 3. 2.** Principal Component Analyses (PCA) of the absorbance of the 31 substrates analysed by Biolog EcoPlates™ after 96 h of incubation. Clusters represent the excluded (Blue) and grazing (Yellow) points. 166
- Figure SM 5. 1.** PCA calculated from the digital values of the images obtained in the National Game Reserve “Ports de Tortosa i Beseit” in Catalonia, northeast Spain (40°46’08” N, 0°20’04” E, 450 m. a. s. l.). Lines represent the recorded bands (variables) and points represent the sampled pixels coloured by species (individuals). Up to 20 individuals of these plant species were marked with a dGPS. *Brachypodium phoenicoides* (BP), *Brachypodium retusum* (BR), *Buxus sempervirens* (BS), *Cistus albidus* (CA), *Chamaerops humilis* (CH), *Erica multiflora* (EM), Graminoids (G), *Genista scorpius* (GS), *Helianthemum marifolium* (H), *Juniperus oxycedrus* (JO), *Phillyrea angustifolia* (PA), *Pistacia lentiscus* (PL), *Pinus nigra* (PN), *Pinus pinaster* (PP), *Quercus coccifera* (QC), *Quercus ilex* (QI), *Rosmarinus officinalis* (RO), *Thymus vulgaris* (TV), *Ulex parviflorus* (UP). 183
- Figure SM 5. 2.** PCA calculated from the digital values of the images obtained in NGRPTB. Lines represent the recorded bands (variables) and points represent groups of plant species consumed by a flock of ibexes (*Capra pyrenaica*) in the National Game Reserve “Ports de Tortosa i Beseit” in Catalonia, northeast Spain (40°46’08” N, 0°20’04” E, 450 m. a. s. l.). Plant groups are the following: *Quercus* spp. as the family Fagaceae (Group F), *Rosmarinus officinalis* and *Thymus vulgaris* as the family Labiatae (Group L), *Erica multiflora* (Group E), *Cistus albidus* (Group C), *Brachypodium phoenicoides*, *B. retusum*, and other grass-like plants as Graminoids (Group G)..... 184

Acknowledgements

A Jordi, Elena y Emmanuel. Por haberme dado la oportunidad de realizar la tesis doctoral con vosotros, por haberme guiado y ayudado tanto durante este periodo. Gracias por vuestra paciencia, por vuestro tiempo y por todo lo que me habéis enseñado, lo cual siempre he sentido recibir de una manera muy generosa. He crecido, y es gracias a vosotros.

A mi familia, especialmente a Alicia y a mis padres que siempre creéis en mi y me apoyáis incondicionalmente.

Abstract

A long history of human presence has shaped Mediterranean mountain landscapes. However, due to socio-economic changes, the exodus of rural people in the middle of the 20th century has induced major changes in land use, land cover, and the dynamics of its ecosystems. Grazing and the use of wood as a source of fuel have historically been the primary factors shaping forest lands. Nowadays, herds of domestic herbivores turned into feral livestock have also influenced ecosystem services in the Mediterranean. These feral herds are getting regulated by resource availability rather than by hunting.

In environmental restoration plans, herbivore control campaigns are carried out to seek a stable plant structure in harmony with the new uses. However, these actions are complex and costly, as well as controversial. The extent of ecosystem response to herbivore control measures is not well known in heterogeneous environments transformed by centuries of human activity and highly dependent on environmental variables.

This doctoral thesis evaluates the functional response of the Mediterranean mountain ecosystems to the control of herbivores at different scales. In addition, given the lack of long-term information, and the complexity and effort of assessing changes at the ecosystem level, remote sensing tools are proposed to support managers in making decisions in regulating herbivore populations.

Chapter 1 examines the effect of excluding the activity of the feral goats (*Capra aegagrus hircus*) in five independent sites in the mountains of Mallorca on the soil's physical, chemical, and biological characteristics. Specifically, vegetation cover and

Abstract

soil properties in ungulate-exclusion plots were compared with adjacent plots where ungulates were present. Microbial activity increased significantly when exclusion occurred. However, all other physical and chemical measurements of the soils did not vary significantly. This may be caused by soil resilience against the effect of herbivores or by the high heterogeneity of soil at a very local scale. A multi-level meta-analysis confirms the notion that ungulate effects are context-dependent, and soil heterogeneity makes it difficult to identify clear patterns. The study results suggest that environmental context persistently drives ground response more than browsing itself, even at very small scales (< 10m).

Management actions are sometimes taken to manage the uncontrolled growth of herbivore populations reducing environmental disturbances caused by herbivores. However, it is often not possible to evaluate the effects of herbivore control on the ecosystem due to the lack of information both before and after management. Furthermore, the cost and complexity of inaccessible sampling areas such as those in the Mediterranean mountains make regular monitoring more difficult. In Chapter 2, this problem is addressed using a remote sensing approach. Twenty-one years of time series of monthly NDVI (proxy of photosynthetic activity) data was obtained from satellite images to evaluate the effects of the eradication of the black rat (*Rattus rattus*) on the productivity of the Mediterranean vegetation in the islet of Sa Dragonera and a near control area in Mallorca. At the time of eradication, the rat population density was one of the highest reported in an insular context. The black rat feeds mainly on seeds, shoots and leaves of woody vegetation. Therefore it is hypothesised that primary production would have increased over a nine-year period after the rodenticide campaign. This study revealed changes in vegetation dynamics throughout the study period. However, a comparison of the historical changes that occurred on the islet to

Abstract

those that occurred within a control zone (i.e., no rats), suggests that the magnitude and trend of changes in vegetation dynamics cannot be explicitly attributed to the presence of the rats. The lack of detection of an effect could be attributed to the resilience of Mediterranean shrub communities to browsing conducted by rats. Changes in herbivory intensity could modify specific plants with little contribution to NDVI values, and environmental factors are likely to overshadow their detection. The results suggest that the current passive restoration scheme imposed after eradication is insufficient to observe effective improvement in vegetation vigour and plant recruitment capacity.

A higher spatial resolution is increasingly required in conservation management programs worldwide to study plant-herbivores interaction. To this end, chapter 3 presents a novel remote sensing approach that uses images obtained with a low-cost Unmanned Aerial System (UAS). The study was carried out in a fenced enclosure with a captive of Iberian ibex (*Capra pyrenaica*) population in the Ports de Tortosa-Beceit Natural Park in Tarragona. The Microhistological analysis of the faecal cuticles was used to assess the dietary preferences of ibexes. Subsequently, the most common plant species individuals were georeferenced to locate them precisely on the multispectral images obtained with the UAS. The spectral signatures of these plant individuals were used to train machine learning algorithms and accurately predict resources at the landscape scale. As a result, it was possible to map the resources of herbivores classified according to dietary preferences with an error of 11.8%. This methodology can help successfully monitor the availability of resources for herbivores in the patchy Mediterranean vegetation in a faster, more accurate, and cheaper way than traditional field surveys.

Abstract

In addition to representing a significant scientific contribution towards a better understanding of the functional response of Mediterranean mountain ecosystems to herbivore control, the results of this thesis represent a contribution to the management of herbivore pressure in these ecosystems. The different approaches used show that remote sensing techniques combined with field data allow for large-scale analysis that helps decision-making on an ecosystem-wide level as well as at the local scale.

Keywords: Ecosystem services; Feral goat, Foodscapes, Iberian ibex, Remote sensing, Vegetation assessment

1. General introduction

The conservation of natural ecosystems is essential to safeguard the ecosystem services they provide. In the last century, many areas worldwide have been under some form of protection to preserve natural biodiversity and cultural history. However, numerous studies have made it clear that nature conservation is not an altruistic option in recent decades but rather a human necessity. Ecosystem services are direct and indirect contributions of ecological structures and natural processes to human wellbeing (De Groot, 1992). Ecosystem services are grouped into broader groups called functional groups. For the terrestrial ecosystems, the productive, environmental, and social functions are the main services (Table 1.1).

Table 1. 1. Ecosystem goods and services in the major functional groups of terrestrial ecosystems according to Rodà et al., 2003.

Productive function	Environmental function	Social function
Supply renewable natural goods such as food, medicines, wood, and non-wood products such as pastures, cork, game, or mushrooms	Biodiversity maintenance, climate regulation, biogeochemical cycles regulation, soil, and water conservation (e.g., erosion prevention), carbon storage	Recreational, educational, and leisure uses. Traditional cultural values, economic activities such as tourism and hiking.

Natural systems provide many ecosystem services in areas of the planet inhabited since ancient times, such as the Mediterranean basin. Still, after thousands of years of adaptation, their preservation requires the regulation of human action. Landscapes in the Mediterranean basin are highly heterogeneous due to the variable climate and the long story of human activities (Blondel et al., 2010). The Mediterranean climate is characterised by contrasting warm dry summers, and mild and wet winters, which

determine a high spatio-temporal environmental variability favouring a complex mosaic of landscapes (Peñuelas et al., 2004). Human activities have contributed significantly to shaping the landscape for more than 50,000 years (Rick et al., 2020). Humans have traditionally burned and cut down trees for grazing (Vernet and Thiebault, 1987). As a result, the Mediterranean is represented by a mosaic of landscapes where human activities and environmental conditions are closely interlinked (Plieninger et al., 2015).

Shifts in livestock management and landscape use in a global warming scenario

Pieces of evidence supporting global warming are increasing daily (IPCC, 2018). The Mediterranean basin is considered a ‘climate change hot spot’ since the temperature increase is greater than the global average, with approximately an increase of 1.3°C compared to 0.85°C worldwide in 2005-2006 (Guiot and Cramer, 2016). Furthermore, in recent decades there has been a reduction in summer rainfall and an increase in autumn rains which are often characterised by torrential rains (Capolongo et al., 2008; Pastor et al., 2015). The changes in the Mediterranean climate as temperatures rise and seasons become drier affect ecosystem functioning and the biological cycles of species. For example, satellite monitoring of phenological cycles of Mediterranean vegetation has revealed an increase in the growing period (i.e., vegetative activity) correlated to the occurrence of early springs and longer autumns (Peñuelas et al., 2017; Vitasse et al., 2011). This increase in the growing period is affecting the ability of ecosystems for carbon sequestration, atmospheric CO₂ reduction, biogeochemical cycling, and thus ecosystem functioning. Furthermore, the increasingly warm and dry environment intensifies the risk of ecosystems and human lives to wildfires (Giannakopoulos et al., 2009; Peñuelas et al., 2004; Turco et al., 2017).

General introduction

Since the mid-twentieth century, socioeconomic changes have resulted in the rural exodus, which in turn has resulted in changes in the land use of the Mediterranean basin. This fact, combined with global warming, contributes to the so-called ‘Global change’ that is profoundly alters forest ecosystem services worldwide (Choe and Thorne, 2017; Lamarque et al., 2014). This process is particularly evident in the Mediterranean basin due to the dramatic decline of traditional activities such as extensive livestock activity (De Rancourt et al., 2006) and the extraction of wood fuels (Lasanta-Martínez et al., 2005; Poyatos et al., 2003). The most obvious consequence is the forest encroachment and the loss of open landscapes due to natural regeneration and the colonisation of bushes and trees in abandoned areas (Figure 1. 1).

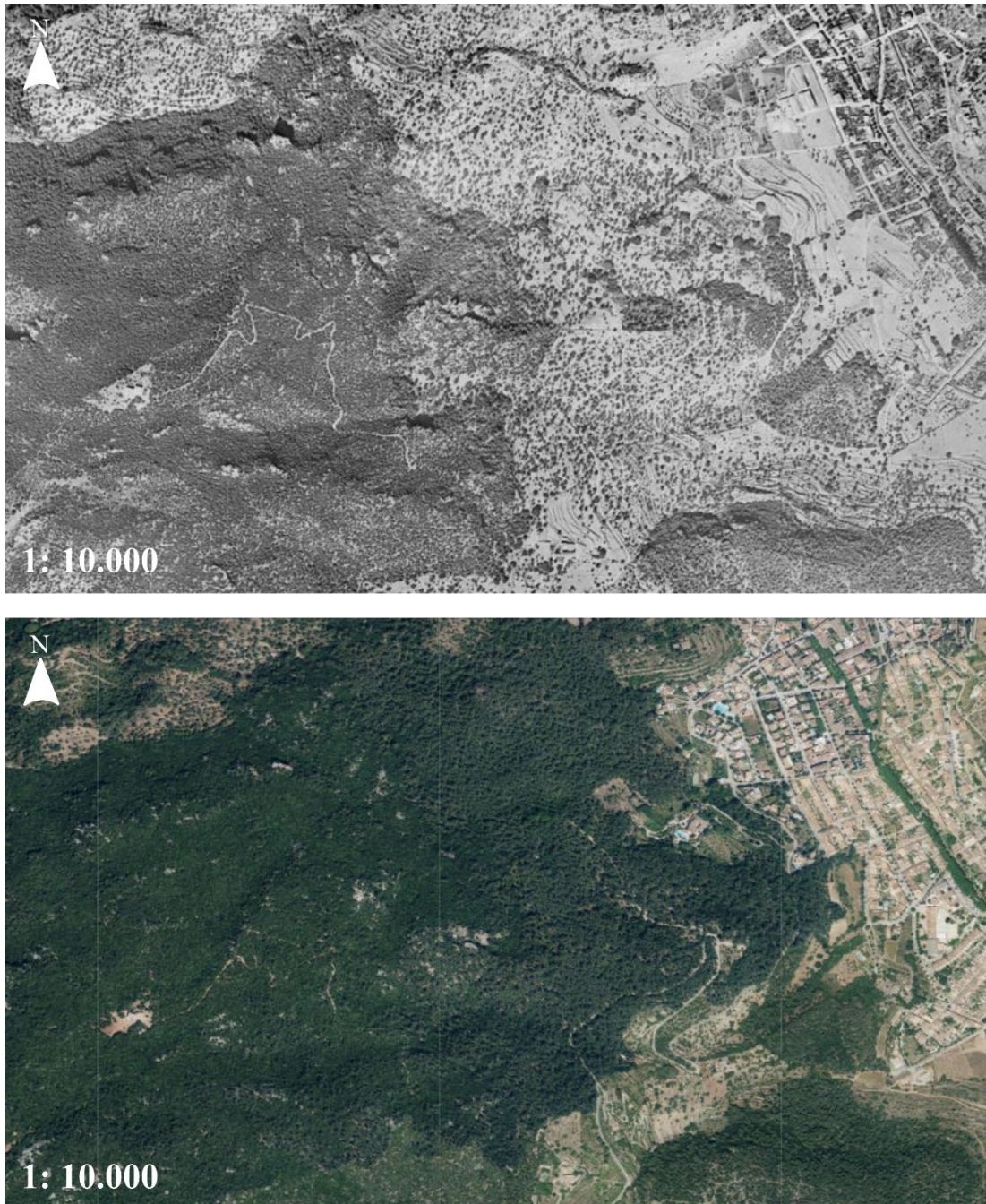


Figure 1. 1. Forest encroachment process due to the cessation of rural activities for 65 years in a Mediterranean mountain area Esporles, Serra de Tramuntana, Mallorca Island, Spain. The upper aerial scene was taken in 1956, while the lower satellite scene was in 2021. The abandoned agricultural areas on the right side have been replaced by an Aleppo pine (*Pinus halepensis*) forest. The orography is better appreciated in the old scene due to the lower holm oak forest (*Quercus ilex*) density. Oak has a finer-grained green colour than pines.

The prevailing criteria for addressing ecosystem degradation have been based on changes in the structure and function of vegetation (Barbero et al., 1990). This biased

vision about the benefit of forests (Pausas and Bond, 2019) has favoured the uncontrolled development of forests in the Mediterranean mountain areas. Some risks, among others, are the loss of productive land, the increased risk of wildfires, and the reduction of open habitats considered important reservoirs of biodiversity (Santos et al., 2008). Furthermore, the increased availability of vegetation biomass combined with the reduced activity of humans has led to growing numbers of wild herbivores (Madhusudan, 2004; Pereira and Navarro, 2015).

Herbivory in the Mediterranean mountains

Herbivores, but in particular rodents, lagomorphs and ungulates, are considered ecosystem engineers due to their ability to modify the environment to suit their needs and change the availability of resources for other species in the process (Hester et al., 2010; Jones et al., 1997, Figure 1.2). For centuries domestic ungulates have been raised at high densities in the downland areas of Mediterranean mountains, whereas wild ungulates have occupied the uplands, usually at low densities (Pereira and Navarro, 2015). This traditional animal husbandry and grazing management have promoted these ecosystems' biodiversity and productivity without apparent damage. In fact, the ability of Mediterranean vegetation to cope with millennia of human activity and wildfire occurrence might have contributed to developing its high resilience (Blondel, 2006). However, since the 60s, tables have turned, and today, livestock farming has become negligible, whereas wild ungulate populations have increased in range and number in practically all temperate ecosystems (Apollonio et al., 2010; Parente, 2011).



Figure 1. 2. Examples of the impact of browsing on the morphology of different plants in the Finca La Victoria, a mountainous area of the Island of Mallorca, Spain. The upper image (A) shows the short term effect of feral goat (*Capra hircus*) browsing (to the right of the fence) on the Mediterranean vegetation. The lower images show intensely browsed trees such as wild olive (*Olea europaea*, B), and Aleppo pine (*Pinus halepensis* together with well-developed grass *Ampelodesmos mauritanica*, a species very tolerant to herbivory, C).

Various factors have contributed to this burgeoning ungulate populations in the Mediterranean basin, such as socio-economic changes, lack of predators, habitat re-naturalization, and the reintroductions for recreational hunting purposes (Acevedo et al., 2011; Milner et al., 2014). These wild ungulate populations can have beneficial natural effects, such as restoring food webs or maintaining open habitats. However, when populations are overabundant, ungulates can cause deleterious effects on the ecosystems due to trampling and browsing, causing environmental damage and

putting emblematic plant species at risk (Augustine and McNaughton, 1998; Fernández-Olalla et al., 2016).

This conservation issue is particularly relevant in Mediterranean islands, where both relict and introduced plant species coexist and the herbivore population often occur at high densities (Terborgh et al., 2001). These insular ecosystems, often hilly and mountainous, have complex orography that plays an important role as a refuge for plant species adapted to insular environments. Conservation plans often begin with the control of herbivory exerted by herbivores introduced centuries or millennia ago, such as ungulates or rodents, which, at high densities, can severely affect primary production and transform the habitat. Some examples in the Balear archipelago are the eradication of rats in the Sa Dragonera islet (Mayol et al., 2012) and the reduction in the feral goat population on the Es Vedrà islet (Capó et al., 2022). Following herbivory control campaigns, recovery of native ecosystems may be quick if communities are sufficiently resilient or may require longer timescales; results vary according to the context (Beltran et al., 2014; Schweizer et al., 2016). Animal population control campaigns are highly controversial, and long-term monitoring studies are needed to assess the efficacy of these campaigns. However, there is often an information gap in ecosystem monitoring both, before and after control campaigns, with just a few studies having a sufficient temporal extension evaluating the response of the ecosystem (Beltran et al., 2014; Carmel and Kadmon, 1999; Jones and Schmitz, 2009; Schweizer et al., 2016).

Herbivores and the ecosystem services associated with the soil

Shifts in animal husbandry and landscape use have significantly changed soil ecosystem services. The vegetation that herbivores browse is directly connected to the

soil through the rhizosphere and the bidirectional plant-soil feedbacks that occur in them (van der Putten et al., 2016). Large herbivores disturb the soil directly compacting the soil by trampling (Alegre and Lara, 1991), increasing site regeneration and soil heterogeneity; and indirectly by driving plants to increase root biomass to compensate for browsed biomass. Therefore herbivores produce changes in biological, physical, and chemical soil properties (e.g., Augustine et al., 2003; Hunter and Price, 1992). There are extensive studies assessing the effect of herbivory on soil features; however, the results are varied and highly dependent on the context in which they occur (Andriuzzi and Wall, 2018; Forbes et al., 2019). These varied responses of soil features to herbivory may be due to the combined effect of the abiotic context of the parent soil and the landscape in which it sits and the high heterogeneity of the soil features from global to local scale.

Establishing well-controlled analysis protocols that consider the environmental context could help analyse the variation in the effect of ungulates on Mediterranean mountainous vegetation.

Remote sensing for monitoring the effects of herbivores

A remote sensing approach can tackle the heterogeneous response of the ecosystem functioning to herbivory action. Changes in the ecosystem occur heterogeneously, and herbivores are an essential source of heterogeneity by trampling on some areas, defecating in others, and consuming vegetation in patches (Cid and Brizuela, 1998). This fact could peter out consistent effects of herbivory when the traditional ecological herbivore exclusion studies are conducted, supporting the old but long-standing idea that climate and soils are the only essential factors shaping large-scale patterns in nature (Pausas and Bond, 2019). Increasing the sampling effort of

traditional ecological surveys is costly and time-consuming, and this does not guarantee to avoid the high heterogeneity of the environmental factors (Andriuzzi and Wall, 2018). Satellite sensors play a crucial role in providing land cover information at different spatial and temporal resolutions and provide an important source of continuous geospatial data for monitoring vegetation health. This remote sensing approach allows for identifying areas of recovery following natural- or human-induced disturbance (Sader and Jin, n.d.; Verbesselt et al., 2010).

Vegetation indices are valuable in studying the structure and functioning of terrestrial vegetation (Peñuelas and Filella, 1998). One of the most well-known vegetation indexes is the Normalized Difference Vegetation Index (NDVI) which can be used for these purposes (Pettorelli et al., 2005). NDVI is a proxy for photosynthetic activity (Sellers, 1985), vegetation productivity, aboveground biomass (Reed et al., 1994), and vegetation dynamics (Myneni et al., 2019; Running, 1990), and has been shown to reliably capture the ecological responses to environmental change, including human- and animal-induced land degradation (Pettorelli et al., 2005). Other indices commonly used for this purpose are the Enhanced Vegetation Index (EVI) and the Photochemical Reflectance Index (PRI). The EVI index is often used as an alternative to NDVI to deal with signal saturation caused by high biomass covers and the influence of bare soil (Huete et al., 2002). On the other hand, the PRI index is used to monitor changes in the efficiency of the use of solar radiation and associated physiological parameters at the leaf, canopy and ecosystem levels (Peñuelas et al., 2011).

Identification of the effect of herbivores on the ecosystem using traditional ecological field surveys can be clouded by climatic dynamics and environmental heterogeneity. In contrast, satellite observation provides longer time-series measurements at a scale where the causes of change, whether natural or human-induced, can be detected and

differentiated (Barbosa et al., 2019; Washington-Allen et al., 2006). Some of the key sensors used to assess herbivore-plant interactions are, among others, Advanced Very High-Resolution Radiometer (AVHRR, Notaro, et al., 2019), Moderate Resolution Imaging Spectroradiometer (MODIS, Jarque-Bascuñana, et al., 2021; Notaro et al., 2019) and Sentinel-2 (Awuah and Aplin, 2021; Qin et al., 2021). Landsat satellites stand out because they constitute the longest continuous satellite moderate-resolution (30 m) record of the global land surface (NASA, 2013). Specifically, the recorded period ranges from 1972 to the present day on a monthly basis. AVHRR and MODIS have a high temporal resolution, sufficient to capture subtle changes in vegetation development but an insufficient spatial resolution to capture plant-specific phenological changes (Shen et al., 2015). Sentinel-2 has been active since 2013 and provides records with a temporal resolution of 5 to 10 days which is advantageous for vegetation analysis. The most relevant characteristics of the main sensors evaluating terrestrial ecosystems are summarised in Table 1.2.

Table 1. 2. Main features of major sensors used to assess terrestrial ecosystems. Useful imagery can be obtained by combining the spectral bands of different spectral ranges (VIS = visible; NIR= Near-Infrared; SWIR = Short Wave Infrared; TIR = Thermal Infrared). To provide higher spatial resolution for multispectral images, some sensors include a panchromatic band (PAN)

Sensor	Running Period	N° Spectral bands/ Spectral range	Spatial Resolution	Temporal resolution
Landsat TM	1982 to present	6 / (PAN, VIS, NIR, SWIR, TIR)	30 m	16 days
Landsat ETM+	1999 to present	8 / (PAN, VIS, NIR, SWIR, TIR)	30 m	16 days
Landsat OLI	2013 to present	9 / (PAN, VIS, NIR, SWIR)	15-30 m	16 days
SPOT (1-5)	1986 to present	5 / (PAN, VIS, NIR, SWIR)	2.5-20 m	1-3 days
MODIS	2000 to present	36 / (VIS, NIR, SWIR, TIR)	250-1000 m	16 days
AVHRR	1980 to present	6 / (VIS, NIR, SWIR, TIR)	1000 m	1-2 days
IKONOS	1999 to present	5 / (PAN, VIS, NIR, TIR)	1-4 m	3-5 days
ASTER	2000 to present	14 / (VIS, NIR, SWIR, TIR)	15- 90 m	1-2 days
HYPERION	2003 to 2017	220 / (VNIR-SWIR)	30 m	16 days
Sentinel-2	2015 to present	12 / (VIS, NIR, SWIR)	10- 60 m	5 days

One fact that has helped popularise the study of land cover with satellite images is computational advances. A large amount of data extracted from satellite images can be automatically harmonised in time-series datasets of vegetation indices (Chen et al., 2004; Verbesselt et al., 2006), as well as robust algorithms for structural change analysis (Verbesselt et al., 2015; Zeileis et al., 2001). The analyses of structural changes of the NDVI time series are especially useful for the evaluation and characterisation of changes in the dynamics of the Mediterranean vegetation since it identifies abnormal changes in the time series, considering the seasonal component and the general trend. Temperature and precipitation are the main environmental factors driving vegetation trends and changes in the Mediterranean basin. Knowing the environmental context of a study area makes it possible to assess the effect of an exogenous intervention in the system, such as herbivore control campaigns.

UAVs and herbivory monitoring

Mapping vegetation at the species scale is essential for monitoring bottom-up (Espunyes et al., 2019) and top-down ecosystem regulation processes (Oates et al., 2019; Peters et al., 2019; Searle et al., 2007) by ungulate populations. Satellites provide long- and short-term information on vegetation dynamics from global (Bernardino et al., 2020) to local scales (Chen et al., 2014; Geng et al., 2019); however, satellite imagery shows specific weaknesses for monitoring herbivore-plant interactions in heterogeneous and dynamic areas such as the Mediterranean mountains. Furthermore, if plant species are rare or do not contribute significantly to the values of global indexes of greens (e.g., NDVI or EVI), then the impact of herbivores would not be detected by satellite sensors. Unmanned Aerial Vehicles

General introduction

(UAV) technology shows promise for monitoring vegetation in heterogeneous landscapes at a species or functional group level. This could be a viable alternative not only to the satellite approach, since the spatial resolution and time intervals of the studies do not depend on satellite orbits, but also to the time-consuming traditional field surveys. Although UAV-based surveys are still costly and beyond the budgeting capabilities of some organisations, businesses and government-funded agencies, they are an up-and-coming surveying tool for monitoring and managing wildlife. Finding accurate and cost-effective ways to map complex vegetation structure landscapes is a challenging and exciting research area that is still in its infancy.

References

- Acevedo, P., Farfán, M.Á., Márquez, A.L., Delibes-Mateos, M., Real, R., Vargas, J.M., 2011. Past, present and future of wild ungulates in relation to changes in land use. *Landsc. Ecol.* 26. <https://doi.org/10.1007/s10980-010-9538-2>
- Alegre, J.C., Lara, P.D., 1991. Efecto de los animales en pastoreo sobre las propiedades físicas de suelos de la región tropical húmeda de Perú. *Pasturas Trop.* 13(1), 18–23.
- Andriuzzi, W.S., Wall, D.H., 2018. Soil biological responses to, and feedbacks on, trophic rewilding. *Philos. Trans. R. Soc. B Biol. Sci.* <https://doi.org/10.1098/rstb.2017.0448>
- Apollonio, M., Andersen, R., Rory, P., 2010. European Ungulates and Their Management in the 21st Century, *European Ungulates and Their Management in the 21st Century*.
- Augustine, D.J., McNaughton, S.J., 1998. Ungulate Effects on the Functional Species Composition of Plant Communities: Herbivore Selectivity and Plant Tolerance. *J. Wildl. Manage.* 62. <https://doi.org/10.2307/3801981>
- Augustine, D.J., McNaughton, S.J., Frank, D.A., 2003. Feedbacks between soil nutrients and large herbivores in a managed savanna ecosystem. *Ecol. Appl.* 13. <https://doi.org/10.1890/02-5283>
- Awuah, K.T., Aplin, P., 2021. Fusion of Sentinel-2 Data with High Resolution Open Access Planet Basemaps for Grazing Lawn Detection in Southern African Savannas. <https://doi.org/10.1109/igarss47720.2021.9554156>
- Barbero, M., Bonin, G., Loisel, R., Quézel, P., 1990. Changes and disturbances of

- forest ecosystems caused by human activities in the western part of the mediterranean basin. *Vegetatio* 87. <https://doi.org/10.1007/BF00042952>
- Barbosa, J.M., Pascual-Rico, R., Eguia Martínez, S., Sánchez-Zapata, J.A., 2019. Ungulates Attenuate the Response of Mediterranean Mountain Vegetation to Climate Oscillations. *Ecosystems*. <https://doi.org/10.1007/s10021-019-00449-8>
- Beltran, R.S., Kreidler, N., Van Vuren, D.H., Morrison, S.A., Zavaleta, E.S., Newton, K., Tershy, B.R., Croll, D.A., 2014. Passive Recovery of Vegetation after Herbivore Eradication on Santa Cruz Island, California. *Wiley Online Libr.* 22, 790–797. <https://doi.org/10.1111/rec.12144>
- Bernardino, P.N., De Keersmaecker, W., Fensholt, R., Verbesselt, J., Somers, B., Horion, S., 2020. Global-scale characterization of turning points in arid and semi-arid ecosystem functioning. *Glob. Ecol. Biogeogr.* 29, 1230–1245. <https://doi.org/10.1111/geb.13099>
- Blondel, J., 2006. The “design” of Mediterranean landscapes: A millennial story of humans and ecological systems during the historic period. *Hum. Ecol.* 34. <https://doi.org/10.1007/s10745-006-9030-4>
- Blondel, J., Aronson, J., Bodiou, J., Boeuf, G., 2010. *The Mediterranean region: biological diversity in space and time.* Oxford University Press, Oxford.
- Capó, M., Cursach, J., Picorelli, V., Baraza, E., Rita, J., 2022. Eradication of feral goats, not population control, as a strategy to conserve plant communities on Mediterranean islets. *J. Nat. Conserv.* 65. <https://doi.org/10.1016/j.jnc.2021.126108>
- Capolongo, D., Diodato, N., Mannaerts, C.M., Piccarreta, M., Strobl, R.O., 2008. Analyzing temporal changes in climate erosivity using a simplified rainfall

erosivity model in Basilicata (southern Italy). *J. Hydrol.* 356.
<https://doi.org/10.1016/j.jhydrol.2008.04.002>

Carmel, Y., Kadmon, R., 1999. Effects of grazing and topography on long-term vegetation changes in a Mediterranean ecosystem in Israel. *Plant Ecol.* 145.
<https://doi.org/10.1023/A:1009872306093>

Chen, J., Jönsson, P., Tamura, M., Gu, Z., Matsushita, B., Eklundh, L., 2004. A simple method for reconstructing a high-quality NDVI time-series data set based on the Savitzky-Golay filter. *Remote Sens. Environ.* 91, 332–344.
<https://doi.org/10.1016/j.rse.2004.03.014>

Chen, L., Michishita, R., Xu, B., 2014. Abrupt spatiotemporal land and water changes and their potential drivers in Poyang Lake, 2000-2012. *ISPRS J. Photogramm. Remote Sens.* 98, 85–93. <https://doi.org/10.1016/j.isprsjprs.2014.09.014>

Choe, H., Thorne, J.H., 2017. Integrating climate change and land use impacts to explore forest conservation policy. *Forests* 8. <https://doi.org/10.3390/f8090321>

Cid, M.S., Brizuela, M.A., 1998. Heterogeneity in tall fescue pastures created and sustained by cattle grazing. *J. Range Manag.* 51.
<https://doi.org/10.2307/4003606>

De Groot, R.S., 1992. *Functions of Nature: Evaluation of Nature in Environmental Planning, Management and Decision Making.*

De Rancourt, M., Fois, N., Lavín, M.P., Tchakérian, E., Vallerand, F., 2006. Mediterranean sheep and goats production: An uncertain future, in: *Small Ruminant Research*. <https://doi.org/10.1016/j.smallrumres.2005.08.012>

Espunyes, J., Bartolomé, J., Garel, M., Gálvez-Cerón, A., Aguilar, X.F., Colom-Cadena, A., Calleja, J.A., Gassó, D., Jarque, L., Lavín, S., Marco, I., Serrano, E.,

2019. Seasonal diet composition of Pyrenean chamois is mainly shaped by primary production waves. *PLoS One* 14. <https://doi.org/10.1371/journal.pone.0210819>

Fernández-Olalla, M., Martínez-Jauregui, M., Perea, R., Velamazán, M., San Miguel, A., 2016. Threat or opportunity? Browsing preferences and potential impact of *Ammotragus lervia* on woody plants of a Mediterranean protected area. *J. Arid Environ.* 129. <https://doi.org/10.1016/j.jaridenv.2016.02.003>

Forbes, E.S., Cushman, J.H., Young, T.P., Klope, M., Young, H.S., 2019. Synthesizing the effects of large, wild herbivore exclusion on ecosystem function 1597–1610. <https://doi.org/10.1111/1365-2435.13376>

Geng, L., Che, T., Wang, X., Wang, H., 2019. Detecting spatiotemporal changes in vegetation with the BFAST model in the Qilian Mountain region during 2000–2017. *Remote Sens.* 11. <https://doi.org/10.3390/rs11020103>

Giannakopoulos, C., Le Sager, P., Bindi, M., Moriondo, M., Kostopoulou, E., Goodess, C.M., 2009. Climatic changes and associated impacts in the Mediterranean resulting from a 2 °C global warming. *Glob. Planet. Change* 68. <https://doi.org/10.1016/j.gloplacha.2009.06.001>

Guiot, J., Cramer, W., 2016. Climate change: The 2015 Paris Agreement thresholds and Mediterranean basin ecosystems. *Science*. 354. <https://doi.org/10.1126/science.aah5015>

Hester, A.J., Bergman, M., Iason, G.R., Moen, J., 2010. Impacts of large herbivores on plant community structure and dynamics, in: *Large Herbivore Ecology, Ecosystem Dynamics and Conservation*. <https://doi.org/10.1017/cbo9780511617461.006>

- Huete, A., Didan, K., Miura, T., Rodriguez, E.P., Gao, X., Ferreira, L.G., 2002. Overview of the radiometric and biophysical performance of the MODIS vegetation indices. *Remote Sens. Environ.* 83. [https://doi.org/10.1016/S0034-4257\(02\)00096-2](https://doi.org/10.1016/S0034-4257(02)00096-2)
- Hunter, M.D., Price, P.W., 1992. Playing chutes and ladders: heterogeneity and the relative roles of bottom-up and top-down forces in natural communities. *Ecology* 73. <https://doi.org/10.2307/1940152>
- IPCC, 2018. Global warming of 1.5°C, *Ipcc - Sr15*.
- Jarque-Bascuñana, L., Calleja, J.A., Ibañez, M., Bartolomé, J., Albanell, E., Espunyes, J., Gálvez-Cerón, A., López-Martín, J.M., Villamuelas, M., Gassó, D., Fernández-Aguilar, X., Colom-Cadena, A., Krumins, J.A., Serrano, E., 2021. Grazing influences biomass production and protein content of alpine meadows. *Sci. Total Environ.* <https://doi.org/10.1016/j.scitotenv.2021.151771>
- Jones, C.G., Lawron, J.H., Shachak, M., 1997. Positive and negative effects of organisms as physical ecosystem engineers. *Ecology*. [https://doi.org/10.1890/0012-9658\(1997\)078\[1946:PANEOO\]2.0.CO;2](https://doi.org/10.1890/0012-9658(1997)078[1946:PANEOO]2.0.CO;2)
- Jones, H.P., Schmitz, O.J., 2009. Rapid recovery of damaged ecosystems. *PLoS One* 4. <https://doi.org/10.1371/journal.pone.0005653>
- Lamarque, P., Lavorel, S., Mouchet, M., Quétier, F., 2014. Plant trait-based models identify direct and indirect effects of climate change on bundles of grassland ecosystem services. *Proc. Natl. Acad. Sci. U. S. A.* 111. <https://doi.org/10.1073/pnas.1216051111>
- Lasanta-Martínez, T., Vicente-Serrano, S.M., Cuadrat-Prats, J.M., 2005. Mountain Mediterranean landscape evolution caused by the abandonment of traditional

primary activities: A study of the Spanish Central Pyrenees. *Appl. Geogr.* 25.
<https://doi.org/10.1016/j.apgeog.2004.11.001>

Madhusudan, M.D., 2004. Recovery of wild large herbivores following livestock decline in a tropical Indian wildlife reserve. *J. Appl. Ecol.* 41.
<https://doi.org/10.1111/j.0021-8901.2004.00950.x>

Mayol, J., Mayol, M., Domenech, O., Oliver, J., McMinn, M., Rodríguez, A., 2012. Aerial broadcast of rodenticide on the island of Sa Dragonera (Balearic Islands, Spain). A promising rodent eradication experience on a Mediterranean island. *Aliens Invasive Species Bull.* 32, 29–32.

Milner, J.M., Van Beest, F.M., Schmidt, K.T., Brook, R.K., Storaas, T., 2014. To feed or not to feed? Evidence of the intended and unintended effects of feeding wild ungulates. *J. Wildl. Manage.* <https://doi.org/10.1002/jwmg.798>

Myneni, R.B., Hall, F.G., Sellers, P.J., Marshak, A.L., 2019. The interpretation of spectral vegetation indexes. *IEEE Trans. Geosci. Remote Sens.* 33, 481–486.
<https://doi.org/10.1109/tgrs.1995.8746029>

NASA, 2013. Program-level Requirements on the Landsat Data Continuity Mission Project: Appendix N to the Earth Systematic Mission Program Plan.

Notaro, M., Emmett, K., O’Leary, D., 2019. Spatio-temporal variability in remotely sensed vegetation greenness across Yellowstone National Park. *Remote Sens.* 11. <https://doi.org/10.3390/rs11070798>

Oates, B.A., Merkle, J.A., Kauffman, M.J., Dewey, S.R., Jimenez, M.D., Vartanian, J.M., Becker, S.A., Goheen, J.R., 2019. Antipredator response diminishes during periods of resource deficit for a large herbivore. *Ecology* 100.
<https://doi.org/10.1002/ecy.2618>

- Parente, G., 2011. Grazing systems and biodiversity in Mediterranean areas: Spain, Italy and Greece. *Grass Forage Sci.* 66. <https://doi.org/10.1111/j.1365-2494.2011.00820.x>
- Pastor, F., Valiente, J.A., Estrela, M.J., 2015. Sea surface temperature and torrential rains in the Valencia region: Modelling the role of recharge areas. *Nat. Hazards Earth Syst. Sci.* 15. <https://doi.org/10.5194/nhess-15-1677-2015>
- Pausas, J.G., Bond, W.J., 2019. Humboldt and the reinvention of nature. *J. Ecol.* <https://doi.org/10.1111/1365-2745.13109>
- Peñuelas, J., Filella, L., 1998. Technical focus: Visible and near-infrared reflectance techniques for diagnosing plant physiological status. *Trends Plant Sci.* 3. [https://doi.org/10.1016/S1360-1385\(98\)01213-8](https://doi.org/10.1016/S1360-1385(98)01213-8)
- Peñuelas, J., Garbulsky, M.F., Filella, I., 2011. Photochemical reflectance index (PRI) and remote sensing of plant CO₂ uptake. *New Phytol.* <https://doi.org/10.1111/j.1469-8137.2011.03791.x>
- Peñuelas, J., Sabaté, S., Filella, I., Gracia, C., 2004. Efectos del cambio climático sobre los ecosistemas terrestres: observación, experimentación y simulación. *Ecología del bosque mediterráneo en un mundo cambiante.* pp. 425–460.
- Peñuelas, J., Sardans, J., Filella, I., Estiarte, M., Llusià, J., Ogaya, R., Carnicer, J., Bartrons, M., Rivas-Ubach, A., Grau, O., Peguero, G., Margalef, O., Pla-Rabés, S., Stefanescu, C., Asensio, D., Preece, C., Liu, L., Verger, A., Barbeta, A., Achotegui-Castells, A., Gargallo-Garriga, A., Sperlich, D., Farré-Armengol, G., Fernández-Martínez, M., Liu, D., Zhang, C., Urbina, I., Camino-Serrano, M., Vives-Inglá, M., Stocker, B.D., Balzarolo, M., Guerrieri, R., Peaucelle, M., Marañón-Jiménez, S., Bórnez-Mejías, K., Mu, Z., Descals, A., Castellanos, A.,

General introduction

- Terradas, J., 2017. Impacts of global change on Mediterranean forests and their services. *Forests*. <https://doi.org/10.3390/f8120463>
- Pereira, H.M., Navarro, L.M., 2015. Rewilding European landscapes, Rewilding European Landscapes. <https://doi.org/10.1007/978-3-319-12039-3>
- Peters, W., Hebblewhite, M., Mysterud, A., Eacker, D., Hewison, A.J.M., Linnell, J.D.C., Focardi, S., Urbano, F., De Groeve, J., Gehr, B., Heurich, M., Jarnemo, A., Kjellander, P., Kröschel, M., Morellet, N., Pedrotti, L., Reinecke, H., Sandfort, R., Sönnichsen, L., Sunde, P., Cagnacci, F., 2019. Large herbivore migration plasticity along environmental gradients in Europe: life-history traits modulate forage effects. *Oikos* 128. <https://doi.org/10.1111/oik.05588>
- Pettorelli, N., Vik, J.O., Mysterud, A., Gaillard, J.M., Tucker, C.J., Stenseth, N.C., 2005. Using the satellite-derived NDVI to assess ecological responses to environmental change. *Trends Ecol. Evol.* <https://doi.org/10.1016/j.tree.2005.05.011>
- Plieninger, T., Hartel, T., Martín-López, B., Beaufoy, G., Bergmeier, E., Kirby, K., Montero, M.J., Moreno, G., Oteros-Rozas, E., Van Uytvanck, J., 2015. Wood-pastures of Europe: Geographic coverage, social-ecological values, conservation management, and policy implications. *Biol. Conserv.* <https://doi.org/10.1016/j.biocon.2015.05.014>
- Poyatos, R., Latron, J., Llorens, P., 2003. Land Use and Land Cover Change After Agricultural Abandonment. *Mt. Res. Dev.* 23. [https://doi.org/10.1659/0276-4741\(2003\)023\[0362:lualcc\]2.0.co;2](https://doi.org/10.1659/0276-4741(2003)023[0362:lualcc]2.0.co;2)
- Qin, Q., Xu, D., Hou, L., Shen, B., Xin, X., 2021. Comparing vegetation indices from Sentinel-2 and Landsat 8 under different vegetation gradients based on a

controlled grazing experiment. *Ecol. Indic.* 133.
<https://doi.org/10.1016/j.ecolind.2021.108363>

Reed, B.C., Brown, J.F., VanderZee, D., Loveland, T.R., Merchant, J.W., Ohlen, D.O., 1994. Measuring phenological variability from satellite imagery. *J. Veg. Sci.* 5, 703–714. <https://doi.org/10.2307/3235884>

Rick, T., Ontiveros, M.Á.C., Jerardino, A., Mariotti, A., Méndez, C., Williams, A.N., 2020. Human-environmental interactions in Mediterranean climate regions from the Pleistocene to the Anthropocene. *Anthropocene.*
<https://doi.org/10.1016/j.ancene.2020.100253>

Rodà, F., Ibáñez, J., Gracia, C., 2003. L'estat dels boscos.

Running, S.W., 1990. Estimating Terrestrial Primary Productivity by Combining Remote Sensing and Ecosystem Simulation. pp. 65–86.
https://doi.org/10.1007/978-1-4612-3302-2_4

Sader, S.A., Jin, S., n.d. MODIS time-series imagery for forest disturbance detection and quantification of patch size effects Article in Remote Sensing of Environment December 2005 SEE PROFILE MODIS time-series imagery for forest disturbance detection and quantification of patch size effects. Elsevier.
<https://doi.org/10.1016/j.rse.2005.09.017>

Santos, K.C., Pino, J., Rodà, F., Guirado, M., Ribas, J., 2008. Beyond the reserves: The role of non-protected rural areas for avifauna conservation in the area of Barcelona (NE of Spain). *Landsc. Urban Plan.* 84.
<https://doi.org/10.1016/j.landurbplan.2007.07.004>

Schweizer, D., Jones, H.P., Holmes, N.D., 2016. Literature Review and Meta-Analysis of Vegetation Responses to Goat and European Rabbit Eradications on

Islands. *Pacific Sci.* 70, 55–71. <https://doi.org/10.2984/70.1.5>

Searle, K.R., Hobbs, N.T., Gordon, I.J., 2007. It's the "Foodscape", not the landscape:

Using foraging behavior to make functional assessments of landscape condition.

Isr. J. Ecol. Evol. 53. <https://doi.org/10.1560/IJEE.53.3.297>

Sellers, P.J., 1985. Canopy reflectance, photosynthesis and transpiration. *Int. J.*

Remote Sens. 6, 1335–1372. <https://doi.org/10.1080/01431168508948283>

Shen, M., Piao, S., Dorji, T., Liu, Q., Cong, N., Chen, X., An, S., Wang, S., Wang,

T., Zhang, G., 2015. Plant phenological responses to climate change on the

Tibetan Plateau: Research status and challenges. *Natl. Sci. Rev.*

<https://doi.org/10.1093/nsr/nwv058>

Terborgh, J., Lopez, L., Nuñez, P. V., Rao, M., Shahabuddin, G., Orihuela, G.,

Riveros, M., Ascanio, R., Adler, G.H., Lambert, T.D., Balbas, L., 2001.

Ecological meltdown in predator-free forest fragments. *Science*, 294.

<https://doi.org/10.1126/science.1064397>

Turco, M., Von Hardenberg, J., AghaKouchak, A., Llasat, M.C., Provenzale, A.,

Trigo, R.M., 2017. On the key role of droughts in the dynamics of summer fires

in Mediterranean Europe. *Sci. Rep.* 7. [https://doi.org/10.1038/s41598-017-](https://doi.org/10.1038/s41598-017-00116-9)

00116-9

van der Putten, W.H., Bradford, M.A., Pernilla Brinkman, E., van de Voorde, T.F.J.,

Veen, G.F., 2016. Where, when and how plant–soil feedback matters in a

changing world. *Funct. Ecol.* 30, 1109–1121. [https://doi.org/10.1111/1365-](https://doi.org/10.1111/1365-2435.12657)

2435.12657

Verbesselt, J., Hyndman, R., Newnham, G., Culvenor, D., 2010. Detecting trend and

seasonal changes in satellite image time series. *Remote Sens. Environ.* 114, 106–

115. <https://doi.org/10.1016/j.rse.2009.08.014>

Verbesselt, J., Jönsson, P., Lhermitte, S., Van Aardt, J., Coppin, P., 2006. Evaluating satellite and climate data-derived indices as fire risk indicators in savanna ecosystems. *IEEE Trans. Geosci. Remote Sens.* 44, 1622–1632. <https://doi.org/10.1109/TGRS.2005.862262>

Verbesselt, J., Zeileis, A., Hyndman, R., 2015. Breaks For Additive Season and Trend (BFAST). Version 1.5.7. Tech. Rep.

Vernet, J.-L., Thiebault, S., 1987. An Approach to Northwestern Mediterranean Recent Prehistoric Vegetation and Ecologic Implications. *J. Biogeogr.* 14. <https://doi.org/10.2307/2845066>

Vitasse, Y., François, C., Delpierre, N., Dufrêne, E., Kremer, A., Chuine, I., Delzon, S., 2011. Assessing the effects of climate change on the phenology of European temperate trees. *Agric. For. Meteorol.* 151. <https://doi.org/10.1016/j.agrformet.2011.03.003>

Washington-Allen, R.A., West, N.E., Ramsey, R.D., Efroymson, R.A., 2006. A protocol for retrospective remote sensing-based ecological monitoring of rangelands. *Rangel. Ecol. Manag.* 59. <https://doi.org/10.2111/04-116R2.1>

Zeileis, A., Leisch, F., Hornik, K., Kleiber, C., 2001. strucchange: An R Package for Testing for Structural Change in Linear Regression Models, *Journal of Statistical Software*.

2. Objectives

The general objective of this thesis is to assess the impact of wild herbivores on the ecosystem functions of the Mediterranean mountain ecosystems. In the context of climate change and land-use change in the Mediterranean mountains, it is necessary to evaluate the new role of wild herbivores that increase their populations and act without the control that humans had exerted on them for thousands of years. The depopulation of the Mediterranean mountains leads administrations to tackle ambitious environmental management plans, which often begin with the control of herbivores. However, this type of intervention needs a solid understanding of how the system works to obtain the expected results. The studies carried out in this thesis seek advanced solutions to assess the response capacity of Mediterranean mountain ecosystems to wild herbivory, considering environmental heterogeneity and the high resilience of these ecosystems to herbivory. In addition, novel ecosystem assessment methodologies are shown that address the limitations of traditional sampling and the lack of long-term information.

In **chapter 1, the objective** is to compare the extent to which feral ungulate populations affect the ecosystem functioning through a herbivore exclusion experiment in Mallorca island mountains. The starting hypothesis was that feral ungulates affect the soil's physical, chemical, and biological characteristics, subsequently to changes exerted over vegetation structure. To address the contextual variation of the effects of herbivory on the ecosystem services, we carry out a multi-level meta-analysis across five different study sites.

Objectives

The **objective of chapter 2** is to evaluate the effect of eradicating the black rat (*Rattus rattus*) on the primary production of the islet of Sa Dragonera in Mallorca, Spain. The public administration carried out a rat eradication campaign in February 2011 in response to the very high-density population of rats, which was thought to lead to intense herbivory pressure on local vegetation and change the ecosystem functions of the island. Specifically, the objective is to fill the information gap on the state of the insular ecosystem both before and after the eradication campaign using a satellite imagery approach and, in this way, determine if vegetation productivity recovered followed the rate of eradication. In particular, we expect to detect an increase (abrupt and/or gradual) in the greenness of the main vegetation due to the natural vegetation recovery following rodent eradication after controlling for climatic conditions.

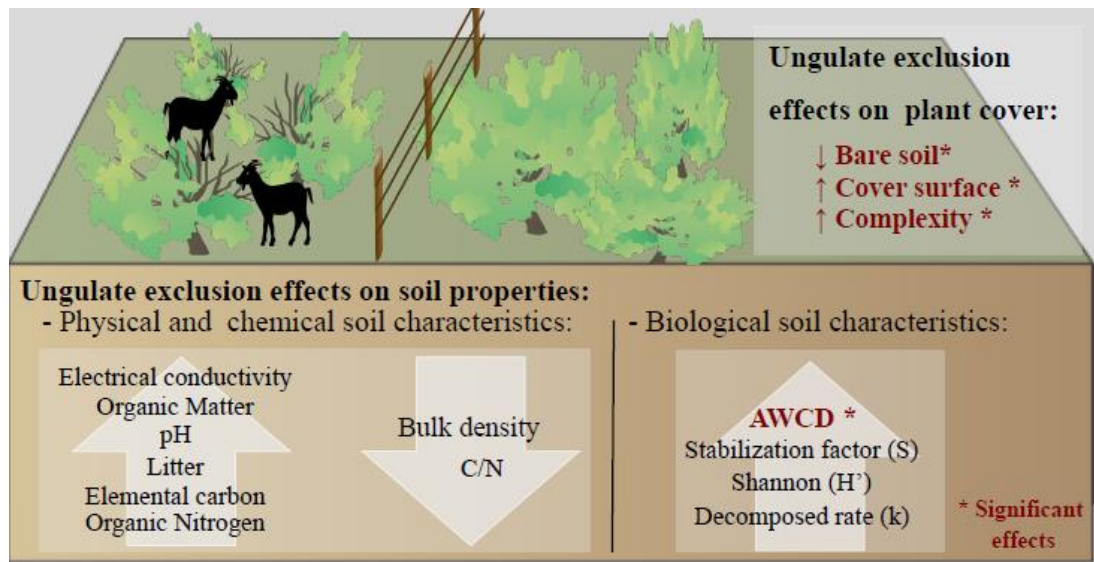
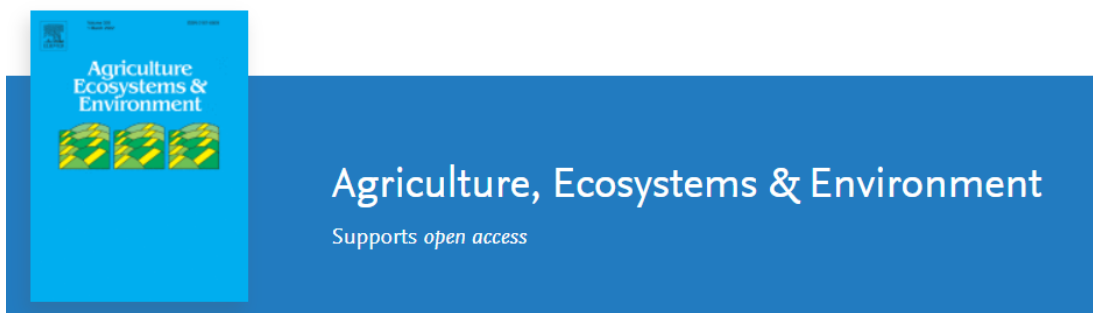
Wild ungulates play a fundamental role in transforming the vegetation structure due to their feeding behaviour and preferences. In **chapter 3, the objective** is to assess the food landscape (vegetation availability) for a mixed-feeding ungulate, the Iberian ibex (*Capra pyrenaica*), in a heterogeneous Mediterranean scrubland using a novel remote sensing approach. Specifically, the main objective is to determine the feasibility of classifying Mediterranean plant species using sensors onboard low-cost Unmanned Aerial Vehicles (UAVs), focusing on the plants that the Iberian ibex feeds on. The methodology lays the foundations to study diet quality and resource availability for herbivores in remote and inaccessible areas such as the Mediterranean mountains, where traditional sampling methods involve hard legwork.

3. Chapter 1

Ungulates alter plant cover without consistent effect on soil ecosystem functioning

Miguel Ibañez-Alvarez, Elena Baraza, Emmanuel Serrano, Antonia Romero-Munar, Carles Cardona, Jordi Bartolome, Jennifer Adams Krumins.

<https://doi.org/10.1016/j.agee.2021.107796>¹.



¹ The citation in this chapter follows the citation style of the Agriculture, Ecosystem & Environment journal.

Abstract

Shifts in animal husbandry and landscape use have significantly changed ungulate grazing effects on ecosystem functioning. These changes are now the subject of extensive research with respect to plant and soil communities, but the results of these studies are highly varied and context-dependent. This study aims to address contextual variation by holding all sampling methods and analytical approaches constant and analyse the effect of the feral goat (*Capra hircus*) population of Mallorca Island, Spain, on soil physical, chemical and biological characteristics across five controlled sites. Specifically, vegetation cover and soil properties in fenced plots excluded from ungulates were compared with adjacent grazed plots in five independent mountain areas of Mallorca. Soil microbial activity measured as Community-Level Physiological Profiles (CLPP) using EcoPlate™ increased when ungulates were excluded. However, all other physical and chemical measures of the soils did not vary significantly when we considered ungulate exclusion across all plots, and this may be caused by a soil community that is simply robust to the effects of the herbivores. Or, it may be due to the high heterogeneity that was detected among pair plot comparisons within each of the five sites. Indeed, we find more variability within a site than among our independent sites leading us to hypothesise that grazing does influence biogeochemical cycles, but it does it by increasing the variability of the system in general. Our well-controlled multilevel meta-analysis confirms the notion that ungulate effects are highly context-dependent, and soil heterogeneity makes resolving clear patterns very challenging. Apparently, context persistently drives the soil response more than the grazing itself, and this is seen even at very small scales.

Keywords: Soil heterogeneity; Ecosystem services; Microbial activity; Grazing exclusion; Ungulate overabundance

1. Introduction

In recent decades, human land use has changed, and this includes animal husbandry and grazing practices. The changes in grazing practice are causing profound transformation of plant productivity and community composition at landscape level scales (Capó et al., 2021, Peco et al., 2006, Sebastià et al., 2008, Sjödin et al., 2007). Therefore, populations of ungulates, especially domestic livestock but also wild species, have been extensively studied to determine their effects on the composition and functioning of plant (Jia et al., 2018) and soil communities (for recent meta-analysis and synthesis see: Andriuzzi and Wall, 2018; Forbes et al., 2019). However, all of this extensive research seems to reveal more questions than answers. Specifically, we know that herbivory directly affects plant growth and plant community dynamics. Therefore, we would expect to find subsequent effects below ground in the soils. This is because soils are directly connected to the plant community via the rhizosphere and bidirectional plant and soil feedbacks that occur therein (van der Putten et al., 2016). As such, they provide important ecosystem services like decomposition and nutrient cycling that sustains soil productivity and future plant growth (Coleman et al., 2004, Crowther et al., 2019, Roger-Estrade et al., 2010) or even plant resistance to abiotic disturbances and stress (Brussaard et al., 2007). However, a clear connection between ungulate effects above-ground on the plant community and that of the soils below-ground has not been realised. This disconnect may be because soils are highly heterogeneous, and their functioning is subject to multiple and varied environmental drivers (Wall et al., 2012). Therefore, we question the role of environmental heterogeneity to moderate when, or under what conditions ungulates can affect soil functioning.

The influence of diverse animal grazers on the landscape and the soils has been highly mixed and context-dependent. The presence of livestock has been shown to significantly degrade soil in some cases (Gizicki et al., 2018), but it can have positive consequences in other cases (Pulido et al., 2018). Grazing by ungulates in high densities is responsible for a reduction in the organic carbon in the soil by reducing the amounts of necromass that is returned to the soil. However, other studies report significant increases in organic matter due to return via faeces (Peco et al., 2006, Pulido et al., 2018). The variability in organic matter return to the soil may be caused by differences in ungulate feeding activity associated with plant quality and ungulate efficiency (*sensu* Krumins et al., 2015). Logically, shifts in carbon allocation to the soil will directly influence the functioning of microbial communities there. However, the responses of microbes to ungulate grazing, as in other responses, can be quite mixed. Microbial biomass can be reduced by high pressure from herbivores and the destruction of structures such as mycelia or bacterial biofilms (Damacena De Souza et al., 2006), although in other studies it has been observed that it can increase at high grazing intensities (Mohr et al., 2005) or differing conditions (Stark et al., 2002). Effects on the microbial community will cascade to ecosystem services like decomposition. Yet again, this is context-dependent. For instance, when moose were excluded from a plot, decomposition was not affected (Ellis and Leroux, 2017, Kolstad et al., 2018). However, in a different environmental context, decomposition was reduced when moose and hares were excluded (Kielland et al., 1997).

All of these varied responses to herbivory may be a product of the abiotic context of the parent soil and the landscape in which it sits. The return of organic carbon to the soil may be directly impacted when grazed soils have greater bulk density. This can be associated with excessive trampling (Alegre and Lara, 1991) and to the reduction

in some areas of the amount of organic matter which is capable of creating clay aggregates that would maintain more porous soils. The pH can also be affected by modifying the microbial and root activity (Jeddi and Chaieb, 2010), although this effect varies according to the environmental conditions and the type of soil (Bardgett et al., 2001, Noe and Abril, 2013). As is likely the case with respect to this work, trampling and therefore its effects on bulk density may be high when water is limiting and soil organic matter is otherwise low (Reichert et al., 2018).

We do know that ungulates are responsible for regulating biogeochemical cycles, the most notable being the acceleration in the nitrogen and carbon cycle (Fleurance et al., 2011, Patra et al., 2005). It has been shown that ungulates are able to inhibit ecosystem functions like nitrification or ammonification due to the reduced return of nitrogen to the soil and/or the compaction of the soil which consequent decrease in soil moisture (Pan et al., 2018, Xu et al., 2008). Simultaneously, grazing may lead to increased nitrogen losses by leaching or volatilization by removing the vegetation cover and making the soil more susceptible to erosion (Núñez et al., 2010). This can be overcome when the presence of ungulates increases nitrogen mineralization due to the contributions of organic nitrogen with faeces and urine (Frank and Groffman, 1998, Furusawa et al., 2016), but this effect will be spatially dispersed as the animals move through the landscape and will be moderated by local environmental conditions. For instance, xeric soils can be more oxygenated, moderating microbially mediated enzyme activities and nitrogen transformations (Ghiloufi et al., 2018), likely interacting with other physical effects of ungulates to the soil.

As a means to address this conundrum in soil ecology, we exploit an existing ungulate exclusion experiment in which anti-herbivory plots were established from 5 to 20 years ago. The objective of this study is to analyse the differences in physical,

chemical and biological characteristics of the soil between areas without ungulates, feral goats (*Capra hircus*) and free-ranging flocks of sheep (*Ovis aries*), compared to areas under continuous ungulate grazing in five distinct mountainous localities with Mediterranean vegetation in Mallorca, Spain. Specifically, we wanted to know if the variability in grazing upon the soil was greater within each site or among the five individual sites. One strength of this study is that we measured response to the same ungulate across well-known (Table 3.1) and climatically and geographically similar sites while maintaining experimenter identity constant. Given that each site is independent, we expected to see differences among them. However, we wanted to know if the differences all followed the same trend. Our results are relevant locally and globally. This information will help in the analysis of the impacts derived from the variation of ungulate populations that many rural areas suffer. However, they are also globally relevant because they help to inform what environmental conditions determine the impact of the ungulates on the soil more broadly.

Table 3. 1. Study site characteristics in Majorca Mountains: type of habitat, soil texture classification, mean elevation, annual mean temperature, Net Primary Production (NPP). The Time of exclusion indicates the approximate years of ungulates exclusion establishment until the data collection, and Design indicates the number of fenced areas with respect to the number of plots inside each fenced area.

Site	Habitat	Textural Soil Class	Elevation (m asl)	T° ^a	NPP kgC/m ² /yr ^b	Time of exclusion	Design
Binifaldó	Forest	Clay	626	13.3°C	1.398	>15	1/2
Sobremunt	Forest	Loam	663	13.9°C	1.303	>20	1/3
Son Moragues	Forest	Loam	522	13.8°C	1.401	>15	3/1
La Victoria	Scrubland	Silty clay	97	17.2°C	1.232	5	1/3
Na Burguesa	Scrubland	Silt loam	479	15.5°C	1.298	>20	3/1

Chapter 1

a Climatological data are from Climatologies at High Resolution for the Earth Land Surface Areas, project CHELSA (Karger et al., 2017).

b Net Primary Production Gap-Filled Yearly L4 Global 500 m SIN Grid (MOD17A3HGF v006) (Running and Zhao, 2019).

2. Materials and methods

2.1. Study sites

We address the role of ungulate grazers on soil factors across five independent sites in the mountainous region on the Island of Mallorca, Spain (Figure 3. 1). Steep slopes predominate the sites, and the soil is generally shallow with limestone outcropping (See Table 3. 1). The climate is Mediterranean and ranges from humid to semiarid subtypes along the topographical gradients. The study sites were named according to the toponym where they are located (Figure 3. 1).

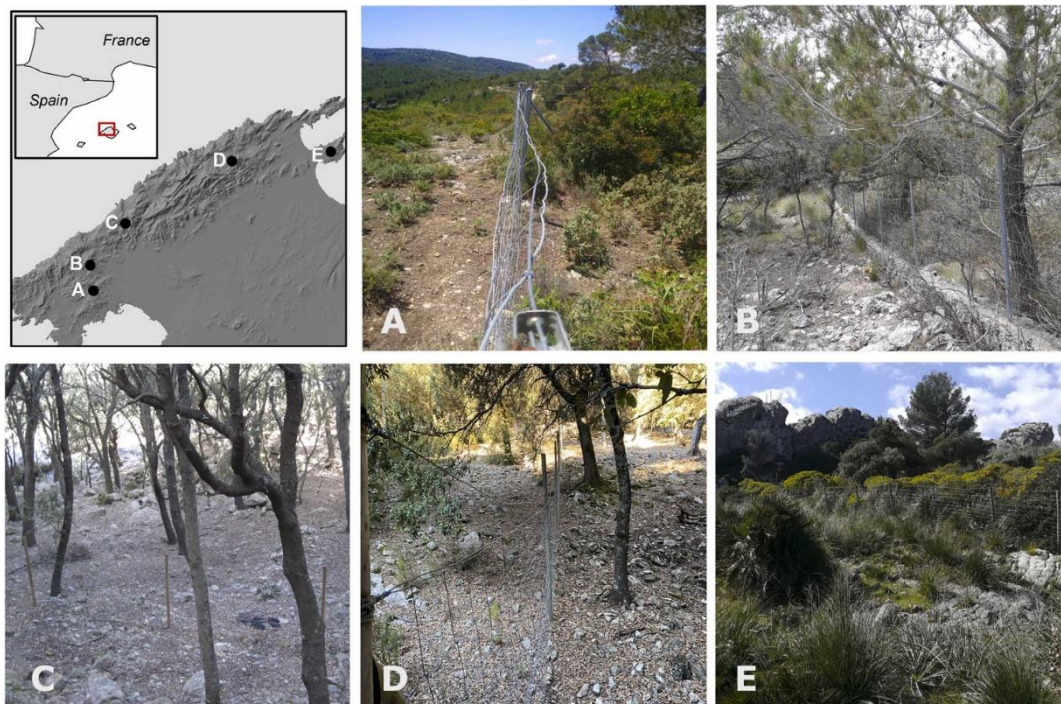


Figure 3. 1. The first slot indicates the geographical location of the study sites. The rest of the slots show photographic details of the habitats for the fenced study sites. A (Na Burguesa) and E (La Victoria) represent scrubland. The forest areas are related to the letters B (Sobremunt), C (Son Moragues) and D (Binifaldó).

All five study sites are located in natural areas with pre-established herbivore exclusion plots. There are two types of habitats between the study sites, holm oak forest and Mediterranean scrubland. Holm oak forest was formed by *Quercus ilex* as the only tree species at Son Moragues, with some pines (*Pinus halepensis*) at Binifaldo or some Strawberry trees (*Arbutus unedo*) and pines at Sobreamunt. In the scrubland areas, La Victoria is dominated by the large tussock grass *Ampelodesmos mauritanica* meanwhile at Na Burguesa predominate the perennial grass *Brachypodium retusum* with *Cistus* sp. scrubs. Within each of the five areas there is at least one fenced ungulate enclosure. Each site allows for two treatments, ungulate herbivore presence (Ungulate) or exclusion (Ungulate-free). Each area has a different size and age of exclusions (Table 3.1), depending on the history of the site, some are designed as a large exclusion that include several study plots within, while in other sites there were multiple small exclusions, including only one plot within each. Outside of the enclosures, in all sites, feral goats (*Capra aegagrus hircus*) graze freely, and in Son Moragues and Binifaldo, domestic sheep herds occasionally graze with the goats. To assess herbivory effects at each site, we established Ungulate/Ungulate-free paired sampling plots for a binary comparison (Table 3.1).

2.2. Sampling protocol

In each study site, we established three 10 × 10 m plots for each treatment, except in Binifaldó, where only two plots per treatment could be established (28 plots in total). Each of these plots within the ungulate excluded zone was compared with a plot in the open zone that was as close as possible (but always >1 m from the fence). We conducted a vegetation survey in all plots using the point intercept technique (Elzinga et al., 1998), in which we measured vegetation and plant species (excluding trees higher than 1.5 m) at 25 m intervals. We measure the percent vegetation cover as the

relative number of points that are vegetated or bare ground. Due to the complexity of the vegetation structure, sometimes multiple individuals of different species occurred at the same point intersection. Therefore, we measure vegetation complexity as the relative number of points that support multiple different species (vertically through the point). We exclude trees higher than 1.5 m because they are not likely relevant to ungulate herbivory in this system.

Within each plot, we randomly established three 0.01 m² sampling frames (84 samples in total) to collect the litter layer and two bulk soil samples. In the laboratory, the litter was oven dried (24 h at 105 °C) and weighed, and the bulk soil samples were stored at 4 °C before further analysis. We used 200 gr of dry, 2 mm sieved soil for chemical analysis. All analyses were performed by Eurofins Laboratories Ltd., Lleida, Spain for the following parameters: pH, electrical conductivity, C (elemental carbon), organic matter content, N (elemental nitrogen) and five soil textural classes (fine sand, coarse sand, fine silt, coarse silt and clay). The C:N ratio was also calculated.

We used the excavation method described in (Blake and Hartge, 1986) to measure the bulk soil density due to the stony nature of the sites (Capó-Bauçà et al., 2019). This procedure included digging a 10 cm³ hole by using the same square frame and a gardening shovel. The volume of the excavation was determined by lining the hole with plastic film and filling it completely with a measured volume of water. Coarse fragments (diameter > 2 mm) were sieved out and bulk density was calculated as the mass of dry, coarse fragment-free soil per volume of the excavated soil, where volume was also calculated on a coarse fragment-free basis. We were not able to assess soil bulk density at Sobremunt since the soil nature is too rocky and there is insufficient depth to extract samples.

2.3. Soil microbial community profiling

We measured the functional diversity of the microbial community in soil with the community-level physiological profiles method (CLPP) (Garland and Mills, 1991) using Biolog EcoPlates™ (Biolog Inc., Hayward, California, USA). EcoPlates contain 31 distinct carbon sources in triplicate as well a colour dye that turns purple if a given carbon source is metabolised by the microbial community present in the well. Following the colour development over time allows one to estimate the rate of carbon source utilisation in addition to which carbon sources were used.

To prepare a microbial inoculum from each soil, we diluted 5gr. sub-samples of fine soil in saline (45 ml, 0.9% NaCl) then centrifuged for 10 min at 2,400rpm. The microbial suspension was left to stand for 30 min at 4 °C then the sub-samples were again diluted 1:100 in saline before inoculation into the EcoPlates at the rate of with 100 µL of sample in each well. We incubated the EcoPlates in the dark at a constant 25 °C and measured optical density (OD) at 590 nm with a plate reader every 12 h for up to 96 h plus an additional reading at 160 h. We scored a carbon source as positive when two out of three wells reached an OD of at least 0.2 after subtraction of the median blank from all wells. We modelled the colour development in each well that we scored as positive with a modified Gompertz equation (Zwietering et al., 1990).

We used the R script and nlsLM function of the package “minpack.lm” 1.2–1 version (Elzhov et al., 2016) to fit the Gompertz function (Roger et al., 2016). The function is a sigmoidal curve describing microbial community growth and is determined by 3 parameters, lag phase (l), maximum uptake rate (r) and maximum population growth (k) (Kahm et al., 2010). Functional diversity was calculated considering each carbon source as a community trait, and the maximum uptake rate (r) of the carbon source was taken as trait value. We weighed all carbon sources by their uptake rate and

calculated the diversity of the community according to the Shannon Index using the diversity function in the vegan package (Oksanen et al., 2019).

The average well colour development (AWCD) parameter represents the metabolic capacity of the soil microorganisms grown in the EcoPlates. AWCD was derived from the mean difference among OD values of the wells following (Garland and Mills, 1991) formula: $AWCD = \sum (C_i - R) / 31$ where C_i is the optical density of the substrate i , R is the optical density of the control wells and 31 is the number of different carbon sources of each well (in triplicate). An AWCD value is generated for each reading increment, and we then select the time increment in which maximum AWCD value occurs to assess soil metabolic capacity.

2.4. Organic matter decomposition

We assessed ungulate effects on soil biological activity by calculating the organic matter degradation rate on standard plant material following the Tea Bag Index (TBI) method of (Keuskamp et al., 2013). The tea bags were labelled with a waterproof marker, oven dried at 70°C for 48 h and weighed (+/- 0.01 g). Subsequently, three replicates of each tea type were buried in each plot in 8-cm deep separate holes of recorded location (a total of 84 sample units). Sample burial was carried out between March 26th to March 29th, 2018, and they were retrieved 90 days later. Post recovery, bags were cleaned of roots and debris, dried and weighed. According to the weight loss, we calculated the TBI parameters: S (stabilisation factor) and k (decomposition rate constant). Green tea has a very labile fraction that has a rapid initial decomposition rate. After 90 days we were able to determine how much of the labile fraction of the material is decomposed (k) and how much is stabilised (S). Rooibos tea decomposes much more slowly. After 90 days, it is still in the first phase of decomposition. Thereby, the weight loss of rooibos tea is a proxy of the initial

decomposition rate (k). TBI parameters were calculated using the spreadsheet template provided by TBI research team in the website <http://www.teatime4science.org>.

2.5. Statistical analysis

Data from the vegetation transects were analysed using mixed regression models considering the treatment (Herbivory Yes or No) as a fixed factor and plot nested in site as a random intercept term. The data fulfilled the assumptions of normality and homoscedasticity. The mixed effect models were conducted in the nlme package 3.1–152 (Pinheiro et al., 2021) in R (R Core Team, 2020).

We detected very high heterogeneity in soil characteristic data including many outliers and significant differences among plots within the same study area. Furthermore, when the sample size is small or the intensity of an effect is low (as was the case in our study), an alternative to control for Type II statistical error is the meta-analysis (Arnquist and Wooster 1995). Following the criteria established by Gómez-Aparicio et al. (2004), the effect of ungulate exclusion (ungulate versus ungulate-free) on soil physicochemical and biological characteristics was analysed using a meta-analysis. We performed a three level meta-analysis to address variation across paired plots while also accounting for the dependency of the ungulate exclusion effects within study sites. Each paired plot was considered as an individual study and weighed according to its robustness to assess the overall effect of herbivory exclusion on soil properties.

In order to structure the multilevel meta-analysis workflow, we compute the effect size and variance for each set of paired plots within each individual study in the context of response ratios described in (Hedges et al., 1999). Summary statistics (mean (μ), standard deviation (sd) and sample size (n)) for each response variable

were reported to determine the weighted effect size for each plot. The effect size of ungulate exclusion on the response variables was calculated as $\ln(\mu_{\text{ungulate-free}} / \mu_{\text{ungulate}})$, hereafter referred to as the log response ratio, $\ln(\text{RR})$ (Hedges et al., 1999). The $\ln(\text{RR})$ quantifies the proportional change that results from herbivore exclusion and is appropriate given that the absolute value in the response variables varied widely among and within sites (Goldberg et al., 1999, Hedges et al., 1999). Negative values of $\ln(\text{RR})$ indicate that the exclusion of ungulates decreases the response variable, so ungulates presence increases it. The overall $\ln(\text{RR})$ was back-transformed and converted to a percentage of change for ease of interpretation.

The response ratios were weighted with the inverse sample variance to ensure a greater contribution of the most robust studies (Rosenberg et al., 2000), therefore, we estimate the variances associated with the response ratio (Hedges et al., 1999) as:

$$V_{\ln(\text{RR})} = \frac{SD_{\text{ungrazed}}^2}{n_{\text{ungrazed}}(X_{\text{ungrazed}})^2} + \frac{SD_{\text{grazed}}^2}{n_{\text{grazed}}(X_{\text{grazed}})^2}$$

We assessed the consistency of the $\ln(\text{RR})$ across studies for each response variable by fitting a three-level meta-analytic model. For this purpose, we use the `rma.mv` function of the `metafor` (Viechtbauer, 2010) package in R, by running the syntax:

```
rma.mv (data, yi, V, random = ~1/site/plot)
```

Data is the dataset containing the summary statistics of each variable; y_i is the effect size Ungulate-free, and V is the sampling variance. Random argument specifies the random-effect structure of the model. In three level meta-analysis, the heterogeneity is distributed between the sampling variance ($I_{\text{Level } 1}^2$), the variance within plots ($I_{\text{Level } 2}^2$) and between site ($I_{\text{Level } 3}^2$). We used the `var.comp` function in the `dmatar` package (Harrer et al., 2019) in R to calculate the multilevel variance I^2 . The

heterogeneity variation between plots and/or sites can be regarded as substantial if less than 75% of the total amount of variance is attributed to sampling variance ($I_{Level\ 1}^2$) (Hunter et al., 1991). When that occurred, we performed a test of moderators by introducing in the model the covariates: elevation, Net Primary Production (NPP), temperature, soil textural classes (summarized with the first component of a Principal Component Analysis with the five texture components) and the categorical covariate of habitat, which may explain the observed heterogeneity. We derived the mean effect of each moderator with the 95% CI and the results of the omnibus test under the test of moderators (Table SM 3. 1, supplementary material). If the p-value associated with the test of moderators Q_M is larger than the significant level of 0.05 we concluded that the overall effect is not moderated by the covariates included (Viechtbauer, 2010).

With respect to the CLPP, we also used a multivariate approach to summarise the data. We first calculated normalized Biolog absorbance of each substrate after 96h of incubation by dividing the mean value of absorbance of the three wells per substrate by the AWCD value of each plate. With these values we conducted a PCA with 'prcomp' function in base R, comparing the carbon source utilization patterns of soil microbial communities with respect to the presence or absence of ungulates (Capó-Bauçà et al., 2019).

3. Results

3.1. Vegetation response to ungulate exclusion

The exclusion of ungulate herbivores generates significant changes in vegetation cover. In the absence of ungulates, vegetation cover and complexity (% coverage with several layers of vegetation) increased significantly (Table 3.2). Likewise, the percent cover of bare soil decreased with the absence of ungulates (Table 3.2).

Table 3. 2. Ungulate exclusion effects on the percentage of bare soil, total vegetation cover and percentage of cover with multiple different species (complexity) as analysed by a mixed general lineal model GLMM.

Plant Cover	Herbivory (mean±SE)	Herbivore-free (mean±SE)	GLMM
Bare soil	46.12±10.11	26.63±9.58	$F_{(13)}=16.14$; $P=0.0015$
Cover	45.52±11.07	62.58±19.95	$F_{(13)}=10.73$; $P=0.0060$
Complexity	17.75±6.29	32.80±8.92	$F_{(13)}=5.22$; $P=0.0398$

3.2. Soil response to ungulate exclusion

For 11 of the 12 variables examined, the CI of the mean effect size overlapped zero (Table 3.3, Figure 3.2). Soil microbes were more active in ungulates excluded plots, since the activity of microbial communities measured by CLPP with EcoPlates, changed significantly (Table 3.3) with higher activity (AWCD) in the absence of ungulates (Figure. 3.2; Table 3.3). All physicochemical parameters measured (BD, Electric conductivity, elemental carbon, soil organic matter, elemental nitrogen, C/N ratio and pH), microbial functional diversity (H) and OM decomposition measured by TBI did not significantly change with ungulates exclusion (Table 3.3). For these soil characteristics, effect size varied from negative to positive across paired plot comparisons inside the same studied area (Figure 3.2, Figure SM 3.1). Forest diagrams representing the estimate of the variance between studies show no consistent effect inside the same area (Figure 3.2, Figure SM 3.2).

Table 3. 3. Statistical results of the overall effects of ungulate exclusion over the response variables analysed by multi-level meta-analytic models. In the first column, a global increase on the studied variable was indicated by \uparrow whereas a decrease was indicated by \downarrow . The p-value of the fitted model is outlined in bold when the effect is statistically significant. LnRR (95% CI) indicates the effect size of the ungulate exclusion and is also shown as a percentage of response (inverse transformation of the logarithm) to facilitate interpretation. N^o indicates the number of pair plot comparisons. The test of heterogeneity Q-test shows significant variation between all effect sizes when p-value < 0.005. The variance is distributed across the sampling variance (*I*Level 12), variance within plots (*I*Level 22), and between site/plot (*I*Level 32)

Variable	p- value	LnRR (95% CI) % Response	N ^o	Q-test (p-value)	I^2_{Level1} I^2_{Level2} I^2_{Level3}
Bulk density \downarrow	0.093	-0.11(-0.23,0.02) -10.0	11	< 0.001	14.47 85.52 0
Litter \uparrow	0.213	0.22(-0.14,0.58) 24.6	14	< 0.001	7.16 92.84 0
Electrical conductivity \uparrow	0.194	0.11(-0.07,0.29) 12.1	14	< 0.001	52.97 47.03 0
Elemental Carbon \uparrow	0.278	0.12(-0.111,0.35) 13.0	14	< 0.001	39.17 60.83 0
Organic Matter \uparrow	0.304	0.13(-0.14,0.40) 14.3	14	< 0.001	15.62 69.17 15.21
Elemental Nitrogen \uparrow	0.152	0.16(-0.07,0.38) 16.9	14	< 0.001	31.57 54.88 13.55
pH \uparrow	0.580	0.01(-0.02,0.03) 0.5	14	< 0.001	100 0 0
C/N \downarrow	0.349	0.03(-0.09,0.03) -2.7	14	< 0.001	31.61 68.39 0
AWCD \uparrow	0.008	0.25(0.08,0.43) 28.9	14	< 0.001	10.03 89.97 0
Shannon (H') \uparrow	0.099	0.13(-0.03,0.28) 13.4	14	0.042	10.13 89.87 0
Stabilization factor (S) \uparrow	0.820	0.01(-0.08,0.10) 1.0	13	< 0.001	34.42 65.58 0
Decomposed rate (k) \uparrow	0.892	0.02(-0.25,0.28) 1.6	8	0.657	10.84 84.81 4.35

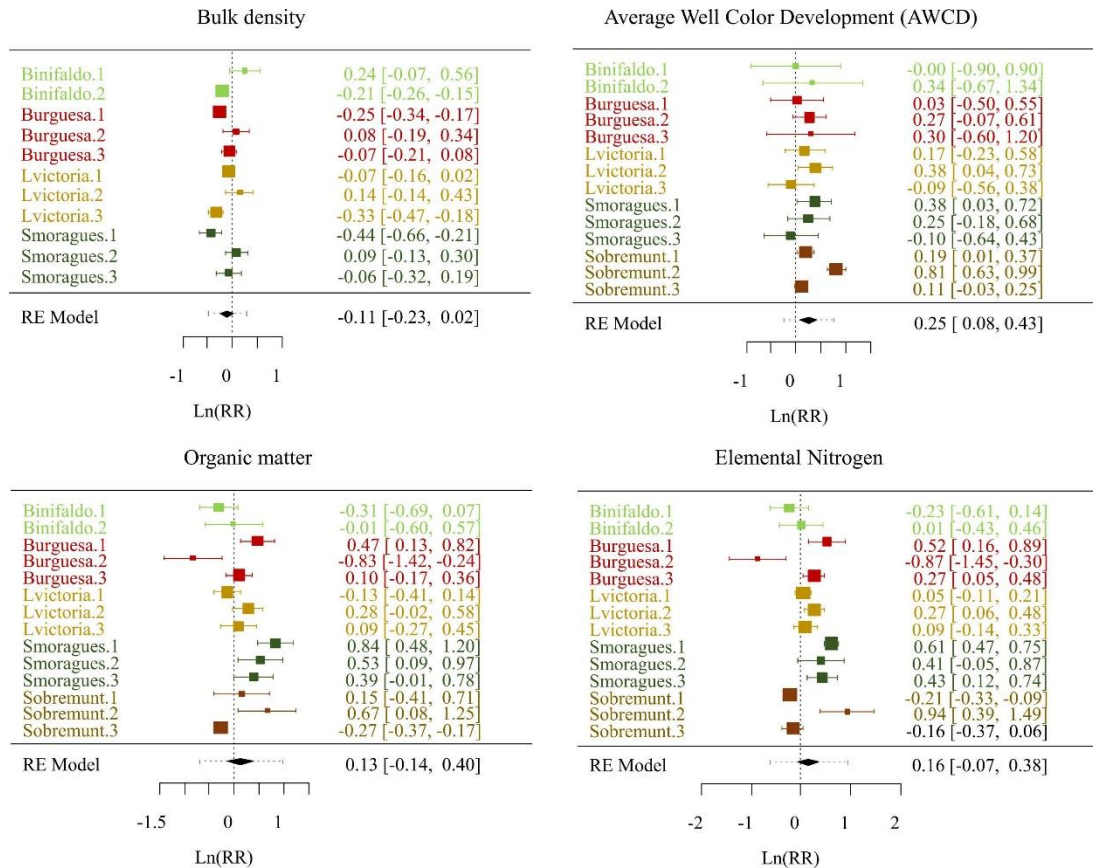


Figure 3. 2. Forest plot of the effect of the herbivory on four key response variables (Bulk density, AWCD, organic matter and soil organic nitrogen content). In each plot, the names on the left identify the individual plots in each of the five study areas. The boxes represent the $\ln(\text{RR})$ of the individual studies, and the horizontal lines their 95% confidence intervals. The size of the boxes expresses the weight (see methods) of each study in the total effect, which is represented by a diamond. Response rates less than zero (vertical dotted line) indicate a negative effect of ungulate exclusion, while values greater than zero indicate a positive effect. If the diamond does not cross the zero line, the overall effect is significant. For a full list of comparisons see Table 3.3 or Table MS 3.1.

In fact, for all the variables, less than 75% of the total amount of variance is attributed to sampling variance ($I_{Level 1}^2$), and the % of variance within plots ($I_{Level 2}^2$) is the highest in all cases. (Table 3.3). However, this could not be explained by geographic factors or even environmental characteristics because meta-regressions showed no significant influence of elevation, NPP, temperature, soil textural classes on the effect sizes within each site (Table MS 3.1). Only the habitat covariate had a marginal

significant effect on the effect size of elemental nitrogen and stabilization factor (S) variables (Table MS 3.1).

With respect to the carbon source utilisation patterns of soil microbial communities, the PCA of the absorbance of all the available substrates in the EcoPlates™ read at 96 h shows no clear variation between ungulate and ungulate-free treatments (Figure SM 3. 2).

4. Discussion

Apparently, local environmental heterogeneity may be a more critical driver of soil ecosystem properties than the effects of ungulate herbivory and subsequent shifts in plant community composition and productivity. These are the findings in a mountainous Mediterranean ecosystem (Mallorca, Spain), but they also inform the broader literature that often finds context dependent and idiosyncratic responses of soils to herbivory (Andriuzzi and Wall, 2018, Forbes et al., 2019, Vermeire et al., 2021). In this experiment, we compared the effects of ungulate exclusions on the above ground vegetation but also on the physical, chemical and bacteriological characteristics of soils. As expected, excluding the ungulates, significantly affected understory vegetation (cover and complexity). However, this was not realised belowground where there were very few meaningful changes to the soil structure, chemistry and biology. We suspect that our results are due to two possible explanations. First, the abiotic and microbiological properties of the soil but not aboveground vegetation were robust to the effects of grazing. This would be in agreement with previous works such as that of Greenwood et al. (1997) where they conclude that soil physical properties appear to be relatively insensitive to stocking rate in the long term. In fact, as Vermeire et al. (2021) suggested, we can expect

relatively small changes in microbial communities due to natural disturbance when soil microbial communities have evolved with disturbance. In our case, microorganisms in the Mediterranean basin have adapted to soils with little availability of water (Yuste et al., 2014) making them resistant to change. And second, we assume that the environmental heterogeneity of the different plots clouds our ability to see consistent effects of ungulate grazing exclusion. In fact, herbivores may even increase this heterogeneity by trampling some areas, defecating in other and consuming vegetation in patches (Eldridge et al., 2019, Zhang et al., 2020). Moreover, it is likely both, as these two hypotheses are not mutually exclusive.

Here, we attempt to tackle heterogeneity and variability of environmental factors across different experimental sites with a three-level meta-analysis in which each of the comparisons among plots was treated as a study dealing with the dependency of the effect sizes within sites. Across our sites, ungulate exclusion had no effect on belowground soil processes and ecosystem functioning such as: decomposition, mineralisation, C/N ratio or nutrient stock. Therefore, we have assumed that other factors controlling the biochemical activity of soil are likely more impactful than ungulate grazers. In reality however, our meta-analysis reveals no consistent driver of soil characteristics in this system but high heterogeneity between plots. Many of the environmental parameters of the soil were highly variable and did not obviously respond to the impacts of ungulates in spite of changes to the vegetation. For instance, the comparison of one pair of plots can result in an important increase of soil organic matter, nitrogen and pH when ungulates are excluded while other pair plot comparisons showed the contrary effect (Figure 3.2, Figure SM 3.1).

Our results here, and those of Ellis and Leroux (2017), found that decomposition rate k of standardised litter was not affected by ungulate exclusion. However, this is in

contrast to Kielland et al. (1997) who found a decrease in decomposition rate of standardised litter (cellulose) inside herbivore exclusion fences in the Alaskan Taiga. But also, Cárdenas et al. (2012) demonstrated that herbivory accelerates the decomposition of organic matter in a neotropical cloud forest. Similarly, we found higher nitrogen concentrations in eight of the twelve ungulate exclusion comparisons (Figure 3.2d). That is, in our study, ungulates reduced soil nitrogen content. This was expected since ungulates have a preference for plants rich in N, and it is documented that their increase is related to a decrease in soil N (Pastor and Naiman, 1992). Similar responses have been observed with *Cervus elaphus* (Bardgett et al., 2001, Donkor et al., 2002, Gass and Binkley, 2011, Kumbasli et al., 2010). However, the relationship of both N and C concentration to ungulate exclusion is mixed but often neutral among our sampling sites with effect size very close to 0 in most of the cases (Figure SM 3.1). No change in the soil C/N ratio is frequently reported in herbivore exclusion studies (Gass and Binkley, 2011, Harrison and Bardgett, 2004, Stark et al., 2010, Wardle et al., 2001).

Although there were few consistent effects of excluding ungulates upon soil properties, the capacity of the microbial communities to metabolise diverse carbon sources increased. The AWCD of the EcoPlates was significantly higher in soils that were excluded from the ungulates. This did not coincide with an increase on soil bacterial functional diversity, but it did coincide with a general decrease in the bulk density of the soil. This result follows the findings of other works with domestic goats by Holdaway (2014), with feral goat and deer by Kardol et al. (2014) and with moose by Gass and Binkley (2011) reporting that ungulate trampling produces soil compaction and may limit microbial activity.

In summary, when all of our five study sites were analysed, we find significant effects of ungulate grazing on vegetation cover but few significant effects on soil properties. Indeed, our lack of statistical significance is due to within plot variability that is greater than the variability between treatments or among sites. We propose the hypothesis that grazing does influence biogeochemical cycles, but it does it by increasing variability of the system in general. This is a testable hypothesis, and we propose that a study of ecosystem stability as opposed to static measures of ecosystem functions may be a more useful metric to study the effects of herbivory and its changing patterns with respect to the landscape. For instance, repeated measures of soil respiration, with respect to variable grazing intensity, would reveal the stability of soil functioning under herbivores. Regardless, increased sampling will always be needed, and even a cross-study meta-analysis has revealed similar clouded results with respect to soil (Andriuzzi and Wall, 2018). Apparently, the spatial variation in the soil biotic and abiotic conditions was so great that our sampling effort was insufficient. This is supported by the high heterogeneity of results among comparison plots inside the same site (Figure 3.2) indicating that most of the variation is at an even smaller spatial scale than site (that is, between plots). A primary goal of this project was to control for methodological differences such that we could resolve the role of ecosystem context (Forbes et al., 2019). In practice, we achieved methodological control. However, apparently variability of an ecosystem is more important than the direct effects of ungulate grazers on the soil.

5. Conclusions

The last century has seen a profound transition in ungulate land use and herd management globally. The outcome of this is major shifts in plant community

dynamics and the distribution of grassland and forested ecosystems. The implications of this span conservation, ecosystem stability and carbon sequestration. The results of our three-level meta-analysis studying 14 ungulate exclosure experiments reveals that although plant communities are directly affected by ungulate activity, apparently, the effects are not consistently realised belowground in the soil. Therefore, we assume that, soil environmental heterogeneity dilutes grazing effects, and this is realised even at very small scales (<10 m). Variability in the soil response to ungulates was greater within each of our experimental plots than among the five sites. This finding is important because soil community processes drive plant community dynamics and ultimately, ecosystem functioning (van der Putten et al., 2016). Our research findings inform a deeper understanding of the role of ungulates in terrestrial ecosystems. However, the spatial and temporal scale at which ungulates affect soil may be difficult to capture in experiments and a challenge for herders and land managers. On the other hand, the impact of ungulate on soil integrity might be different in more homogenous biomes with a lower micro-landscape complexity and more homogeneous vegetation cover.

6. References

- Alegre, J.C., Lara, P.D., 1991. Efecto de los animales en pastoreo sobre las propiedades físicas de suelos de la región tropical húmeda de Perú. *Pasturas Trop.* 13(1), 18–23.
- Andriuzzi, W.S., Wall, D.H., 2018. Soil biological responses to, and feedbacks on, trophic rewilding. *Philos. Trans. R. Soc. B Biol. Sci.* <https://doi.org/10.1098/rstb.2017.0448>

Chapter 1

- Bardgett, R.D., Jones, A.C., Jones, D.L., Kemmitt, S.J., Cook, R., Hobbs, P.J., 2001. Soil microbial community patterns related to the history and intensity of grazing in sub-montane ecosystems. *Soil Biol. Biochem.* 33, 1653–1664. [https://doi.org/10.1016/S0038-0717\(01\)00086-4](https://doi.org/10.1016/S0038-0717(01)00086-4)
- Blake, G.R., Hartge, K.H., 1986. Particle Density, in: *Methods of Soil Analysis: Part 1 Physical and Mineralogical Methods.* pp. 377–382. <https://doi.org/10.2136/sssabookser5.1.2ed.c14>
- Brussaard, L., de Ruiter, P.C., Brown, G.G., 2007. Soil biodiversity for agricultural sustainability. *Agric. Ecosyst. Environ.* 121, 233–244. <https://doi.org/10.1016/j.agee.2006.12.013>
- Capó-Bauçà, S., Marqués, A., Llopis-Vidal, N., Bota, J., Baraza, E., 2019. Long-term establishment of natural green cover provides agroecosystem services by improving soil quality in a Mediterranean vineyard. *Ecol. Eng.* 127, 285–291. <https://doi.org/10.1016/j.ecoleng.2018.12.008>
- Capó, M., Engelbrecht, C., Cardona, C., Castells, E., Bartolomé, J., Ramoneda, M., Baraza, E., 2021. Mildly toxic shrubs as indicators of goats herbivory give information for the management of natural landscapes on Mediterranean islands. *Sci. Total Environ.* 786, 147391. <https://doi.org/10.1016/J.SCITOTENV.2021.147391>
- Cárdenas, R.E., Dangles, O., 2012. Do canopy herbivores mechanically facilitate subsequent litter decomposition in soil? A pilot study from a Neotropical cloud forest. *Ecol. Res.* 2012 275 27, 975–981. <https://doi.org/10.1007/S11284-012-0979-8>

- Coleman, M.D., Isebrands, J.G., Tolsted, D.N., Tolbert, V.R., 2004. Comparing soil carbon of short rotation poplar plantations with agricultural crops and woodlots in North Central United States. *Environ. Manage.* 33. <https://doi.org/10.1007/s00267-003-9139-9>
- Crowther, T.W., Riggs, C., Lind, E.M., Borer, E.T., Seabloom, E.W., Hobbie, S.E., Wubs, J., Adler, P.B., Firn, J., Gherardi, L., Hagenah, N., Hofmockel, K.S., Knops, J.M.H., McCulley, R.L., MacDougall, A.S., Peri, P.L., Prober, S.M., Stevens, C.J., Routh, D., 2019. Sensitivity of global soil carbon stocks to combined nutrient enrichment. *Ecol. Lett.* 22, 936–945. <https://doi.org/10.1111/ele.13258>
- Damacena De Souza, E., Aurélio, M., Carneiro, C., Barbosa Paulino, H., Silva, C.A., Buzetti, S., 2006. Frações do carbono orgânico, biomassa e atividade microbiana em um Latossolo Vermelho sob cerrado submetido a diferentes sistemas de manejos e usos do solo. *Acta Sci. Agron.* 28, 323–329.
- Donkor, N.T., Gedir, J. V., Hudson, R.J., Bork, E.W., Chanasyk, D.S., Naeth, M.A., 2002. Impacts of grazing systems on soil compaction and pasture production in Alberta. *Can. J. Soil Sci.* 82, 1–8. <https://doi.org/10.4141/S01-008>
- Eldridge, D.J., Travers, S.K., Val, J., Wang, J.T., Liu, H., Singh, B.K., Delgado-Baquerizo, M., 2019. Grazing Regulates the Spatial Heterogeneity of Soil Microbial Communities Within Ecological Networks. *Ecosystems.* <https://doi.org/10.1007/s10021-019-00448-9>
- Ellis, N.M., Leroux, S.J., 2017. Moose directly slow plant regeneration but have limited indirect effects on soil stoichiometry and litter decomposition rates in

disturbed maritime boreal forests. *Funct. Ecol.* 31, 790–801.
<https://doi.org/10.1111/1365-2435.12785>

Elzhov, T., Mullen, K., Spiess, A., Bolker, B., 2016. Package “minpack. lm.”
<https://Cran.R-Project.Org/Web/Packages/Minpack.Lm/Minpack.Lm.Pdf>.

Elzinga, C.L., Salzer, D.W., Willoughby, J.W., 1998. Measuring and monitoring plant populations. Denver, CO.

Fleurance, G., Duncan, P., Farruggia, A., Dumont, B., Lecomte, T., 2011. Impact of equine pasture land on the diversity of fauna and flora in grazing lands. *Fourrages* 207, 189–199.

Forbes, E.S., Cushman, J.H., Young, T.P., Klope, M., Young, H.S., 2019. Synthesizing the effects of large, wild herbivore exclusion on ecosystem function 1597–1610. <https://doi.org/10.1111/1365-2435.13376>

Frank, D.A., Groffman, P.M., 1998. Ungulate vs. Landscape Control of Soil C and N Processes in Grasslands of Yellowstone National Park. *Ecology* 79, 2229.
<https://doi.org/10.2307/176818>

Furusawa, H., Hino, T., Takahashi, H., Kaneko, S., 2016. Nitrogen leaching from surface soil in a temperate mixed forest subject to intensive deer grazing. *Landsc. Ecol. Eng.* 12, 223–230. <https://doi.org/10.1007/s11355-016-0296-4>

Garland, J.L., Mills, A.L., 1991. Classification and characterization of heterotrophic microbial communities on the basis of patterns of community-level sole-carbon-source utilization. *Appl. Environ. Microbiol.* 57, 2351–2359.
<https://doi.org/10.1128/aem.57.8.2351-2359.1991>

- Gass, T.M., Binkley, D., 2011. Soil nutrient losses in an altered ecosystem are associated with native ungulate grazing. *J. Appl. Ecol.* 48, 952–960. <https://doi.org/10.1111/j.1365-2664.2011.01996.x>
- Ghiloufi, W., Seo, J., Kim, J., Chaieb, M., Kang, H., 2018. Effects of Biological Soil Crusts on Enzyme Activities and Microbial Community in Soils of an Arid Ecosystem. *Microb. Ecol.* 2018 771 77, 201–216. <https://doi.org/10.1007/S00248-018-1219-8>
- Gizicki, Z. S., Tamez, V., Galanopoulou, A. P., Avramidis, P., Foufopoulos, J., 2018. Long-term effects of feral goats (*Capra hircus*) on Mediterranean island communities: results from whole island manipulations. *Biol. Invasions*, 20(6), 1537-1552. <https://doi.org/10.1007/s10530-017-1645-4>
- Goldberg, D.E., Rajaniemi, T., Gurevitch, J., Stewart-Oaten, A., 1999. Empirical approaches to quantifying interaction intensity: competition and facilitation along productivity gradients, *Special Feature Ecology*. John Wiley & Sons, Ltd. [https://doi.org/10.1890/0012-9658\(1999\)080\[1118:EATQII\]2.0.CO;2](https://doi.org/10.1890/0012-9658(1999)080[1118:EATQII]2.0.CO;2)
- Gómez-Aparicio, L., Zamora, R., Gómez, J.M., Hódar, J.A., Castro, J., Baraza, E., 2004. Applying plant facilitation to forest restoration: a meta-analysis of the use of shrubs as nurse plants. *Ecol. Appl.* 14, 1128–1138. <https://doi.org/10.1890/03-5084>
- Greenwood, K.L., MacLeod, D.A., Hutchinson, K.J., 1997. Long-term stocking rate effects on soil physical properties. *Aust. J. Exp. Agric.* 37, 413–419. <https://doi.org/10.1071/EA96131>

- Harrer, M., Cuijpers, P., Furukawa, T., Ebert, D.D., 2019. dmetar: Companion R Package For The Guide “Doing Meta-Analysis in R”. R package version 0.0.9000. URL <http://dmetar.protectlab.org/>.
- Harrison, K.A., Bardgett, R.D., 2004. Browsing by red deer negatively impacts on soil nitrogen availability in regenerating native forest. *Soil Biol. Biochem.* 36, 115–126. <https://doi.org/10.1016/j.soilbio.2003.08.022>
- Hedges, L. V, Gurevitch, J., Curtis, P.S., 1999. THE META-ANALYSIS OF RESPONSE RATIOS IN EXPERIMENTAL ECOLOGY, Special Feature Ecology.
- Holdaway, R., 2014. Footprint pressures and locomotion of moas and ungulates and their effects on the New Zealand indigenous biota through trampling.
- Hunter, J.E., Raudenbush, S.W., Schmidt, F.L., 1991. Methods of Meta-Analysis: Correcting Error and Bias in Research Findings. *J. Am. Stat. Assoc.* 86, 242. <https://doi.org/10.2307/2289738>
- Jeddi, K., Chaieb, M., 2010. Changes in soil properties and vegetation following livestock grazing exclusion in degraded arid environments of South Tunisia. *Flora Morphol. Distrib. Funct. Ecol. Plants* 205, 184–189. <https://doi.org/10.1016/j.flora.2009.03.002>
- Jia, S., Wang, X., Yuan, Z., Lin, F., Ye, J., Hao, Z., Luskin, M.S., 2018. Global signal of top-down control of terrestrial plant communities by herbivores. *Proc. Natl. Acad. Sci. U. S. A.* 115, 6237–6242. <https://doi.org/10.1073/pnas.1707984115>
- Kahm, M., Hasenbrink, G., Lichtenberg-Fraté, H., Ludwig, J., Kschischo, M., 2010. Grofit: Fitting biological growth curves with R. *J. Stat. Softw.* 33, 1–21. <https://doi.org/10.18637/jss.v033.i07>

- Kardol, P., Dickie, I.A., St. John, M.G., Husheer, S.W., Bonner, K.I., Bellingham, P.J., Wardle, D.A., 2014. Soil-mediated effects of invasive ungulates on native tree seedlings. *J. Ecol.* 102, 622–631. <https://doi.org/10.1111/1365-2745.12234>
- Keuskamp, J.A., Dingemans, B.J.J., Lehtinen, T., Sarneel, J.M., Hefting, M.M., 2013. Tea Bag Index: A novel approach to collect uniform decomposition data across ecosystems. *Methods Ecol. Evol.* 4, 1070–1075. <https://doi.org/10.1111/2041-210X.12097>
- Kielland, K., Bryant, J.P., Ruess, R.W., 1997. Moose herbivory and carbon turnover of early successional stands in interior Alaska. *Oikos* 25–30.
- Kolstad, A.L., Austrheim, G., Solberg, E.J., Venete, A.M.A., Woodin, S.J., Speed, J.D.M., 2018. Cervid Exclusion Alters Boreal Forest Properties with Little Cascading Impacts on Soils. *Ecosystems* 21, 1027–1041. <https://doi.org/10.1007/s10021-017-0202-4>
- Krumins, J.A., Krumins, V., Forgoston, E., Billings, L., van der Putten, W.H., 2015. Herbivory and Stoichiometric Feedbacks to Primary Production. *PLoS One* 10, e0129775. <https://doi.org/10.1371/journal.pone.0129775>
- Kumbasli, M., Makineci, E., Cakir, M., 2010. Long term effects of red deer (*Cervus elaphus*) grazing on soil in a breeding area. *J. Environ. Biol.* 31, 185–188.
- Mohr, D., Cohnstaedt, L.W., Topp, W., 2005. Wild boar and red deer affect soil nutrients and soil biota in steep oak stands of the Eifel. *Soil Biol. Biochem.* 37, 693–700. <https://doi.org/10.1016/j.soilbio.2004.10.002>
- Noe, L., Abril, A., 2013. Is the nitrification a redundant process in arid regions?: Activity, abundance and diversity of nitrifier microorganisms. *Rev. Chil. Hist. Nat.* 86, 325–335. <https://doi.org/10.4067/s0716-078x2013000300009>

- Núñez, P.A., Demanet, R., Misselbrook, T.H., Alfaro, M., de la Luz Mora, M., 2010. Pérdidas de nitrógeno bajo diferentes frecuencias e intensidades de pastoreo en un suelo volcánico del sur de Chile. *Chil. J. Agric. Res.* 70, 237–250. <https://doi.org/10.4067/S0718-58392010000200007>
- Oksanen, J., Blanchet, F.G., Friendly, M., Kindt, R., Legendre, P., Mcglinn, D., Minchin, P.R., O'hara, R.B., Simpson, G.L., Solymos, P., Henry, M., Stevens, H., Szoecs, E., Maintainer, H.W., 2019. Package “vegan” Title Community Ecology Package. *Community Ecol. Packag.* 2, 1–297.
- Pan, H., Xie, K., Zhang, Q., Jia, Z., Xu, J., Di, H., Li, Y., 2018. Archaea and bacteria respectively dominate nitrification in lightly and heavily grazed soil in a grassland system. *Biol. Fertil. Soils* 54, 41–54. <https://doi.org/10.1007/s00374-017-1236-7>
- Pastor, J., Naiman, R.J., 1992. Selective foraging and ecosystem processes in boreal forests. *Am. Nat.* 139, 690–705. <https://doi.org/10.1086/285353>
- Patra, A.K., Abbadie, L., Clays-Josserand, A., Degrange, V., Grayston, S.J., Loiseau, P., Louault, F., Mahmood, S., Nazaret, S., Philippot, L., Poly, F., Prosser, J.I., Richaume, A., Le Roux, X., 2005. EFFECTS OF GRAZING ON MICROBIAL FUNCTIONAL GROUPS INVOLVED IN SOIL N DYNAMICS. *Ecol. Monogr.* 75, 65–80. <https://doi.org/10.1890/03-0837>
- Peco, B., Sánchez, A.M., Azcárate, F.M., 2006. Abandonment in grazing systems: Consequences for vegetation and soil. *Agric. Ecosyst. Environ.* 113, 284–294. <https://doi.org/10.1016/j.agee.2005.09.017>
- Pinheiro, J., Bates, D., DebRoy, S., Sarkar, D., Team, R.C., 2021. nlme: Linear and nonlinear mixed effects models. R package version 3.1-152.

- Pulido, M., Schnabel, S., Lavado Contador, J.F., Lozano-Parra, J., González, F., 2018. The Impact of Heavy Grazing on Soil Quality and Pasture Production in Rangelands of SW Spain. *L. Degrad. Dev.* 29, 219–230. <https://doi.org/10.1002/ldr.2501>
- R Core Team, 2020. R: A language and environment for statistical computing. R Foundation for Statistical Computing, Vienna, Austria. URL <https://www.R-project.org/>.
- Reichert, J.M., Mentges, M.I., Rodrigues, M.F., Cavalli, J.P., Awe, G.O., Mentges, L.R., 2018. Compressibility and elasticity of subtropical no-till soils varying in granulometry organic matter, bulk density and moisture. *CATENA* 165, 345–357. <https://doi.org/10.1016/J.CATENA.2018.02.014>
- Roger-Estrade, J., Anger, C., Bertrand, M., Richard, G., 2010. Tillage and soil ecology: Partners for sustainable agriculture. *Soil Tillage Res.* <https://doi.org/10.1016/j.still.2010.08.010>
- Roger, F., Bertilsson, S., Langenheder, S., Osman, O.A., Gamfeldt, L., 2016. Effects of multiple dimensions of bacterial diversity on functioning, stability and multifunctionality. *Ecology* 97, 2716–2728. <https://doi.org/10.1002/ecy.1518>
- Rosenberg, M., Adams, D., Gurevitch, J., 2000. *MetaWin: Statistical Software for Meta-Analysis, version 2.0*. Sinauer Associates, Inc. New York.
- Sardans, J., Peñuelas, J., 2013. Plant-soil interactions in Mediterranean forest and shrublands: impacts of climatic change. *Plant Soil* 2013 3651 365, 1–33. <https://doi.org/10.1007/S11104-013-1591-6>

- Sebastià, M., Bello, F., Puig, L., Taull, M., 2008. Grazing as a factor structuring grasslands in the Pyrenees. *Appl. Veg. Sci.* 11, 215–222. <https://doi.org/10.3170/2008-7-18358>
- Sjödin, N.E., Bengtsson, J., Ekbom, B., 2007. The influence of grazing intensity and landscape composition on the diversity and abundance of flower-visiting insects. *J. Appl. Ecol.* 45, 763–772. <https://doi.org/10.1111/j.1365-2664.2007.01443.x>
- Stark, S., Männistö, M.K., Smolander, A., 2010. Multiple effects of reindeer grazing on the soil processes in nutrient-poor northern boreal forests. *Soil Biol. Biochem.* 42, 2068–2077. <https://doi.org/10.1016/j.soilbio.2010.08.001>
- Stark, S., Strömmer, R., Tuomi, J., 2002. Reindeer grazing and soil microbial processes in two suboceanic and two subcontinental tundra heaths. *Oikos* 97, 69–78. <https://doi.org/10.1034/j.1600-0706.2002.970107.x>
- van der Putten, W.H., Bradford, M.A., Pernilla Brinkman, E., van de Voorde, T.F.J., Veen, G.F., 2016. Where, when and how plant–soil feedback matters in a changing world. *Funct. Ecol.* 30, 1109–1121. <https://doi.org/10.1111/1365-2435.12657>
- Vermeire, M.L., Thoresen, J., Lennard, K., Vikram, S., Kirkman, K., Swemmer, A.M., Te Beest, M., Siebert, F., Gordijn, P., Venter, Z., Brunel, C., Wolfaard, G., Krumins, J.A., Cramer, M.D., Hawkins, H.J., 2021. Fire and herbivory drive fungal and bacterial communities through distinct above- and belowground mechanisms. *Sci. Total Environ.* 785, 147189. <https://doi.org/10.1016/J.SCITOTENV.2021.147189>
- Viechtbauer, W., 2010. *Conducting Meta-Analyses in R with the metafor Package*, JSS Journal of Statistical Software.

Chapter 1

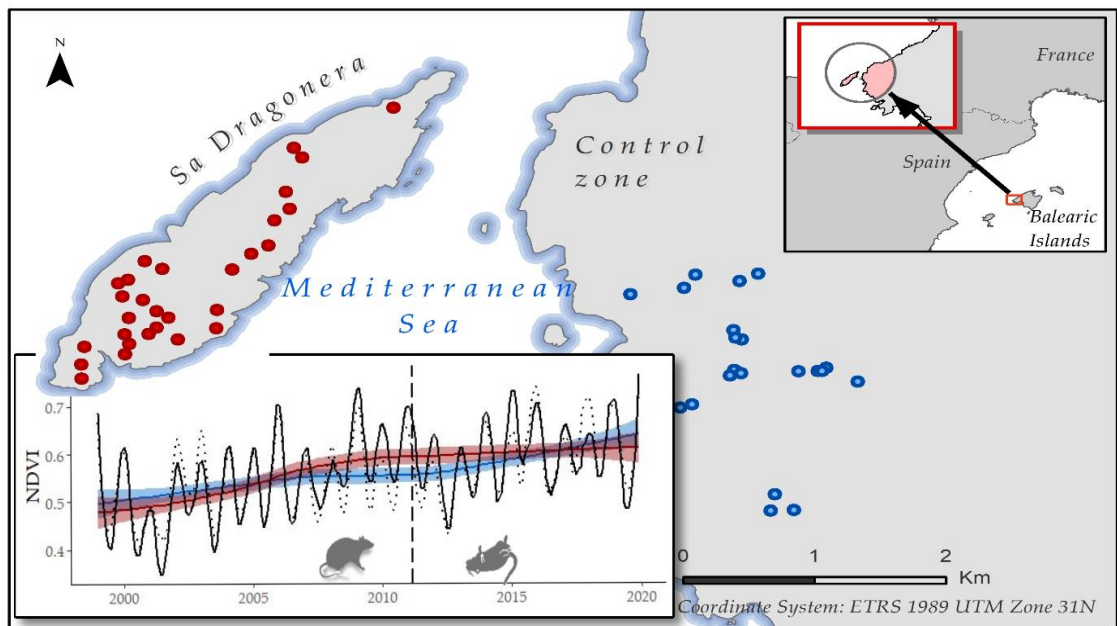
- Wall, D.H., Behan-Pelletier, V., Ritz, K., Jones, T.H., Six, J., Strong, D.R., van der Putten, W.H., 2012. Soil ecology and ecosystem services, Oxford University Press.
- Wardle, D.A., Barker, G.M., Yeates, G.W., Bonner, K.I., Ghani, A., 2001. Impacts of introduced browsing mammals in New Zealand forests on decomposer communities, soil biodiversity and ecosystem properties. *Ecol. Monogr.* 71, 587–614.
- Xu, Y., Wan, S., Cheng, W., Li, L., 2008. Impacts of grazing intensity on denitrification and N₂O production in a semi-arid grassland ecosystem. *Biogeochemistry* 88, 103–115. <https://doi.org/10.1007/s10533-008-9197-4>
- Zhang, M., Li, G., Liu, B., Liu, J., Wang, L., Wang, D., 2020. Effects of herbivore assemblage on the spatial heterogeneity of soil nitrogen in eastern Eurasian steppe. *J. Appl. Ecol.* 57, 1551–1560. <https://doi.org/10.1111/1365-2664.13655>
- Zwietering, M.H., Jongenburger, I., Rombouts, F.M., van 't Riet, K., 1990. Modeling of the Bacterial Growth Curve. *Appl. Environ. Microbiol.* 56.

4. Chapter 2

Satellite-Based Monitoring of Primary Production in a Mediterranean Islet Post Black Rat Eradication

Miguel Ibañez-Álvarez, Pol Farràs Santasusana, Juan A. Calleja, Carlos Rouco, Matthew Brolly, Niall G. Burnside, Elena Baraza, Jordi Bartolomé, Emmanuel Serrano. 2022. Satellite-Based Monitoring of Primary Production in a Mediterranean Islet Post Black Rat Eradication. *Remote Sensing* 14, 1: 101.

<https://doi.org/10.3390/rs14010101>¹



¹ The citation in this chapter follows the citation style of the Remote sensing journal.

Abstract

Invasive rodents have a detrimental impact on terrestrial ecosystem functioning, this is often exacerbated on small islands. Rat eradication campaigns are often used to deal with this environmental perturbation given their classification as invasive species. Studies assessing the effects of rodent control at ecosystem scale are scarce and thus little is known about the subsequent functional response of vegetation subsequent to rat control. In this work, we use remote sensing to assess the effects of black rat (*Rattus rattus*) eradication on Mediterranean vegetation productivity in the Sa Dragonera Islet, Mallorca (Spain). Rats feed on seeds, sprouts, and leaves of woody vegetation and hence we expect primary production to increase nine years after the rodenticide campaign. The Break Detection approach for additive season and trend (BFAST method) was adopted to examine changes in vegetation density before and after the eradication campaign in Sa Dragonera Islet (Balearic Islands), using a temporal series of monthly NDVI data extracted from Landsat imagery. The same temporal trends were examined for a control zone where no rat eradication took place, in order to control for weather-driven changes. The results of this study revealed changes across the 21-year monthly NDVI time series. However, the dates, magnitude, and trend of these changes could not be explicitly attributed to the action of rats, when compared to the historical changes on the islet and the changes found to co-occur within the control zone. These finding could, perhaps, be explained by the high resilience of Mediterranean shrubs to browsing including that of rat invasion. However, the results from the study appear to show that rat damage on specific plant species, with little contribution to global NDVI values, would be overshadowed by the effects of broader environmental factors in this remote sensing approach. The

results suggest that the current passive restoration scheme imposed following eradication is not sufficient for effective ecosystem restoration.

Keywords: BFAST method; invasive species; Landsat Time Series; rodent eradication

1. Introduction

Invasive alien species (IAS) are those that have reached new geographic areas by way of human introduction, and are populations which can survive, reproduce and spread over the natural environment leading to major impacts on the environment or society [1]. IAS can cause serious disturbance to other indigenous species and the ecosystems they invade, often altering ecosystem structure and function, trophic relationships (e.g., plant-animal interactions), and reducing the biodiversity of the invaded ecosystems [2–5].

Island communities which have evolved in isolation are typically the most vulnerable to IAS [6]. One of the most harmful invasive species are rodents belonging to the genus *Rattus*, in particular, the black rat (*Rattus rattus*), brown rat (*R. norvegicus*) and Pacific rat (*R. exulans*) [7–9]. The impact of rats is often density-dependent [10–12] and regulated by primary production [13–15], thus, in many biomes rat populations fluctuate seasonally [16]. Records of black rat density are highly variable ranging from 36.4 rats ha⁻¹ in New Zealand islands [15], to 50 rats ha⁻¹ in some Mediterranean islands [17]. In the Mediterranean basin the black rat is the most invasive species due to its broad tolerance to dry climates [18,19]. These species have already invaded 80% of the world's islands [12,20–22] and they cause a cascade of damage to ecosystems, resulting in the decline and extinction of native birds, mammals, reptiles, invertebrates and plants of many archipelago ecosystems [7,8,18]. The black rat tends to consume

more plants than animals [23], showing a preference for seeds, sprouts, and leaves of adult plants [24,25], and thus directly affecting photosynthetic and reproductive parts. As a result, black rats affect the composition and structure of plant communities, plant recruitment, and the viability of the plant population on the islets and islands they infest. This has been recorded in some islands of New Zealand [26,27], and in islands and small islets of Spanish archipelagos (Canarias and Balearic Islands) where the presence of black rat has altered the structure of the vegetation; depressing or limiting some plant species and favouring others [19].

In islands where rats are removed at an early stage of their invasion, vegetation recovers quickly [28,29]. However, in places with prolonged history of rat colonisation, recovery is much slower due to critical changes in vegetation structure [30,31]. Rodent eradication is a common measure [8] for recovering invaded areas [32] with accompanying environmental monitoring necessary to evaluate the effectiveness of rat eradication campaigns in terms of ecosystem restoration [33]. However, ecosystem recovery is often affected by other confounding factors (e.g., climatic events) [34,35], or is limited to specific plant or animal species [36,37]. Conversely, the lack of environmental information prior to rat invasion [38] can hamper the evaluation of ecosystem restoration programs [39]. In fact, ecosystem monitoring post rodent eradication is uncommon [13,40]. Remote sensing therefore has a clear role to play in assessing ecosystem restoration post rodent eradication [41] given its spatial and temporal extents.

Satellite sensors are capable of providing land cover information at different spatial, spectral, and temporal resolutions, allowing the monitoring of vegetation extent and health, and through this indicate areas of recovery post natural or human-induced disturbance [42,43]. A range of spectral vegetation indices, such as the Normalized

Difference Vegetation Index (NDVI), can be used for these purposes [44]. NDVI is a proxy for photosynthetic activity [45], vegetation productivity, aboveground biomass [46], and vegetation dynamics [47,48], and has been shown to reliably capture ecological response to environmental change including human and animal-driven land degradation [44]. In most terrestrial biomes, long-term NDVI time series follow a non-linear pattern that comprises alternating cycles of greening (increasing NDVI) or browning (decreasing NDVI). The dating and quantification of frequency and magnitude of these NDVI cycles is generally used as a proxy for ecosystem dynamics [44,48,49]. NDVI time series are particularly useful in periods longer than 10 years [50], as this makes it feasible to analyse the seasonal and trend components over time. The nature of the change in NDVI time series can be interpreted according to the affected component. For example, modifications of the seasonal oscillation could indicate phenological changes, while changes in the trend, including the magnitude, may point to a disturbance event [43], precipitation variability [51–53] or drought event [53,54].

In this work, we evaluate the impact of a rodent eradication campaign in a Mediterranean scrubland located in the Balears Archipelago (western Mediterranean basin, Spain) using twenty-one years of monthly NDVI data for the Sa Dragonera and for a nearby control zone on the island of Mallorca. Changes in vegetation productivity, before and after the eradication campaign, across the two zones was examined using the breaks for additive seasonal and trend analysis (BFAST, [43,55]). BFAST is especially useful here to address the lack of information regarding the magnitude of change on primary production after deratization management, because unlike other methods, BFAST does not restrict the data to a specific season since it considers a seasonal fit over the entire time series. Additionally, its change detection

approach based on signal-to-noise ratio does not require setting a change threshold. BFAST has the sensitivity to differentiate the normal phenological cycle from abnormal changes and has been used to monitor the recovery of vegetation [56,57] after a broad range of environmental catastrophes including wildfires, insect outbreaks [58] and floods [59]. Due to the devastating effect that black rat infestations can have on small islet ecosystems reported worldwide [19] and the ability of BFAST to detect changes at the local scale [55,60,61], we hypothesized that primary productivity on Sa Dragonera Islet would differ before and after the rodenticide campaign; due to vegetation regeneration following black rat eradication. In particular, we expect to detect an increase (abrupt and/or gradual) in the greenness of the main vegetation due to the natural vegetation recovery following rodent eradication after controlling for climatic conditions.

2. Materials and methods

2.1. Study Area

The focal geographic area of the study is in the Balears Archipelago (western Mediterranean basin, Spain). It comprises Sa Dragonera Islet, referred to hereafter as treatment zone. In addition, a control zone was included, some 800m away on Mallorca Island, due to its similarity in orography, lithology and vegetation type. Importantly, both zones are an extension of the UNESCO designated World Heritage Site of the Serra de Tramuntana Mountain Range. The treatment zone is a 276 ha islet extending 350 meters above sea level, with the north-west exposure terminating in a cliff face.

The climate at both sites is Mediterranean, with annual average temperatures above 16 degrees and little annual rainfall (<400 mm); but with high inter-annual variability.

According to the Spanish Meteorological Agency (AEMET) [62], drought periods typically last 5 months; yet these events are partially mitigated by maritime influence. Limestone is the predominant bedrock and overlying soils are poorly developed or skeletal. The main vegetation consists of a mosaic of scrub communities. There are tree patches, and the herbaceous taxa are scarce (other than non-palatable plants such as *Urginea maritima* and *Crithmum maritimum*) due to the poor climatic and edaphic conditions. Sclerophyllous woody species of Mediterranean optimum predominate, such as *Pinus halepensis*, *Pistacia lentiscus*, *Olea europaea*, *Anthyllis cytisoides*, *Chamaerops humilis*, *Cistus monspeliensis*, *Cneorum tricoccon*, *Ephedra fragilis*, *Euphorbia dendroides*, *Phillyrea angustifolia* [63,64]. Most of these species can resprout following disturbance, exhibiting some resilience to fires or/and browsing, which are typical characteristics of sclerophyllous flora of the Mediterranean basin [65–67].

The islet is currently uninhabited; however, human activity has shaped its landscape as well as that of Mallorca Island over the last five millennia, fostering deforestation and soil erosion processes [63,68]. Natural resources, such as woodcutting, crop growing, and domestic animal breeding, were common until the 1975 [69,70]. Feral goats (*Capra hircus*) were eradicated in the 1980s, European wild rabbits (*Oryctolagus cuniculus*), and house mouse (*Mus musculus*) were also present in the treatment zone, yet black rats have been by far the most common invasive mammal in the islet reaching up to 50 individuals ha⁻¹ [71]. This density of rats equals the maximum reported in Mediterranean islands [17,72] and is higher than that historically recorded in the islands of New Zealand (36.4 rats ha⁻¹) [15].

Sa Dragonera is the main islet of an archipelago which was awarded the status of Natural Park in 1995 and forms part of the Natura 2000 Special Protection Area and Site of Community Importance (SPA and SCI, EU Birds and Habitats Directive) [73].

The majority of the islet is considered a reserve area devoted to the conservation of natural values in the absence of active management measures [74]. Field observations revealed severe damage by rodents on vegetation cover, for example, in 2010 partial or total damage on branches of juvenile individuals of *Ficus carica*, *Ceratonia siliqua* and *Olea europaea* var. *sylvestris* were reported (Figure 4.1). Likewise, the endangered populations of Balearic shearwater (*Puffinus mauretanicus*) were impacted by rat predation [71]. Hence, conservationists have performed several ground-based rodent eradication attempts between 2001 and 2008 using rodenticide baits in the most accessible areas, but with little long-term success as rat populations have recovered to high densities. In February 2011 the local government organized an eradication campaign using Brodifacoum rodenticide. Brodifacoum baits were aurally distributed twice over the entire islet at rates of 14 kg ha⁻¹ [71]. Since this eradication effort, the treatment zone has been rodent free [75,76], despite the high risk of reinvasion due to the proximity of the coast of Mallorca [77]. Four years after Brodifacoum baiting, unsystematic and occasional field observations have reported the increase of vegetation cover [78], however evidence of this recovery remains lacking.

The Sierra Tramuntana in Mallorca is also a landscape shaped by human activity, which suddenly ceased from the 1960s in the rural mountain areas, becoming focused on rapid development of the tourism sector in the urbanised areas. The abandonment of the rural sector led to the cessation of domestic animal grazing but also to the proliferation of the feral goat which continues today [79,80].



Figure 4. 1. Damage caused by the black rat (*Rattus rattus*) in 2010 in Sa Dragonera Islet. (Top left) Wild olive tree (*Olea europaea* var. *sylvestris*) with damaged bark. (Top right) Damage in a perennial herb (*Urginea maritima*). (Bottom right) Damage in a pinecone (*Pinus halepensis*). Author of the photos: Martí Mayol (Director of the Sa Dragonera Natural Park at the time of the deratization campaign).

2.2. NDVI time series construction

To identify whether the rodenticide eradication campaign affected primary production in the treatment zone, we compare its NDVI time series with that in the control zone. NDVI time series are here based on Landsat surface reflectance (SR) data for a period ranging from 1999 to 2020. February 2011 was set as the base date for detecting changes due to rat eradication. Therefore, the study period was divided into: (i) a historical period of 12 years where vegetation was impacted by rats (1999–2010) and (ii) a recovery period of 9 years post rat eradication (2012–2020).

2.2.1. Satellite images

Chapter 2

This study used the Landsat satellite archive due to the temporal continuity across the analysis time period. Landsat imagery Collection 1 provided by USGS (United States Geological Survey) was accessed via the web site <https://earthexplorer.usgs.gov/> on 14 November, 2020. Landsat Collection 1 images are calibrated and aligned across all Landsat satellites. 333 Landsat SR images were obtained for the period January 1999 to December 2019 from Landsat 5 TM, Landsat 7 ETM+ and Landsat 8 OLI sensors. SR images are a Landsat level-2 product that provide the bottom of atmosphere surface spectral reflectance as it would be measured at ground level (i.e., with atmospheric correction applied). The availability of a high number of images favours the temporal consistency of the radiometric data across time series, since gaps produced due to the presence of clouds or due to SLC off-Data error, inherent to Landsat 7 [81] acquisitions post May 2003, can be replaced with optimal values recorded by another sensor at a close date (Figure 4.2).

Once Landsat SR images were downloaded, R script was coded to search for the red and NIR spectral bands of each satellite observation, combining them according to the NDVI formula [82] using the "Raster" package [83] in the R statistical software [84]. Thus, NDVI layers were produced for all observations. All layers were stacked creating a multi-variable raster dataset called RasterStack object.

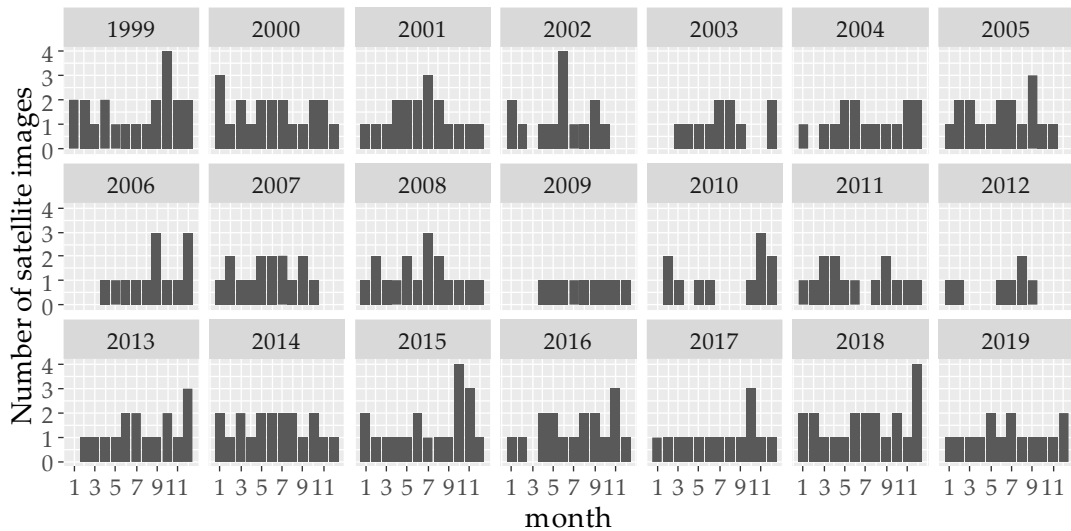


Figure 4. 2. Temporal distribution of Landsat Collection 1 Surface Reflectance (SR) imagery. More images were used (when available) where clouds obstructed data collection or where SLC off-data error in Landsat 7 was detected over study zones.

2.2.2. Plot selection procedure

Time series are created by averaging NDVI values from selected sampling plots. The plots were located using a pair of UTM coordinates indicating the centre and extended to the spatial resolution of a Landsat image (i.e., 900 m²). To select sampling plots where vegetation shows similar temporal dynamics of NDVI, a sampling procedure was used to choose plots meeting the following features: I) same vegetation cover, (scrubland, because it is the principal vegetation cover of the islet), based on Sentinel-2 Global Land Cover (S2GLC, [85]); II) similar NDVI values avoiding scattered scrub areas and cliffs. For this purpose, a NDVI composition map was created where each pixel represented the 5-year average NDVI prior to the rodenticide event (i.e., from 2006 to 2011). This map was classified into the major categories (i.e., coniferous forest, scrubland, scattered thicket and bare soil) using the Jenks natural breaks classification method to maximise the variation between classes and to best group similar values [86]. With the help of a high resolution orthophoto (15 cm spatial

resolution aerial orthophotography from the PNOA (National Plan for Aerial Orthophotography) available in <http://www.scne.es/#ORTOPNOA>) on 17 October, 2020, we photo-interpreted and established that the values of the target vegetation cover in the NDVI composition map ranges from 0.45 to 0.62. To address NDVI differences due to slope, altitude and orientation issues [87], sampling plots were selected if they were between 50 to 300 meters asl, had a slope less than 30 degrees, and had an east or south facing-orientation. This selection was carried out using a 5 × 5-meter resolution Digital Elevation Model (DEM) raster layer in ArcGIS 10.7. A workflow of the sampling procedure is shown in Figure 4.3. A total of fifty-four sampling plots, 29 in the treatment zone and 25 in the control zone, met these criteria (Figure 4.4).

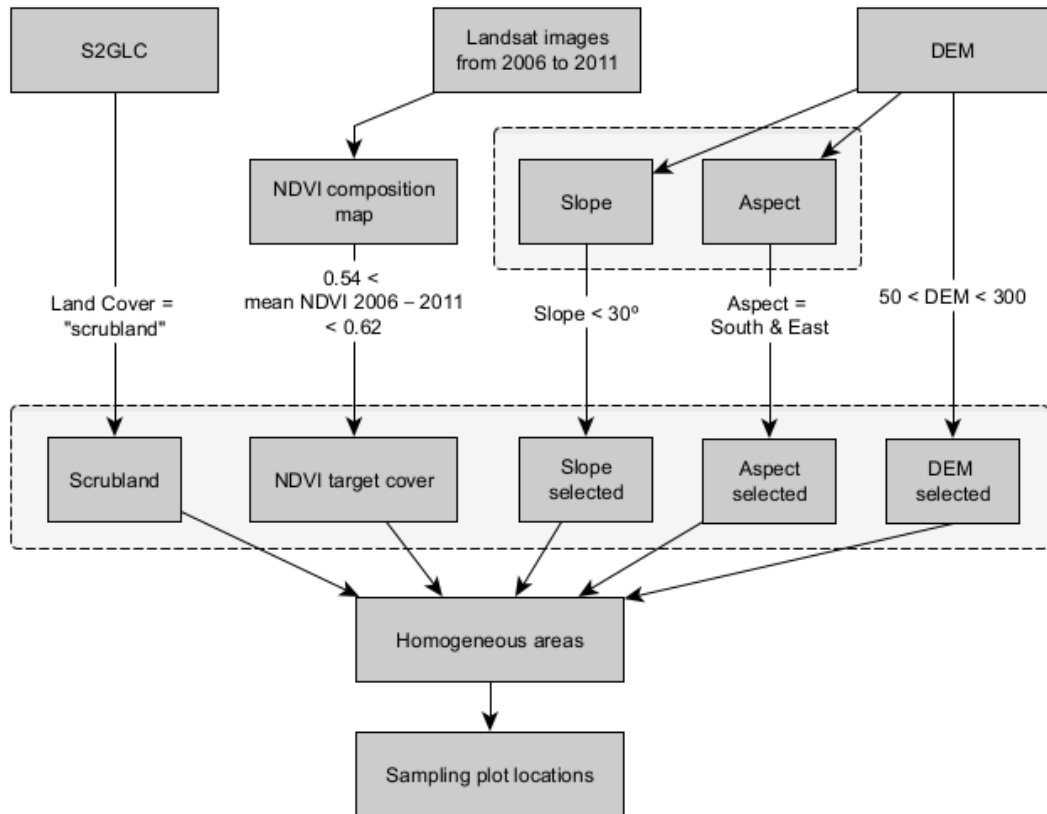


Figure 4. 3. Workflow of spatial criteria to select fifty-four $30 \times 30\text{m}^2$ plots (29 in the treatment zone and 25 in the control zone represented by pink dots in Figure 4) to compare NDVI time series.

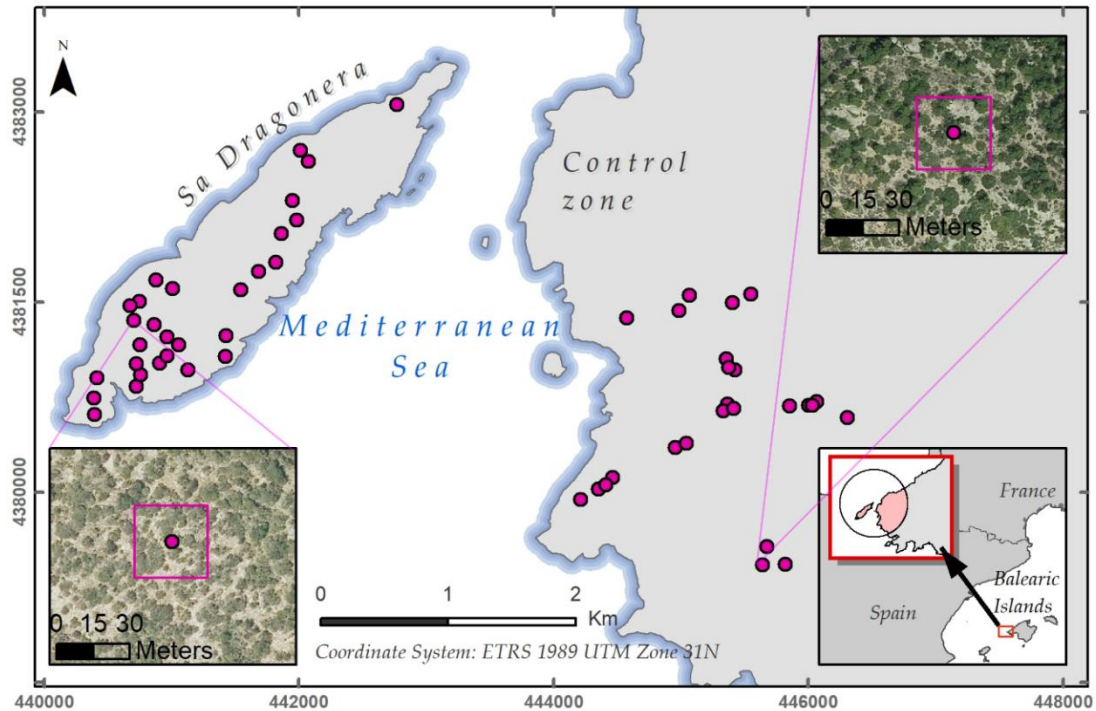


Figure 4. 4. Map showing locations of selected sampling plots (pink dots) to create the NDVI time series for both treatments. On the left are the sampling plots of Dragonera Islet (the treatment zone), and on the right those of Mallorca Island (the control zone). High-resolution aerial orthophotos (15×15 cm) show two examples of the 30×30 m sampling plots of both treatments. Spatial reference map in the bottom right corner.

2.2.3. Monthly Landsat NDVI time series construction

For each sampling plot, NDVI values were extracted from a multilayer raster object (Section 2.2.1) using the “raster” 3.4–10 package [83] in the R statistical software [84]. The cleaning, gap-filling and smoothing procedure summarised below was followed:

- a) NDVI values outside the range of the target vegetation index range, below 0.2 or over 1, were removed. The NDVI values were then selected according to maximum-value composite (MVC) criterion.

b) a gap-filling with linear interpolation between neighbouring values [88] was performed, to fill NDVI gaps (31 observations in the treatment zone and 32 in Mallorca Island, the control zone).

c) the Savitzky–Golay [89] smoothing algorithm was applied to smooth out the noise in both time series. It is appropriate to apply it on seasonal data [90] since it follows within-season variations and therefore captures subtle dynamics during seasons [91].

By applying the steps described here, clean and consistent time series were constructed for each treatment to feed the BFAST algorithms (Figure 4.5), since a temporal consistency of observations is critical for understanding ecosystems dynamics [92].

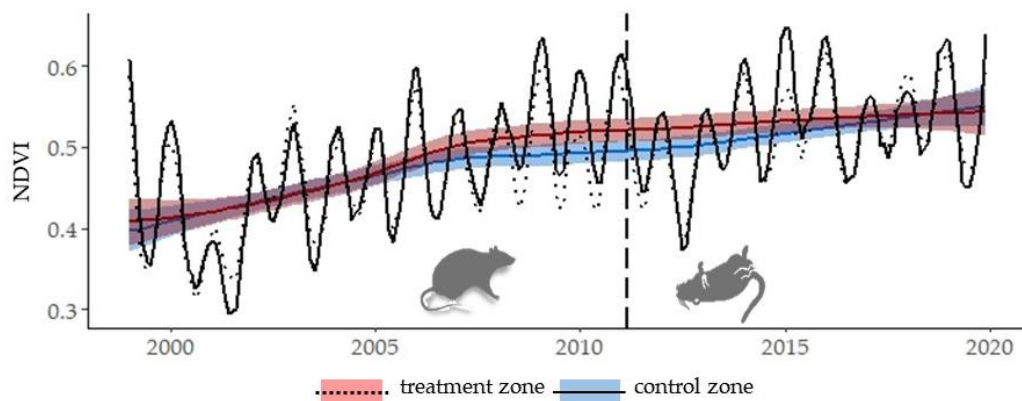


Figure 4. 5. Monthly NDVI time series showing the average NDVI of the sampling plots for each zone. The coloured lines (Red = Sa Dragonera; Blue = Mallorca Island, i.e., control zone) represent the trend throughout the study period, with a LOESS smoothing and standard deviation shown with the corresponding colours. The black lines represent the real data for each treatment (Solid = Sa Dragonera; Dotted= control zone), in which the seasonal variation can be observed. The dashed vertical line dates the rodent eradication campaign (February 2011).

2.3. Historical time series analysis

To detect and characterise changes in the ecosystem dynamics, the BFAST protocol described in [43] was applied to the monthly NDVI time series. BFAST interactively

decomposes time series into trend, seasonal, and remainder components [43,55]. The iteration begins using a Seasonal-Trend decomposition (STL) method. STL first detrends the time series by subtracting the trend from the observed values resulting in a new time series that exposes seasonality. The detrended time series is then used to compute the average seasonality. The amount of NDVI beyond the combination of the seasonal and trend components is considered random noise or the remainder component (Figure 4.6). Subsequently, BFAST function detects breakpoints by applying ordinary least squares residuals-based moving sum (OLS-MOSUM). This tests the null hypothesis that the linear trend of the NDVI values remain constant over the observations against the alternative of significant changes ($p < 0.05$). The optimal number of breakpoints is determined by minimising the Bayesian Information Criterion (BIC) and the position of the breakpoints (dates and its confidence intervals) are chosen by globally minimising the residual sum of squares. BFAST iterates along these steps until the number and position of the breakpoints remains constant. The basis and the process carried out by BFAST is described in detail in [43] and is available in the BFAST package for R (<https://cran.r-project.org/web/packages/bfast/index.html>) on 9 September, 2021. All BFAST analyses were performed using R statistical software [84].

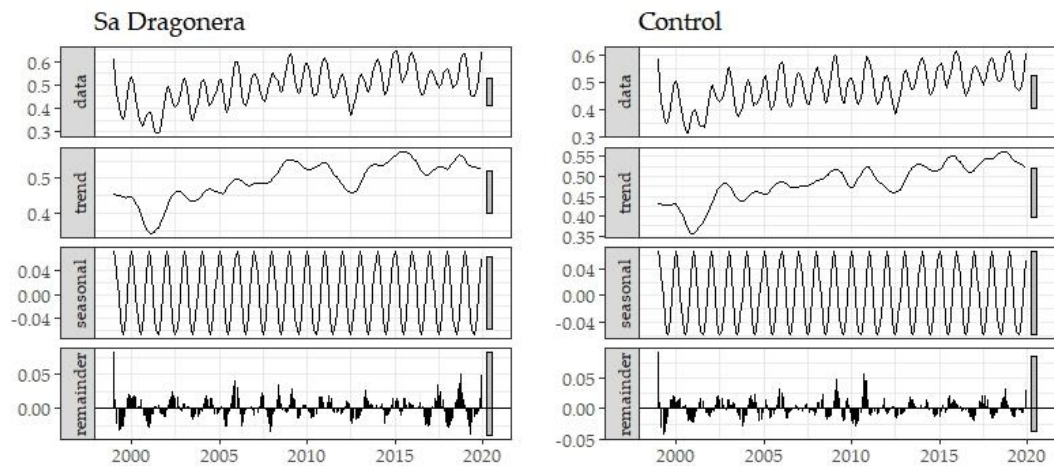


Figure 4. 6. The STL decomposition of the monthly NDVI time series of Sa Dragonera and control zone (Mallorca Island) into the seasonal, trend, and remainder components. In each plot, NDVI units are plotted against time. The seasonal component is estimated by taking the mean of all seasonal sub-series (e.g., for a monthly time series the first sub-series contains the January values). The sum of the seasonal, trend, and remainder components equals the data series. The solid bars on the right-hand side of the plots act as a reference to show the same data range and aid comparison.

BFAST transforms the NDVI time series into a piecewise model, whose maximum number of linear regressions depends on the parameter h . The h parameter sets the minimal segment size between potentially detected breaks in the trend model given as a fraction relative to the sample size. The sample size of each of our time series consists of 252 observations (i.e., 21 years at a monthly frequency). We established the value of $h = 1/7$ in order to set significant trend periods following the recommendations of [59]. For our dataset, this implies that a maximum of seven linear regressions with $252/7 = 36$ minimum observations each (i.e., a minimum of three years). The difference between the NDVI value at the end of a preceding linear model and the intercept of the following linear model defines the magnitude of the abrupt change and the slope of each linear model defines the gradual change between breakpoints.

Chapter 2

For better understanding of the vegetation dynamics and to avoid misinterpretation of the effect of rat removal, we compared the BFAST outcomes between zones and with historical environmental records. Because changes in hydrological regimes are considered the main drivers of vegetation dynamic changes [52,54], and closely related to shifts in NDVI time series in water limited ecosystems [93,94], we compared the BFAST results with the hydrological drought index (HDI). This is reported by the General Directorate of Water Resources (DGRH) of the government of the Balearic Islands [95] in the Hydrological Demand Unit (HDU) of Sierra Tramuntana Sur. This corresponds to our study area. In the report they categorise HDI in 4 groups which describe the state of water resources. These categories, from highest to lowest hydric abundance are: normality, pre-alert, alert and emergency. The years 1999, 2001, 2004, 2007 and 2011 are key dates to consider due to the area entering alert or emergency states. Similar to the majority of zones in Mallorca, as a result of the high rainfall in 2009 and 2010, our study area was at optimal HDI levels, although from 2015 onwards a rapid decline was observed, leading to the alert situation in late 2015.

The BFAST outputs are compared between zones. This, on the one hand, gives us an idea of whether the process of selection of plots was efficient at the time of selecting areas whose vegetation follows the same dynamics. On the other hand, the comparison of the dates when the breaking points occur tries to find the singularity of the effect of the eradication campaign. In addition, the magnitude of the breakpoints is used as a proxy for the vegetation resistance facing a disturbance event; and the slope of the linear regressions as a proxy of the recovery rate (greening when positive rate or browning when negative rate) [96].

A more detailed explanation of the R code workflow can be seen in the Supplementary Material chapter 2 section.

3. Results

3.1. Historical time series results

BFAST decomposed the original NDVI data (Y_t) into seasonal (S_t), trend (T_t) and remainder (et) components (Figure 4.7). The algorithm identified four breakpoints at both the treatment and control zones in the NDVI trend component (Figure 4.7A,B, respectively), two of them following the eradication campaign. The seasonal component showed no abrupt changes, and the seasonal amplitude was approximately 0.05 NDVI.

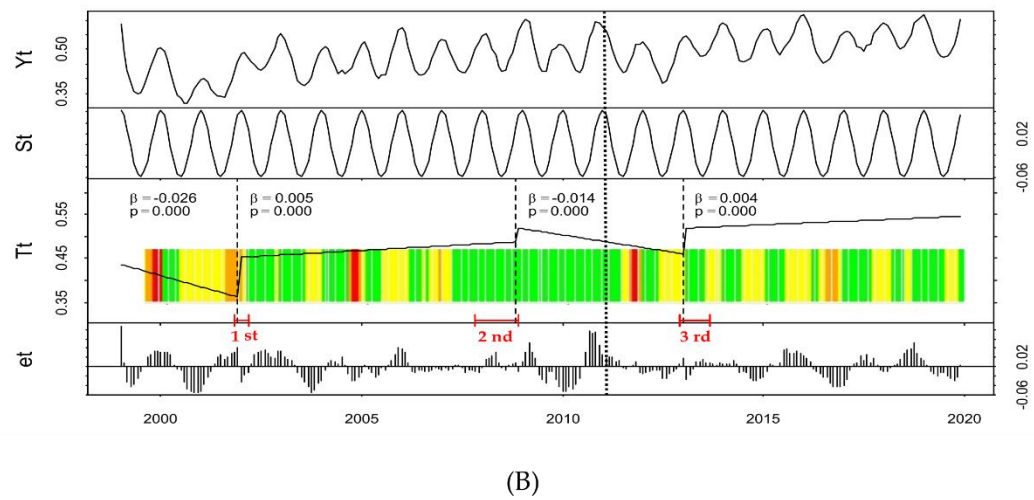
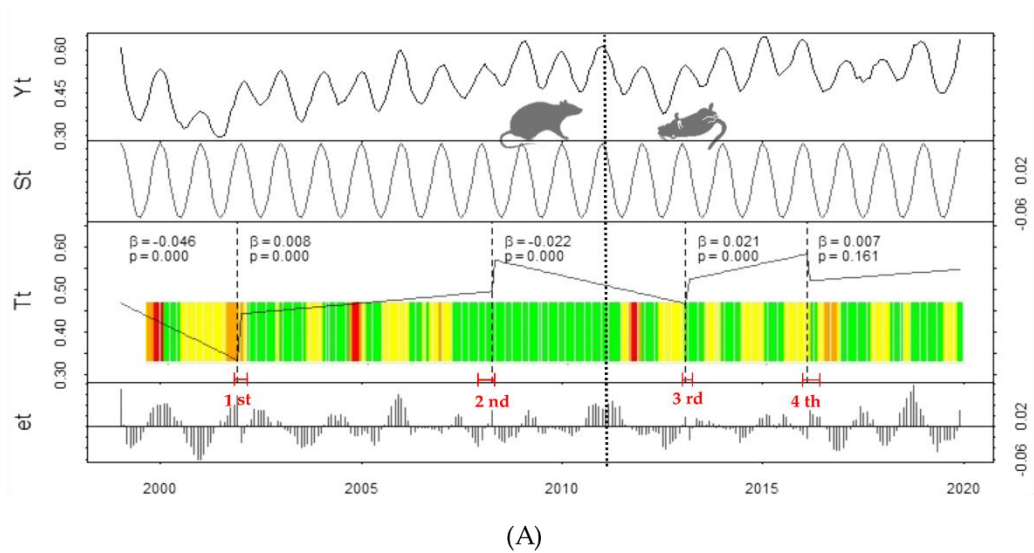


Figure 4. 7. Decomposed NDVI data (Y_t) into seasonal (St), trend (Tt) and remainder (et) components for NDVI time series between 1999 and 2020 for both treatment zone (A), and control zone (B), using the breaks for additive seasonal and trend (BFAST) method. The dotted vertical line shows when the rodent eradication campaign took place (February 2011). The dashed lines in Tt represent the timing of each significant NDVI change ($p < 0.05$), together with its 95% confidence intervals (horizontal red bars). Ordinal numbers are used to name the breakpoints. Vertical axis units are absolute NDVI values. The slope coefficient (β) and p-value is shown for each fitted trend segment. Coloured slots represent Hydrological Drought Index (HDI) between March 1999 and December 2019 [95] which describes the water resources state from more to less abundant for: normality (green), pre-alert (yellow), alert (orange), and emergency (red).

Table 4.1 summarizes the date of abrupt changes, their magnitude and direction, and the regression parameters of the piecewise model, which provides information about the NDVI on the break date (intercept) and on the recovery rate (slope). The timing

of occurrence and the direction of all four abrupt changes were similar for both treatment and control zones, since their breakpoint dates (95% CI) overlapped. All identified breakpoints occurred immediately after environmental disturbances (i.e., anomalies in water resources in this study). In the first and second abrupt changes an increase in NDVI was observed associated with normal hydric states (HDI) arising after recurrent states of alert or emergency. Conversely, the third and fourth abrupt change occurred along with an emergency or alert state just after the observed NDVI values moved between normality and pre-alert states of water resources. The magnitudes observed at the four breakpoints were always higher for treatment zone than for the control zone (Table 4.1).

Likewise, the recovery rates (Slope in Table 4.1) were of a similar level in all four modelled linear regressions, highlighting that these rates are not higher in the modelled segments of the treatment zone after the rat eradication campaign date.

Table 4. 1. Timing and NDVI magnitudes of breaks in the trend component of Sa Dragonera (treatment zone) and Mallorca (control zone) time series. The left and right limits of the breakpoint dates indicate a 95% confidence interval of date estimation. 1 = Timing indicated by year and month. Data format: Year (Month). 2: Difference between the NDVI value at the end of a linear model and the intercept of the next one. 3: Linear regression parameters of segments after the breakpoints date, where the intercept represents the starting NDVI, and the slope represents the greening (+) or browning (-) ratio of the vegetation. The parameters of the starting segment are omitted in this table.

Zone	Breakpoint	Breakpoints Dates			Change magnitude (absolute NDVI Units)	Linear regression parameters of trend component	
		2.5% CI limit	Breakpoint timing	97.5% CI limit		Intercepts	Slopes
Treatment	1st	2001(11)	2001(12)	2002(03)	0.109	0.442	0.008
	2nd	2007(12)	2008(04)	2008(05)	0.074	0.569	-0.022
	3rd	2013(01)	2013(02)	2013(04)	0.057	0.523	0.021
	4th	2016(01)	2016(02)	2016(06)	-0.063	0.521	0.007
Control	1st	2001(11)	2001(12)	2002(03)	0.091	0.453	0.005
	2nd	2007(11)	2008(11)	2008(12)	0.031	0.519	-0.014
	3rd	2012(12)	2013(01)	2013(09)	0.059	0.519	0.004

Together, the BFAST approaches consistently describe the dynamics of the vegetation and show similar shift dates of NDVI between zones, as well as the direction of the changes, and trends of the piecewise models. These results indicate that the variability of rainfall and water reserves were the main factors controlling the vegetation dynamics following the rat eradication campaign as observed in its previous data and in the control zone data. Furthermore, in terms of the magnitude of the changes and the recovery rates observed, there was no relationship between the elimination of rats and the processes of resistance or recovery of the studied vegetation of the islet

4. Discussion

The presented results indicate that the 2011 rodent eradication campaign in Sa Dragonera Islet (treatment zone) had a negligible effect on the primary production dynamics detected at the Landsat resolution scale. The observed changes in NDVI before and after the eradication campaign appear to be driven by water-related environmental events, which could be deemed characteristic of a Mediterranean system [43,53,55,97]. Positive changes detected are followed by segments with a negative or almost zero recovery rate. These patterns coincide with the transition of HDI from alert or pre-alert prolonged states to states of normality. These vegetation dynamics arise in regions with prolonged periods of water limitation interrupted by wet episodes [54] that may trigger a fast germination of short-lived plants and subsequent increase in NDVI followed by a gradual decrease [50]. Other papers such as [59] have used the visual comparison of the rain patterns with dates of abrupt changes of NDVI to evaluate the BFAST algorithm facing known flood events. In this study, we do not validate the dates of the abrupt changes observed due to hydrological factors, since we do not have enough temporal precision in the dates that categorise

the HDI. However, the abrupt and gradual change patterns in the NDVI time series of both treatments is used to reject the hypothesis that deratization drove changes in NDVI.

The comparison between the timing of eradication campaign with the timing of the first break following, indicated that BFAST was unable to detect abrupt changes in vegetation response caused by rat elimination. The gradual NDVI increase shown in the fourth segment in the treatment time series (Figure 4.7A) could reflect the recovery of the ecosystem. However, the BFAST algorithm indicated a non-significant linear relationship, which may have been a relic of noise rather than the signal [59], resulting in the detection of this abrupt change. It is not believed that this represents the response of the vegetation to the demise of rats. The choice of h parameter influences the decomposition of the time series, affecting the change detection process, which is based on signal-to-noise ratio. It is possible that the low h parameters caused the linear models to fit the noise rather than the signal, resulting in the detection of this abrupt change but being non-significant verifies our interpretation. We considered the optimal value of $h = 1/7$ following the recommendations of [59]. Values of h lower than $1/8$ generated additional changes with non-significant linear fits (for example, it identified negative abrupt breaks in 2011), and values greater than $1/6$ generated longer segments, which limited the level of detection detail (here it removed changes detected at the end of 2001). No seasonal changes were detected, however Seasonal-Trend decomposition (STL) showed that a seasonal component was present in the time series, therefore it was convenient to remove seasonal effects before analysing the long-term trends.

The BFAST method dates and quantifies the changes in vegetation from global to local scale, which can be geolocated pixel by pixel at the satellite spatial resolution

[43,55]. Often studies using BFAST validate results by prior knowledge of the study area or by subsequent field visits. Our study, however, has been carried out in an entirely remote manner where the NDVI refer to averaged pixels from the sample plots selected under strict spatial criteria, rather than to geolocated pixels. Thus, changes detected characterise the dynamics on the targeted area over time. Averaged pixels allow comparison of the time series of the study area with that of a control zone, where sampling plots that follow similar dynamics could be selected. By doing this the study overcomes the lack of information available about the previous state of the rodenticide campaign.

The presented results do, however, demonstrate that using BFAST is a suitable approach to detect abrupt and gradual changes in NDVI, for example due to the effects of rodenticide campaigns which are known to lead to recovery of vegetation productivity. Within the treatment zone the BFAST model dates and quantifies the NDVI abnormal behaviour, considering seasonal variations. In this study, we cannot conclusively attribute NDVI recovery, detectable on a 30m spatial scale across the treatment zone, to the eradication campaign, particularly as meteorological drivers in such settings are evident as the dominant influence.

The recovery of an island ecosystem invaded by rats must necessarily begin with their eradication. However, the time and rate of recovery depends on multiple factors such as the frequency, severity and duration of the impacts. There are some studies that have reported the recovery of the vegetation cover in deratized islands through field work, but in an extension and magnitude appreciable by the Landsat sensors. For example, eight years after the deratization of a small island in the Indian Ocean, they reported, through field work, an increase in vegetation cover (from 30% to 70%) validated through aerial images. However, it was due only to the regeneration of the

herbaceous stratus [29]. In a study to assess rodent eradication in the Montebello archipelago, Western Australia, vegetation density was monitored for 26 years with Landsat images [34], and the authors reported a trend of vegetation recovery on the islands just two years after rat eradication. Interestingly, and converse to the findings of our study, they observed that the positive relationship typically exhibited between precipitation and vegetation cover was nullified in the rat-infested islands [34].

That said, in the case of Sa Dragonera Islet, some signs of recovery have been described such as the presence of new plant species, the greater presence of other plants that were previously rare, or the greater abundance of arthropods [78].

The original hypothesis suggests the greening of vegetation, especially considering that plants can keep sprouts (and hence NDVI increment) after rat browsing demise. However, our results reflect the lack of change to primary production.

It appears likely that the lack of rat herbivory pressure that could lead to higher plant recruitment and increase in existing plant biomass, did not translate into an abrupt change in the NDVI time series; and that the NDVI values recorded in the Mediterranean ecosystem, before and after the eradication campaign, are principally driven by water-related environmental events. The remote sensing record would therefore offer no signs of long-term recovery.

The vegetation of Sa Dragonera Islet and Mallorca Island exhibit a long history of permanent pressures by natural and domestic animals plus recurrent natural and human-induced fires [79,80]. The herbivorous mammals such as *Myotragus balearicus* lived in Balears archipelago till its extinction shortly before the introduction of goats 4000 years ago [98]. Feral goats are currently common in Mallorca Island and they were also in Sa Dragonera Islet until its eradication in 1975 [69,70]. Thus, it could be suggested that the prolonged coexistence of the dominant

plant taxa with herbivores in Balears archipelago, might explain the resistance of vegetation dynamics to herbivory by rats in Dragonera Islet.

Ecosystem recovery is complex and involves cascading processes, and, when it has been severely impacted, recovery could take thousands of years [99,100]. Thus, the absence of remotely detectable NDVI recovery in the treatment zone may be due to the action of disturbance within an environment with inherently stressful conditions (e.g., xeric environment). The presence of black rats could go back several centuries [17] and contribute to disturbance through extremely high population densities. That, combined with historical anthropogenic activity make the islet ecosystem particularly susceptible to land degradation [101]. Therefore, due to an intense and prolonged disturbance the ecosystem compositions could have drastically changed, resulting in a limited recovery following removal of an early driver of degradation in the location [17,30,102,103].

Alternatively, the null response of the vegetation could be due to the fact that the pressure exerted by rats on the plants is not sufficiently high to impact the primary productivity of the island and therefore the recorded NDVI. It could be argued that the ecosystem tolerates the rat herbivore in an already naturally stressed environment [67,104], with most of the dominant plants in the landscape also being sprouting species adapted to browsing and associated disturbance [65–67,104]. To assume or discard this option, it would be necessary to have more detailed information on the situation prior to the arrival of the rats on the islet. Likewise, more detailed data on the influence of rats on the richness of plant species, growth rates and periods, seed production, and the consequent population recruitment on the islet would prove vital to deeper functional understanding.

Although records of the ecological past of the islet are sparsely available and limited, the evolution of the ecosystem following elimination of the rats can be monitored in this manner to determine long term trends. The effects of rats on the structure of vegetation are sufficiently reported in the literature, however monitoring eradication outcomes is sporadic and limited [32,35,40], and pre-management data is usually lacking [38]. Hence, this satellite-driven approach represents a consistent methodology that is critical to understanding the ongoing and evolving dynamics of island ecosystems following rat eradication.

5. Conclusion

This study is the first of its kind to examine the effectiveness of remote sensing and BFAST timeseries analysis in island ecosystems post black rat eradication. Given the general lack of reports assessing the effect of rat eradication on island ecosystems, a satellite approach to assess changes in vegetation productivity over time is proposed. Addressing this generalised information gap, the BFAST model is found to be an appropriate tool to monitor NDVI time series due to its sensitivity to reflect the long-term and short-term changes in vegetation growth at local scales accurately. To interpret the changes found, a 21-year time series of NDVI data extracted from satellite images was analysed and compared with hydrological data, which was found to be the likely driver of NDVI changes in water limited environments as is the case for our study area. These climatological influences are deemed to mask the detectable effects of rat eradication in remotely sensed NDVI data.

The BFAST results reveal that the primary production in the treatment area is sensitive to water cycles but not immediately to cessation of rat activity. In the short term there was no abrupt increase in vegetation primary productivity as a response to the

cessation of rat browsing with this significant ecological event being overshadowed by the state of water emergency that occurred close to the time of the eradication campaign. Nor were changes observed in the long term, since facing the aforementioned environmental stress events, the recovery rates in the treatment zone did not overcome those found in the control zone, rather, they continued to show similar trends. Changes may have only occurred at a small spatial scale, as evidenced by the reported field observations of the anecdotal studies in the area. Thus, given the spatial resolution of the core satellite data these changes had little impact on the averaged NDVI produced over the islet. Unlike other studies, changes were not widespread over the island's surface, so it is not possible to detect them at the scale at which Landsat sensors record. We suggest that the non-response of NDVI to rat eradication on Dragonera Islet is due to a high resistance of vegetation to rat predation achieved during a long period of colonisation in an already naturally stressed environment.

6. References

1. Richardson, D.M.; Pyšek, P.; Carlton, J.T. A compendium of essential concepts and terminology in invasion ecology. *Fifty years invasion Ecol. Leg. Charles Elton*, **2011**, 409–420.
2. Dukes, J.S.; Mooney, H.A. Does global change increase the success of biological invaders? *Trends Ecol. Evol.* 1999, *14*, 135–139.
3. Berger, J.J. Ecological Restoration and NonIndigenous Plant Species: A Review. *Restor. Ecol.* 1993, *1*, 74–82.
4. Tsutsumida, N.; Saizen, I.; Matsuoka, M.; Ishii, R. Land cover change detection in Ulaanbaatar using the breaks for additive seasonal and trend method. *Land*

2013, 2, 534–549, doi:10.3390/land2040534.

5. Vilà, M. Efectos de la introducción de especies vegetales en el funcionamiento de los ecosistemas terrestres. *Montes* **1999**, 55, 26–30.
6. Tershy, B.R.; Shen, K.W.; Newton, K.M.; Holmes, N.D.; Croll, D.A. The importance of islands for the protection of biological and linguistic diversity. *Bioscience* 2015, 65, 592–597.
7. Towns, D.R.; Atkinson, I.A.E.; Daugherty, C.H. Have the harmful effects of introduced rats on islands been exaggerated? *Biol. Invasions* **2006**, 8, 863–891, doi:10.1007/s10530-005-0421-z.
8. Howald, G.; Donlan, C.J.; Galván, J.P.; Russell, J.C.; Parkes, J.; Samaniego, A.; Wang, Y.; Veitch, D.; Genovesi, P.; Pascal, M.; et al. Invasive rodent eradication on islands. *Conserv. Biol.* **2007**, 21, 1258–1268, doi:10.1111/j.1523-1739.2007.00755.x.
9. Capizzi, D.; Bertolino, S.; Mortelliti, A. Rating the rat: global patterns and research priorities in impacts and management of rodent pests. *Mamm. Rev.* **2014**, 44, 148–162, doi:10.1111/MAM.12019.
10. Cheylan, G. Prédation du rat noir *Rattus rattus* sur les oiseaux de mer qui nichent dans les îles méditerranéennes. *Ann. Crop* **1985**, 2, 27–29.
11. Igual, J.M.; Forero, M.G.; Gomez, T.; Orueta, J.F.; Oro, & D. Rat control and breeding performance in Cory's shearwater (*Calonectris diomedea*): effects of poisoning effort and habitat features. *Anim. Conserv.* **2006**, 9, 59–65.
12. Atkinson, I.A. The spread of commensal species of *Rattus* to oceanic islands and their effects on island avifaunas. *ICPB Tech Publ*, **1985**, 3, 35–81.

13. Russell, J.C.; Holmes, N.D. Tropical island conservation: Rat eradication for species recovery. *Biol. Conserv.* **2015**, *185*, 1–7, doi:10.1016/j.biocon.2015.01.009.
14. Ruffino, L.; Russell, J.; Vidal, E. Anthropogenic subsidies mitigate environmental variability for insular rodents. *Oecologia* **2013**, *172*(3), 737–749, doi:10.1007/s00442-012-2545-z.
15. Harper, G.; Rutherford, M. Home range and population density of black rats (*Rattus rattus*) on a seabird island: A case for a marine subsidised effect? *N. Z. J. Ecol.* **2016**, *40*(2), 219–228, doi:10.20417/nzj ecol.40.25.
16. Opper, S.; McClelland, G.T.W.; Lavers, J.L.; Churchyard, T.; Donaldson, A.; Duffield, N.; Havery, S.; Kelly, J.; Proud, T.; Russell, J.C.; et al. Seasonal variation in movements and survival of invasive Pacific rats on sub-tropical Henderson Island: implications for eradication. *Int. Conf. Isl. Invasives 2017* **2019**, *62*, 200–208.
17. Ruffino, L.; Bourgeois, K.; Vidal, E.; Duhem, C.; Paracuellos, M.; Escribano, F.; Sposimo, P.; Baccetti, N.; Pascal, M.; Oro, D. Invasive rats and seabirds after 2,000 years of an unwanted coexistence on Mediterranean islands. *Biol. Invasions* **2009**, *11*, 1631–1651, doi:10.1007/s10530-008-9394-z.
18. Martin, J.L.; Thibault, J.C.; Bretagnolle, V. Black rats, island characteristics, and colonial nesting birds in the Mediterranean: Consequences of an ancient introduction. *Conserv. Biol.* **2000**, *14*, 1452–1466, doi:10.1046/j.1523-1739.2000.99190.x.
19. Traveset, A.; Nogales, M.; Alcover, J.A.; Delgado, J.D.; López-Darias, M.; Godoy, D.; Igual, J.M.; Bover, P. A review on the effects of alien rodents in

the Balearic (western Mediterranean sea) and Canary islands (eastern Atlantic ocean). *Biol. Invasions* **2009**, *11*, 1653–1670, doi:10.1007/s10530-008-9395-y.

20. Russell, J.C.; Jones, H.P.; Doug, ; Armstrong, P.; Courchamp, F.; Peter, ; Kappes, J.; Philip, ; Seddon, J.; Oppel, S.; et al. Importance of lethal control of invasive predators for island conservation. *islandconservation.org* **2016**, *30*, 670–672, doi:10.1111/cobi.12666.
21. Campbell, D.J.; Atkinson, I.A.E. Effects of kiore (*Rattus exulans* Peale) on recruitment of indigenous coastal trees on northern offshore islands of New Zealand. *J. Ren. Socieh New Zeal.* **1999**, *29*, 290, doi:10.1080/03014223.1999.9517597.
22. Borchert, M.I.; Jain, S.K. The effect of rodent seed predation on four species of California annual grasses. *Oecologia* **1978**, *33*, 101–113, doi:10.1007/BF00376999.
23. Shiels, A.B.; Drake, D.; Daehler, C.; Hunt, T.; Ticktin, T.; Pitt, W. *Ecology and impacts of introduced rodents(Rattus spp. and Mus musculus) in the Hawaiian islands*; 2010;
24. Grant-Hoffman, M.N.; Barboza, P.S. Herbivory in invasive rats: Criteria for food selection. *Biol. Invasions* **2010**, *12*, 805–825, doi:10.1007/s10530-009-9503-7.
25. Auld, T.D.; Hutton, I.; Ooi, M.K.J.; Denham, A.J. Disruption of recruitment in two endemic palms on Lord Howe Island by invasive rats. *Biol. Invasions* **2010**, *12*, 3351–3361, doi:10.1007/s10530-010-9728-5.
26. Campbell, D.J.; Atkinson, I.A.E. Depression of tree recruitment by the Pacific

- rat (*Rattus exulans* Peale) on New Zealand's northern offshore islands. *Biol. Conserv.* **2002**, *107*, 19–35, doi:10.1016/S0006-3207(02)00039-3.
27. Grant-Hoffman, M.N.; Mulder, C.P.; Bellingham, P.J. Effects of invasive rats and burrowing seabirds on seeds and seedlings on New Zealand islands. *Oecologia* **2010**, *162*(4), 1005–1016, doi:10.1007/s00442-009-1500-0.
28. Hunt, T. Rethinking the fall of Easter Island. New evidence points to an alternative explanation for a civilization's collapse. *Am. Sci.* **2006**, *94*, 412–419.
29. Le Corre, M.; Danckwerts, D.K.; Ringler, D.; Bastien, M.; Orlowski, S.; Morey Rubio, C.; Pinaud, D.; Micol, T. Seabird recovery and vegetation dynamics after Norway rat eradication at Tromelin Island, western Indian Ocean. *Biol. Conserv.* **2015**, *185*, 85–94, doi:10.1016/j.biocon.2014.12.015.
30. Weber, C. *Ecological Impacts of Invasive Rat Removal on Mediterranean Sea Islands. Graduate thesis, University of Michigan, Ann Arbor, Michigan, USA.*; 2014;
31. Blackburn, T.M.; Cassey, P.; Duncan, R.P.; Evans, K.L.; Gaston, K.J. Avian extinction and mammalian introductions on oceanic islands. *Science* (80-.). **2004**, *305*, 1955–1958, doi:10.1126/science.1101617.
32. Jones, H.P. Prognosis for ecosystem recovery following rodent eradication and seabird restoration in an island archipelago. *Ecol. Appl.* **2010**, *20*, 1204–1216, doi:10.1890/09-1172.1.
33. Block, W.M.; Franklin, A.B.; Ward, J.P.; Ganey, J.L.; White, G.C. Design and implementation of monitoring studies to evaluate the success of ecological restoration on wildlife. *Restor. Ecol.* **2001**, *9*, 293–303, doi:10.1046/j.1526-

100X.2001.009003293.x.

34. Lohr, C.; Van Dongen, R.; Huntley, B.; Gibson, L.; Morris, K. Remotely monitoring change in vegetation cover on the Montebello Islands, Western Australia, in response to introduced rodent eradication. *PLoS One* **2014**, *9*, 1–15, doi:10.1371/journal.pone.0114095.
35. Bastille-Rousseau, G.; Gibbs, J.P.; Campbell, K.; Yackulic, C.B.; Blake, S. Ecosystem implications of conserving endemic versus eradicating introduced large herbivores in the Galapagos Archipelago. *Biol. Conserv.* **2017**, *209*, 1–10, doi:10.1016/j.biocon.2017.02.015.
36. Graham, M.F.; Veitch, C.R. Changes in bird numbers on Tiritiri Matangi Island, New Zealand, over the period of rat eradication. *Turn. tide Erad. invasive species, Occas. Pap. IUCN Species Surviv. Comm. No. 27, IUCN, Gland. Switz. Cambridge, UK.* **2002**, 120–123.
37. McClelland, P.J. Eradication of Pacific rats (*Rattus exulans*) from Whenua Hou Nature Reserve (Codfish Island), Putauhinu and Rarotoka Islands, New Zealand. *Turn. tide Erad. invasive species, Occas. Pap. IUCN Species Surviv. Comm. No. 27, IUCN, Gland. Switz. Cambridge, UK.* **2002**, 173–181.
38. Towns, D.R.; Atkinson, I.A.E.; Daugherty, C.H. *Reconstructing the ambiguous: can island ecosystems be restored*; Ecological restoration of New Zealand islands. Department of Conservation, Ed.; Wellington, 1990;
39. Schweizer, D.; Jones, H.P.; Holmes, N.D. Literature Review and Meta-Analysis of Vegetation Responses to Goat and European Rabbit Eradications on Islands. *Pacific Sci.* **2016**, *70*, 55–71, doi:10.2984/70.1.5.
40. Jones, H.P.; Holmes, N.D.; Butchart, S.H.M.; Tershy, B.R.; Kappes, P.J.;

- Corkery, I.; Aguirre-Muñoz, A.; Armstrong, D.P.; Bonnaud, E.; Burbidge, A.A.; et al. Invasive mammal eradication on islands results in substantial conservation gains. *Proc. Natl. Acad. Sci. U. S. A.* **2016**, *113*, 4033–4038, doi:10.1073/pnas.1521179113.
41. Pettorelli, N.; Safi, K.; Turner, W. Satellite remote sensing, biodiversity research and conservation of the future. *Philos. Trans. R. Soc. B Biol. Sci.* **2014**, *369*, doi:10.1098/rstb.2013.0190.
42. Sader, S.A.; Jin, S. MODIS time-series imagery for forest disturbance detection and quantification of patch size effects Article in Remote Sensing of Environment · December 2005 SEE PROFILE MODIS time-series imagery for forest disturbance detection and quantification of patch size effects. *Elsevier*, doi:10.1016/j.rse.2005.09.017.
43. Verbesselt, J.; Hyndman, R.; Newnham, G.; Culvenor, D. Detecting trend and seasonal changes in satellite image time series. *Remote Sens. Environ.* **2010**, *114*, 106–115, doi:10.1016/j.rse.2009.08.014.
44. Pettorelli, N.; Vik, J.O.; Mysterud, A.; Gaillard, J.M.; Tucker, C.J.; Stenseth, N.C. Using the satellite-derived NDVI to assess ecological responses to environmental change. *Trends Ecol. Evol.* 2005, *20*, 503–510.
45. Sellers, P.J. Canopy reflectance, photosynthesis and transpiration. *Int. J. Remote Sens.* **1985**, *6*, 1335–1372, doi:10.1080/01431168508948283.
46. Reed, B.C.; Brown, J.F.; VanderZee, D.; Loveland, T.R.; Merchant, J.W.; Ohlen, D.O. Measuring phenological variability from satellite imagery. *J. Veg. Sci.* **1994**, *5*, 703–714, doi:10.2307/3235884.
47. Running, S.W. Estimating Terrestrial Primary Productivity by Combining

Remote Sensing and Ecosystem Simulation. In; 1990; pp. 65–86.

48. Myneni, R.B.; Hall, F.G.; Sellers, P.J.; Marshak, A.L. The interpretation of spectral vegetation indexes. *IEEE Trans. Geosci. Remote Sens.* **2019**, *33*, 481–486, doi:10.1109/tgrs.1995.8746029.
49. Potter, C.; Tan, P.N.; Steinbach, M.; Klooster, S.; Kumar, V.; Myneni, R.; Genovese, V. Major disturbance events in terrestrial ecosystems detected using global satellite data sets. *Glob. Chang. Biol.* **2003**, *9*, 1005–1021, doi:10.1046/j.1365-2486.2003.00648.x.
50. De Jong, R.; Verbesselt, J.; Zeileis, A.; Schaepman, M.E. Shifts in global vegetation activity trends. *Remote Sens.* **2013**, *5*, 1117–1133, doi:10.3390/rs5031117.
51. Gaitán, J.J.; Bran, D.; Oliva, G.; Ciari, G.; Nakamatsu, V.; Salomone, J.; Ferrante, D.; Buono, G.; Massara, V.; Humano, G.; et al. Evaluating the performance of multiple remote sensing indices to predict the spatial variability of ecosystem structure and functioning in Patagonian steppes. *Ecol. Indic.* **2013**, *34*, 181–191, doi:10.1016/j.ecolind.2013.05.007.
52. Helman, D.; Mussery, A.; Lensky, I.M.; Leu, S. Detecting changes in biomass productivity in a different land management regimes in drylands using satellite-derived vegetation index. *Soil Use Manag.* **2014**, *30*, 32–39, doi:10.1111/sum.12099.
53. Alcaraz-Segura, D.; Cabello, J.; Paruelo, J. Baseline characterization of major Iberian vegetation types based on the NDVI dynamics. *Plant Ecol. 2008 2021* **2008**, *202*, 13–29, doi:10.1007/S11258-008-9555-2.
54. Vicente-Serrano, S.M.; Gouveia, C.; Camarero, J.J.; Beguería, S.; Trigo, R.;

- López-Moreno, J.I.; Azorín-Molina, C.; Pasho, E.; Lorenzo-Lacruz, J.; Revuelto, J.; et al. Response of vegetation to drought time-scales across global land biomes. *Proc. Natl. Acad. Sci. U. S. A.* **2013**, *110*, 52–57, doi:10.1073/pnas.1207068110.
55. Verbesselt, J.; Zeileis, A.; Herold, M. Near real-time disturbance detection using satellite image time series. *Remote Sens. Environ.* **2012**, *123*, 98–108, doi:10.1016/j.rse.2012.02.022.
56. Geng, L.; Che, T.; Wang, X.; Wang, H. Detecting spatiotemporal changes in vegetation with the BFAST model in the Qilian Mountain region during 2000–2017. *Remote Sens.* **2019**, *11*, doi:10.3390/rs11020103.
57. Gillespie, T.W.; Ostermann-Kelm, S.; Dong, C.; Willis, K.S.; Okin, G.S.; MacDonald, G.M. Monitoring changes of NDVI in protected areas of southern California. *Ecol. Indic.* **2018**, *88*, 485–494, doi:10.1016/j.ecolind.2018.01.031.
58. Fang, X.; Zhu, Q.; Ren, L.; Chen, H.; Wang, K.; Peng, C. Large-scale detection of vegetation dynamics and their potential drivers using MODIS images and BFAST: A case study in Quebec, Canada. *Remote Sens. Environ.* **2018**, *206*, 391–402, doi:10.1016/j.rse.2017.11.017.
59. Watts, L.M.; Laffan, S.W. Effectiveness of the BFAST algorithm for detecting vegetation response patterns in a semi-arid region. *Remote Sens. Environ.* **2014**, *154*, 234–245, doi:10.1016/j.rse.2014.08.023.
60. Bernardino, P.N.; De Keersmaecker, W.; Fensholt, R.; Verbesselt, J.; Somers, B.; Horion, S. Global-scale characterization of turning points in arid and semi-arid ecosystem functioning. *Glob. Ecol. Biogeogr.* **2020**, *29*, 1230–1245, doi:10.1111/geb.13099.

61. Chen, L.; Michishita, R.; Xu, B. Abrupt spatiotemporal land and water changes and their potential drivers in Poyang Lake, 2000-2012. *ISPRS J. Photogramm. Remote Sens.* **2014**, *98*, 85–93, doi:10.1016/j.isprsjprs.2014.09.014.
62. Spanish Meteorology Agency – AEMET Government of Spain, 2021 Available online: <http://www.aemet.es/> (accessed on Feb 25, 2021).
63. Ginés, Á.; Ginés, J.; Gómez-Pujol, L.; Onac, B.; Fornós, J. *Mallorca: a Mediterranean benchmark for Quaternary studies*; Societat d’Història Natural de les Balears, Ed.; 2012;
64. Vogiatzakis, I.N.; Pungetti, G.; Mannion, A.M. (Eds. *Mediterranean island landscapes: natural and cultural approaches* ; Springer Science & Business Media, Ed.; 2008; Vol. 9;.
65. Focardi, S.; Tinelli, A. Herbivory in a Mediterranean forest: browsing impact and plant compensation. *Acta Oecologica* **2005**, *28*, 239–247, doi:10.1016/J.ACTAO.2005.05.010.
66. Bashan, D.; Bar-Massada, A. Regeneration dynamics of woody vegetation in a Mediterranean landscape under different disturbance-based management treatments. *Appl. Veg. Sci.* **2017**, *20*, 106–114, doi:10.1111/AVSC.12274.
67. Dell, B.; Hopkins, A. j. M.; Lamont, B.B. *Resilience at the level of the plant community. In Resilience in mediterranean-type ecosystems*; Tasks for vegetation science; Springer Netherlands: Dordrecht, 1986; Vol. 16; ISBN 978-94-010-8637-0.
68. Morey, M.; Ruiz-Pérez, M. The Balearic Islands. In: *Mediterranean Island Landscapes*. In *Springer, Dordrecht*; Springer, D., Ed.; 2008; pp. 271–296.
69. CAMPBELL, K.; DONLAN, C.J. Feral Goat Eradications on Islands. *Conserv.*

- Biol.* **2005**, *19*, 1362–1374, doi:10.1111/j.1523-1739.2005.00228.x.
70. Genovesi, P. Eradications of invasive alien species in Europe: a review. *Biol. Invasions 2004 71* **2005**, *7*, 127–133, doi:10.1007/S10530-004-9642-9.
71. Mayol, J.; Mayol, M.; Domenech, O.; Oliver, J.; McMinn, M.; Rodríguez, A. Aerial broadcast of rodenticide on the island of Sa Dragonera (Balearic Islands, Spain). A promising rodent eradication experience on a Mediterranean island. *Aliens Invasive Species Bull.* **2012**, *32*, 29–32.
72. GRANJON, L.; CHEYLAN, G.; DURYADI, D.; PIRAUD, N.; GANEM, G. Premières données sur l'écologie et l'évolution des populations de rats noirs (*Rattus rattus*, L. 1758) des îles Cerbicale (Corse du Sud). *Trav. Sci. du Parc Nat. régional des réserves Nat. Corse* **1992**, *39*, 97–111.
73. NATURA 2000 Standard Data Form Available online: <https://natura2000.eea.europa.eu/natura2000/SDF.aspx?site=ES0000221> (accessed on Feb 24, 2021).
74. BOIB núm. 73 de 19 de juny de 2001 *Pla Rector d'Ús i Gestió del Parc natural de sa Dragonera*; 2001; pp. 9181–9182;.
75. McMinn, M.; Sevilla, G.; Rodríguez, A.; Pons, G.X. Verificación de la presencia de roedores en el Parque Natural de sa Dragonera. *Soc. d'Història Nat. les Balear.* **2017**.
76. Grivé, M.M. Acciones con aves marinas 2010 *Phalacrocorax aristotelis* Cormorán Moñudo Acciones aves marinas 2009 *Phalacrocorax aristotelis* Cormorán Moñudo. **2010**, 1–13.
77. Russell, J.C.; Beaven B, B.M.; Mackay, J.W.B.; Towns, D.R.; Clout, M.N. Testing island biosecurity systems for invasive rats. *CSIRO* **2008**,

doi:10.1071/WR07032.

78. Alomar, G.; Mayol, M.; González, J.M. Notes naturalístiques del parc natural de sa Dragonera (2011-2014). *Monogr. la Soc. d'Historia Nat. les Balear.* **2015**, *2015-Janua*, 355–358.
79. Alcover, J.A.; Alcover, J.A. The First Mallorcans: Prehistoric Colonization in the Western Mediterranean. *J. World Prehistory* **2008**, *21*, 19–84, doi:10.1007/S10963-008-9010-2.
80. Seguí, B.; Payeras, L.; Ramis, D.; Martínez, A.; Delgado, J.V.; Quiroz, J. La cabra salvaje mallorquina: Origen, genética, morfología, notas ecológicas e implicaciones taxonómicas. *Bolleti la Soc. d'Historia Nat. les Balear.* **2005**, *48*, 121–151.
81. Landsat 7 science data users handbook; 1998; USGS... - Google Acadèmic.
82. Gutman, G.G. Vegetation indices from AVHRR: An update and future prospects. *Remote Sens. Environ.* **1991**, *35*, 121–136, doi:10.1016/0034-4257(91)90005-Q.
83. Hijmans, R.J. raster: Geographic Data Analysis and Modeling. R package version 3.5-9. *Cran* 2021.
84. R Core Team (2021). R: A language and environment for statistical computing. R Foundation for Statistical Computing, Vienna, Austria. URL <https://www.R-project.org/>.
85. Gromny, E.; Lewiński, S.; Rybicki, M.; Malinowski, R.; Krupiński, M.; Nowakowsk, A.; Jenerowicz, M. Creation of training dataset for Sentinel-2 land cover classification. In Proceedings of the Photonics Applications in Astronomy, Communications, Industry, and High-Energy Physics Experiments

- 2019; Romaniuk, R.S., Linczuk, M., Eds.; SPIE, 2019; Vol. 11176, p. 106.
86. North, M.A. A method for implementing a statistically significant number of data classes in the Jenks algorithm. In Proceedings of the 6th International Conference on Fuzzy Systems and Knowledge Discovery, FSKD 2009; 2009; Vol. 1, pp. 35–38.
87. Thomas, W. A three-dimensional model for calculating reflection functions of inhomogeneous and orographically structured natural landscapes. *Remote Sens. Environ.* **1997**, *59*, 44–63, doi:10.1016/S0034-4257(96)00078-8.
88. Verbesselt, J.; Jönsson, P.; Lhermitte, S.; Van Aardt, J.; Coppin, P. Evaluating satellite and climate data-derived indices as fire risk indicators in savanna ecosystems. *IEEE Trans. Geosci. Remote Sens.* **2006**, *44*, 1622–1632, doi:10.1109/TGRS.2005.862262.
89. Chen, J.; Jönsson, P.; Tamura, M.; Gu, Z.; Matsushita, B.; Eklundh, L. A simple method for reconstructing a high-quality NDVI time-series data set based on the Savitzky-Golay filter. *Remote Sens. Environ.* **2004**, *91*, 332–344, doi:10.1016/j.rse.2004.03.014.
90. Zeng, L.; Wardlow, B.D.; Xiang, D.; Hu, S.; Li, D. A review of vegetation phenological metrics extraction using time-series, multispectral satellite data. *Remote Sens. Environ.* **2020**, *237*, doi:10.1016/j.rse.2019.111511.
91. Stanimirova, R.; Cai, Z.; Melaas, E.K.; Gray, J.M.; Eklundh, L.; Jönsson, P.; Friedl, M.A. An empirical assessment of the MODIS land cover dynamics and TIMESAT land surface phenology algorithms. *Remote Sens.* **2019**, *11*, 2201, doi:10.3390/rs11192201.
92. Kennedy, R.E.; Andréfouët, S.; Cohen, W.B.; Gómez, C.; Griffiths, P.; Hais,

- M.; Healey, S.P.; Helmer, E.H.; Hostert, P.; Lyons, M.B.; et al. Bringing an ecological view of change to Landsat-based remote sensing. *Front. Ecol. Environ.* **2014**, *12*, 339–346, doi:10.1890/130066.
93. Funk, C.; Budde, M.E. Phenologically-tuned MODIS NDVI-based production anomaly estimates for Zimbabwe. *Remote Sens. Environ.* **2009**, *113*, 115–125, doi:10.1016/j.rse.2008.08.015.
94. Vrieling, A.; de Beurs, K.M.; Brown, M.E. Variability of African farming systems from phenological analysis of NDVI time series. *Clim. Change* **2011**, *109*, 455–477, doi:10.1007/s10584-011-0049-1.
95. Conselleria medi ambient i pesca. Direcció general recurs hídrics. *Plan especial de actuación en situaciones de alerta y eventual sequía*; Palma de Malloca, 2017;
96. von Keyserlingk, J.; de Hoop, M.; Mayor, A.G.; Dekker, S.C.; Rietkerk, M.; Foerster, S. Resilience of vegetation to drought: Studying the effect of grazing in a Mediterranean rangeland using satellite time series. *Remote Sens. Environ.* **2021**, *255*, 112270, doi:10.1016/j.rse.2020.112270.
97. Verbesselt, J.; Hyndman, R.; Zeileis, A.; Culvenor, D. Phenological change detection while accounting for abrupt and gradual trends in satellite image time series. *Remote Sens. Environ.* **2010**, *114*, 2970–2980, doi:10.1016/j.rse.2010.08.003.
98. ALCOVER, J.A.; PEREZ-OBIOL, R.; YLL, E.-I.; BOVER, P. The diet of *Myotragus balearicus* Bate 1909 (Artiodactyla: Caprinae), an extinct bovid from the Balearic Islands: evidence from coprolites. *Biol. J. Linn. Soc.* **1999**, *66*, 57–74, doi:10.1111/j.1095-8312.1999.tb01917.x.

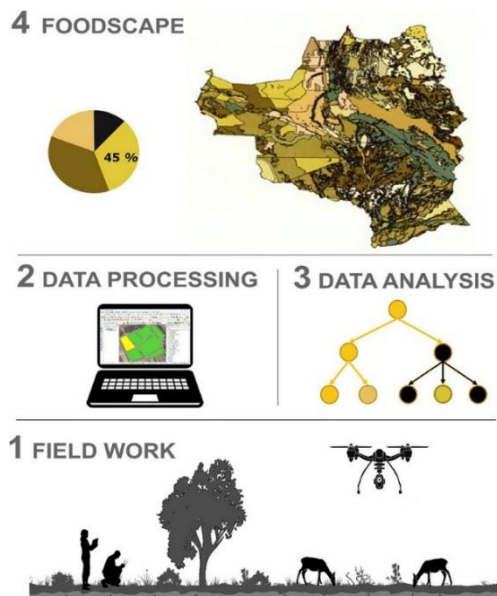
99. Dobson, A.P.; Bradshaw, A.D.; Baker, A.J.M. Hopes for the future: Restoration ecology and conservation biology. *Science* (80-.). **1997**, *277*, 515–522, doi:10.1126/science.277.5325.515.
100. Foley, J.A.; DeFries, R.; Asner, G.P.; Barford, C.; Bonan, G.; Carpenter, S.R.; Chapin, F.S.; Coe, M.T.; Daily, G.C.; Gibbs, H.K.; et al. Global consequences of land use. *Science* (80-.). 2005, *309*, 570–574.
101. Ginés, À.; Ginés, J. La Cova de sa Font (o Cova des Moro) i l'origen del topònim de s' illa de sa Dragonera: una hipòtesi espeleològica. *Endins: publicació d'espeleologia* **2010**, 9–18.
102. Zavaleta, E.S.; Hobbs, R.J.; Mooney, H.A. Viewing invasive species removal in a whole-ecosystem context. *Trends Ecol. Evol.* **2001**, *16*, 454–459, doi:10.1016/S0169-5347(01)02194-2.
103. Strayer, D.L.; Eviner, V.T.; Jeschke, J.M.; Pace, M.L. Understanding the long-term effects of species invasions. *Trends Ecol. Evol.* 2006, *21*, 645–651.
104. Blondel, J.; Aronson, J.; Bodiou, J.; Boeuf, G. *The Mediterranean region: biological diversity in space and time*; 2010;

5. Chapter 3

Remote mapping of foodscapes using sUAS and a low cost BG-NIR sensor

Laura Alonso-Martínez, Miguel Ibañez-Álvarez, Matthew Brolly, Niall G. Burnside, Juan A. Calleja, Marta Peláez, Aida López-Sánchez, Jordi Bartolomé, Helena Fanlo, Santiago Lavín, Ramón Perea, Emmanuel Serrano. 2020. Remote mapping of foodscapes using sUAS and a low cost BG-NIR sensor. *Science of the Total Environment*, 718: 137357.

<https://doi.org/10.1016/j.scitotenv.2020.137357>¹²



¹ The citation in this chapter follows the citation style of the Science of The Total Environment journal.

² This scientific publication declares an equal contribution of the first two authors. A declaration signed by Laura Alonso-Martínez guarantees the right to use this article as a chapter of this thesis. See supplementary material for chapter 3, page 182.

Abstract

The assessment of landscape condition for large herbivores, also known as foodscapes, is fast gaining interest in conservation and landscape management programs worldwide. Although traditional approaches for assessment of landscape condition are now being replaced by satellite imagery, several technical issues, such as the selection of the optimum sensor, still need to be addressed before full standardisation of remote sensing methods to capture the availability of vegetal resources. In this work we present a low-cost method, based on the use of a modified blue/green/near-infrared (BG-NIR) camera housed on a small-Unmanned Aircraft System (sUAS), to create foodscapes for a generalist Mediterranean ungulate: the Iberian Ibex (*Capra pyrenaica*). The work was performed in an enclosure covered by natural Mediterranean vegetation in the Tortosa i Beceit National Game Reserve, Northeast Spain. Faecal cuticle micro-histological analyses was used to assess the dietary preferences of ibexes and then individuals of the most common plant species (n = 19) were georeferenced to use as test samples. Because of the seasonal pattern in vegetation activity, based on the NDVI (Smooth term Month = 21.5, p-value < 0.01, R² = 43%, from a GAM), images were recorded in winter and spring to represent contrasting vegetation phenology using two flight heights above ground level (30 and 60 m). Additionally, images were processed at multiple resolutions (1.4, 1.5, 3.5 pixels/cm). Boosted Trees, a form of stochastic gradient boosting, was used to classify plant taxa, using t spectral reflectance data, to create a foodscape of the study area. The number of target species, the sampling season, the height of flight and the image resolution were analysed to determine the accuracy of mapping the foodscape. The highest classification error (70.66%) was present when classifying all plant species at 3.0 pixels/cm resolution from acquisitions at 30 m height. The lowest error (18.7%),

however, was present when predicting plants preferred by ibexes (e.g., *Cistus albidus*, *Erica multiflora*, Fagaceae and Graminoids), at 3.5 pixels/cm resolution acquired at 60 m height. This methodology can help to successfully monitor food availability and seasonality and to identify individual species. Better results are expected by incorporating more complex cameras into the analysis but with the requirement of higher budget costs that may reduce accessibility and up-take of remotely based methodologies.

Key words: *Capra pyrenaica*, Food resources monitoring, Remote sensing, sUAS, Vegetation assessment

1. Introduction

The spatiotemporal assessment of food resources for large herbivores, also called foodscapes is fast gaining interest within landscape and wildlife management, and associated research agendas worldwide. Knowing the distribution and availability of specific plants (i.e., used by ungulates see Espunyes et al., (2019a)), has become essential not only to understand population dynamics of herbivores but also those of their predators (Oates et al., 2019; Peters et al., 2019; Searle et al., 2007). Mapping vegetation is also essential for ecologists (Moore et al., 2010) and wildlife conservation agents (Schweiger et al., 2015a). Likewise, plant biodiversity conservation strongly depends on the interaction between plants and large herbivores, among others, (Boulanger et al., 2018; Stout et al., 2018) and the modelling of these interactions is fast gaining interest (Weisberg et al., 2010) ; particularly by exploring plant communities at different spatial and temporal scales (Golodets et al., 2011; Schweiger et al., 2015a). Assessment of foodscapes is also of major concern for forest managers, as both wild and domestic ungulates influence forest regeneration, tree

growth and forest development (Bergqvist et al., 2018; Rooney et al., 2015; López-Sánchez et al. 2017; Valle Júnior et al., 2019). Vegetation modulates both habitat and diet selection in large herbivores, which in turn affects the sign (mutualist vs. antagonist) and strength of plant-herbivore interactions (Gill 1992; Perea et al. 2013) and their associated ecosystem services and disservices (Velamazán et al. 2019). In addition ungulate species serve societal needs as game animals or subsistence foods, and can also affect agricultural crops which add importance to the understanding of nutritional resources and habitat use of large herbivores (Rowland et al., 2018; Duparc et al., 2019).

Traditionally, vegetation cover mapping has been done using field-based or *in situ* measurements (Karl et al., 2011). Although field studies are still required for calibration, and validation of other indirect approaches (e.g., based on remote sensing), they are time-consuming and often unfeasible when covering large areas. This is complicated further when studying complex landscapes across different seasons and years (Manousidis et al., 2016; Moore et al., 2010; Petersen et al., 2014; Royo et al., 2017). Remote sensing is thus becoming the main alternative to overcome the limitations of, and complement the advantages of, field-based study (Kerr and Ostrovsky, 2003; Pettorelli, 2013a; Sankey et al., 2019; Skidmore et al., 2010). In fact, satellite derived-measurements are becoming popular for mapping vegetation cover, structure, composition, and condition in wide geographic areas and over long time periods (Harris et al., 2014, Wachendorf et al., 2017). However, several technical issues need to be addressed before remote sensing approaches can be fully established to create foodscapes. In homogeneous landscapes, for example, remote sensing methods are useful for mapping specific food resources (e.g., lichens in tundra used by reindeer, see Falldorf et al., 2014), or linking the greenness of mixed-grass

communities to diet quality of alpine ungulates (Schweiger et al., 2015b; Villamuelas et al., 2016). Few efforts, however, have been made to create foodscapes in complex, bushy and encroached landscapes such as those common in the Mediterranean region. To date, the most ambitious contributions in this area of science have achieved the assessment of the nutritional quality of specific tree species commonly used by African ungulates (Skidmore and Ferwerda, 2008), and by Australian marsupials (Youngentob et al., 2012). Implementation and evaluation of the use of remote sensing to assess the availability of specific woody species used by ungulates in complex landscapes are still scarce but necessary.

One alternative, to gain definition in such heterogeneous environments, is the use of hyperspectral sensors set in unmanned aircraft systems (UAS, see Beeri et al., 2007; Schweiger et al., 2015b; Skidmore et al., 2010; Youngentob et al., 2012), or in combination with lidar (Insua et al., 2019; Lone et al., 2014; Pullanagari et al., 2018). Lamentably, these approaches are still expensive and remain outside of the budget capabilities of most organisations and companies, as well as government-funded bodies. Additionally, they show complexities that require additional expertise which inhibits the broader uptake and use by non-expert researchers and land managers alike. Thus, timely research in this field of remote sensing is required to support decision making, oriented towards the most appropriate, timely and low-cost methods available while also offering suitably high levels of accuracy (Wachendorf et al., 2017). Furthermore, although there are studies focused on estimating primary production and nutrient content, few of them integrate quality assessment and dietary species identification (food availability), and almost no studies focus simultaneously on heterogeneous environments and wide-ranging feeders.

In any case, several methodological issues have to be solved to create foodscapes based on remote sensing. For example, when using UAS mounted sensors, it is important to define the altitude above ground level (AGL) to ensure coverage of the study area while also balancing against the pixel size and subsequent spatial resolution requirements of the study (Tømmervik et al., 2014). Additionally, the spectral range and resolution requirements must be met by the sensor to ensure that detailed spectral responses for each pixel can be obtained. This is particularly relevant to accurately distinguish plant species and monitor their spectral responses and variations across different seasons (Hesketh and Sánchez-Azofeifa, 2012).

For these reasons, this study aims to address both challenges; heterogeneous environmental assessment and mixed feeder diet classification, using a simple and low cost 3 spectral band camera (modified to detect Blue, Green, and Near-Infrared (BG-NIR)) mounted on a small-Unmanned Aircraft System (sUAS). The study seeks to create a foodscape assessment for a mixed feeder ungulate, the Iberian Ibex (*Capra pyrenaica*), in a heterogeneous Mediterranean scrubland. Many sUAS are low-cost machines capable of carrying a wide range of sensors and imaging equipment to work in complex and heterogeneous scenarios (Anderson and Gaston, 2013), and similar sensors have successfully been employed in other vegetation studies (e.g., Pekkonen and Laakso, 2012; Gillan et al., 2019; Lu and He, 2017; Strong et al., 2017).

The Iberian Ibex is a mixed feeder with a diet including herbaceous and woody species (Alados and Escos, 1987; Martínez et al. 1985; Martínez and Martínez, 1987; Granados et al. 2001). This mountain ungulate shows great dietary plasticity but is influenced by plant phenology (Del et al., 1994; Martínez, 2014) and landscape characteristics (Martínez and Martínez, 1987; Moco et al. 2014; Perea et al. 2015).

In this paper, the primary aim is to determine the feasibility of remotely classifying Mediterranean plant species, in two periods of contrasting phenology, growing in a high diversity and physiognomically heterogeneous plant community, with special focus on the plants grazed or browsed by the Iberian Ibex diet. We do so by using a novel methodology and low budget equipment and seek to set a basis for further remote studies aimed at diet quality in complex environments.

2. Materials and methods

2.1. Study area

The study was undertaken in the National Game Reserve ‘‘Ports de Tortosa i Beseit’’ (NGRPTB) in Catalonia, northeast Spain (40°46’08’’ N, 0°20’04’’ E, 450 m. a.s.l., Figure 4.1). The average temperature in winter is from 0.4°C to 10°C and in summer from 11°C to 25°C. Precipitation is concentrated in spring and autumn, with a mean rainfall of 133.7mm and 116.6 mm respectively. Summer is characterised by drought conditions, with an average precipitation of 29.97mm (Meteocat, 2019).

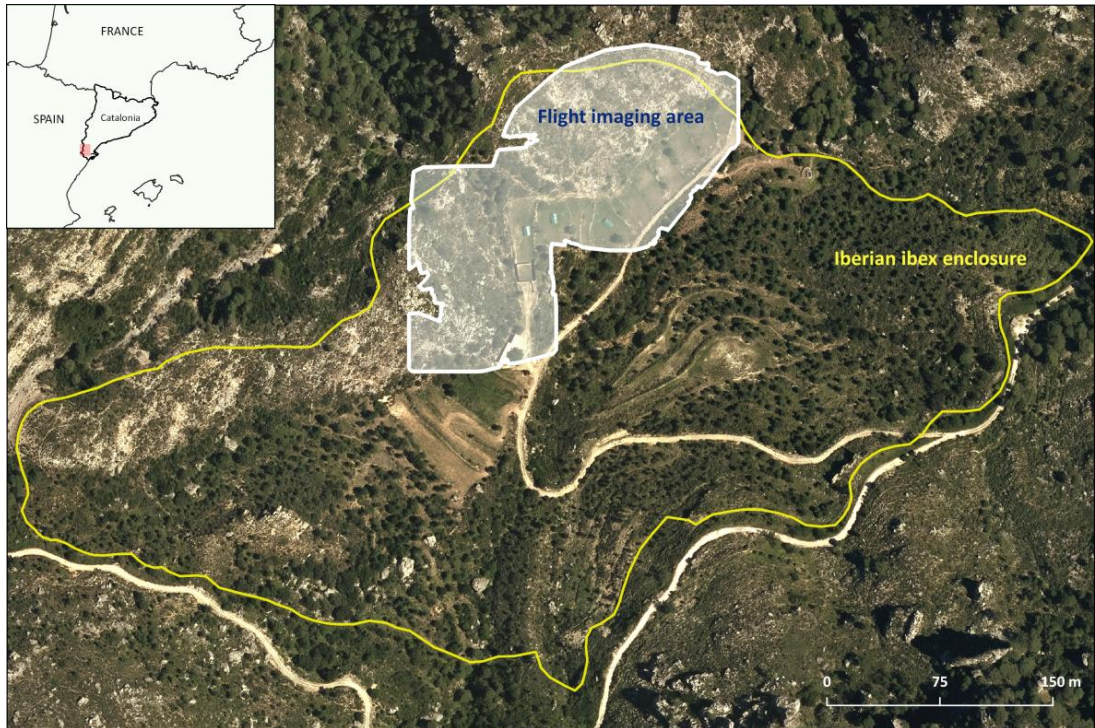


Figure 5. 1. The study area is placed in the National Game Reserve “Ports de Tortosa i Beseit” (NGRPTB) in Catalonia, northeast Spain ($40^{\circ}46'08''$ N, $0^{\circ}20'04''$ E, 450m.a.s.l.) marked in the upper inset. The yellow line marks the Iberian Ibex enclosure. The white area indicates the flight area. (For interpretation of the references to colour in this figure legend, the reader is referred to the web version of this article.)

The study area is characterised by a Mediterranean sclerophyllous woody landscape, dominated by *Quercus ilex* and a dense scrubland integrated by more than 30 woody plants codominated by *Pistacia lentiscus*, *Erica multiflora*, *Quercus coccifera*, *Rosmarinus officinalis*, *Genista scorpius*, and *Ulex parviflorus*. Natural and planted Pine stands and isolated individuals (*Pinus nigra* and *Pinus pinaster*) were also present across the study area. More specifically, the investigation was conducted in a fenced scientific enclosure of 17 ha (see Figure 5.1), which maintained an introduced herd of 18 Iberian Ibexes. The enclosure facilitated the control of Ibex population numbers and represented all relevant vegetation communities and plant species typical of this Mediterranean landscape.

2.2. Field data collection

Field data were collected in both June 2018 and March 2019. The June period was selected to evaluate plants with new and well developed shoots and leaves, and the March period represented an inactive period (late winter) with plants harboring old shoots and leaves. It is hypothesised that spectral variations will be apparent across all species on the two dates. In particular, higher NDVI values are expected in winter than in spring because the higher photosynthetically active radiation of evergreen Mediterranean plants (Garbulsky et al., 2013).

Inside the study enclosure, two sites were selected randomly, and 11 plots of 15x15m were randomly distributed to obtain a representative vegetation sample from within the enclosure. Up to 20 individuals, of the most representative plant species in the area were sampled; and the height, shape, diameter of the vegetative crown and phenological stage were recorded and specifically sampled (for subsequent discernment in aerial imagery, Figure 5.2). The location of sampled individuals was recorded using a differential-GPS (Leica GS07) for image matching and all species coded for analysis (see Table 5.1). A total of 19 plant species (from 12 family groups) were identified and sampled in the study sites within the enclosure. The number of individuals sampled ranged between 6 and 20 dependent upon species and vegetation state (see Table 5.1 and Figure 5.2). In addition, plant fragments were collected for further cuticle micro-histological analysis with up to 10 plants of each diet species sampled.

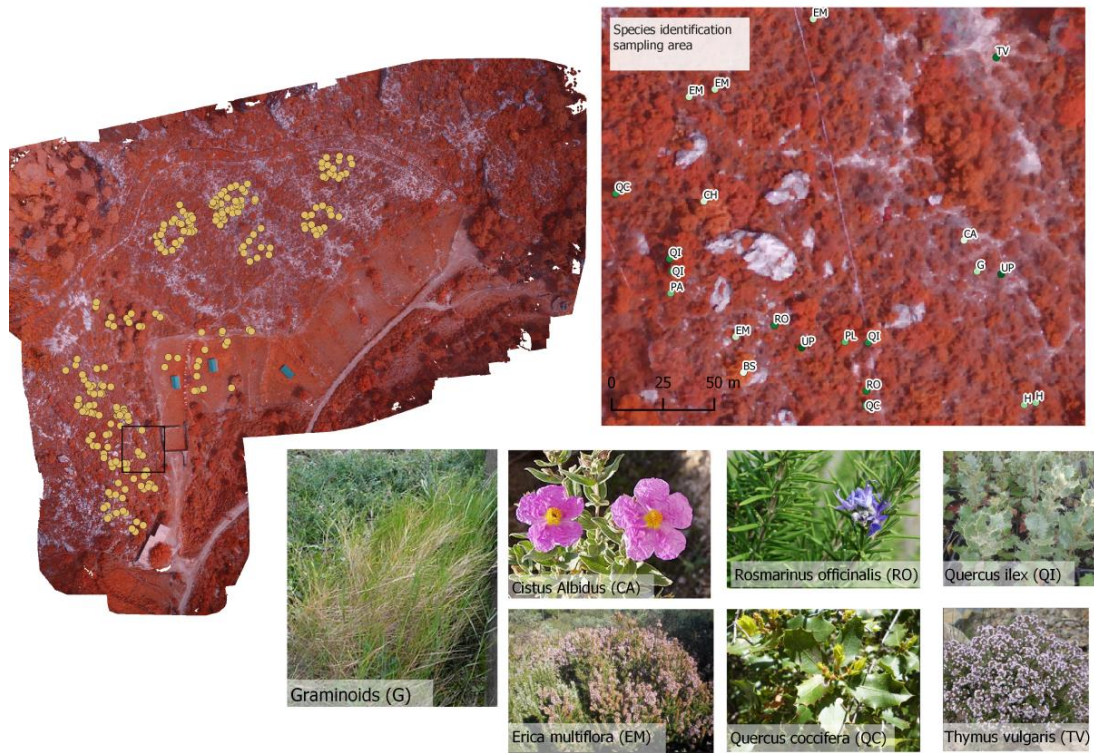


Figure 5. 2. Field sampling in the Iberian Ibex enclosure in the NGRPTB. Up to 20 individuals of the most representative species of the area were marked with a dGPS. In sets present the species most consumed by Iberian ibex in the enclosure.

Finally, 10 fresh Ibex faecal samples were collected from around the enclosure. Fresh faecal samples were placed in individual plastic bags, labelled and then transported via a cool-box to the laboratory. Once at the laboratory, samples were stored in a freezer, at -20°C , until further processing.

Table 5. 1. Species and number of individuals (n) sampled in NGRPTB Iberian ibex enclosure. species are grouped by families and given a code to simplify the interpretation of the consequent analysis. Plant life-forms agree with Raunkier's classification (1934).

Family	Specie	CODE	n	Physiognomy
Amacardiaceae	<i>Pistacia lentiscus</i>	PL	20	Evergreen microphanerophyte with compound broad-leaves
Buxaceae	<i>Buxus sempervirens</i>	BS	6	Evergreen microphanerophyte with simple broad-leaves
Cistaceae	<i>Cistus albidus</i>	CA	8	Evergreen nanophanerophyte with simple broad-leaves covered by dense white tomentous

	<i>Helianthemum marifolium</i>	H	8	Evergreen loosely branched chamaephyte with tiny (< 10x10 mm) simple and hairy broad-leaves
Cupressaceae	<i>Juniperus oxycedrus</i>	JO	20	Evergreen microphanerophyte with simple needle-leaves.
Ericaceae	<i>Erica multiflora</i>	EM	20	Evergreen nanophanerophyte with tiny (< 10 mm length) simple linear-leaves
Fageceae	<i>Quercus coccifera</i>	QC	20	Evergreen microphanerophyte with simple broad-leaves
	<i>Quercus ilex</i>	QI	20	Evergreen mesophanerophyte with simple broad-leaves
Labiatae	<i>Rosmarinus officinalis</i>	RO	20	Evergreen nanophanerophyte with simple linear-leaves
	<i>Thymus vulgaris</i>	TV	20	Evergreen chamaephyte with tiny (< 5 mm length) simple linear-leaves
Leguminosae	<i>Genista scorpius</i>	GS	8	Evergreen thorny and promptly leafless nanophanerophyte
	<i>Ulex parviflorus</i>	UP	11	
Oleaceae	<i>Phillyrea angustifolia</i>	PA	7	Evergreen microphanerophyte with simple lanceolate broad-leaves
Pinaceae	<i>Pinus nigra</i>	PN	10	Evergreen mesophanerophyte with simple needle-leaves
	<i>Pinus pinaster</i>	PP	10	
Palmae	<i>Chamaerops humilis</i>	CH	8	Evergreen nanophanerophyte with compound fan-like leaves
Graminoids	<i>Brachypodium phoenicoides</i>	BP	10	Evergreen tussock-like hemicryptophyte
	<i>Brachypodium retusum</i>	BR	10	
	<i>Graminoids</i>	G	10	

2.3. Image acquisition and processing

A DJI Inspire 1 sUAS (DJI, Europe) was used to capture high resolution aerial imagery of both study sites. The sUAS captured imagery in consistent weather conditions (temperature *circa* 25°C, wind speed < 7ms⁻¹, clear skies), and flights were conducted at solar noon. On two consecutive days in June 2018, two separate flights were undertaken at each site; with a target altitude of 30 m AGL followed by 60 m AGL. On 25th of March 2019, one flight was undertaken at both sites; with a target altitude of 30m. All flights followed a cross-hatched flight plan to ensure maximum overlap (> 80%), at a 5m line spacing. A low-cost payload sensor was used

to collect imagery. More specifically, the payload sensor was a BG-NIR modified version of the DJI X3 RGB sensor (12 megapixels, DJI, Europe). The modified sensor was adjusted using a custom filter to pass infrared light from the “red edge” at 680-800 nm, where plants actively reflect wavelengths, and to block wavelengths over 800 nm. The filter ensured that the blue and green channels only received visible light whilst allowing the detection of NIR light at 680-800 nm (LDP LLC, Carlstadt, NJ, USA).

In addition, a total of 34 Ground Control Points (GCP) were located within the study site to georeference the image in the later processing phase. A Leica GS07 dGPS was used to record their coordinates. The sUAS was flown manually, and image capture ranged between 83-162 images for 60 m AGL flights, and 450-563 images for 30m AGL flights in June, and between 190-1068 images in March (see table 5. 2). All images were recorded in JPEG file format and georeferenced to EXIF GPS coordinates and altitude levels obtained from the DJI Inspire 1 sUAS.

Table 5. 2. Image processing information for each flight executed in NGRPTB ibex enclosure. The table includes final resolution (ppcm, pixel per centimetre) of the image, surface recorded by the image, number of ground control points (GCP), calibration error (mean RMS error), and number of recorded images and number of images used to create the model.

Month	Flight (m)	Resolution (ppcm)	Surface (ha)	GCP	Mean RMS error (m)	N of images	Calibrated images
June	30	1.44	2.8457	18	0.04-0.28	1013	868
June	60	3.51	5.8915	16	0.23-0.08	245	245
March	30	1.52	5.1267	21	0.03-0.07	2188	2152

The Pix4D Mapper® software was used to process all images. Initially, Structure-from-Motion (SfM) was used to generate a Digital Surface Model of the study sites (Westoby et al., 2012), and then an orthomosaic generated by orthorectification of the

aerial imagery (Pix4D, 2018). This method removes perspective distortions from the images using the Digital Surface Model.

To ensure consistency across all orthomosaics, the image resolution and pixel size were matched to the coarsest resolution across all final images using ArcGIS (v10.1). A nearest neighbour sampling method was used to resample discrete pixel data to larger pixel sizes, in order to test the possible influence on the image classification. The range of image pixel sizes was 3.5 cm – 30 cm, with the smallest pixel size representing the highest resolution consistently achievable during the sUAS flights.

Finally, using dGPS locations of the plants sampled in the field, a buffer was generated (25% of the smallest measured diameter of each specific plant) and used to extract the pixel values relative to each plant individually sampled. Pixel sampling of each plant was conducted in this way to avoid plant edges and soil reflectance where possible which may have caused disruptive pixel mixing. The resultant data provided BG-NIR pixel data for each plant sampled in the field which was used to perform subsequent analysis.

2.4. NDVI mapping

NDVI is a good indicator to reflect plant growth, quality, and phenology in Mediterranean ecosystems (Ogaya et al., 2015). NDVI represents the Normalised Difference Vegetation Index which is determined by calculating the difference in reflectance between the NIR band and a chosen visible band which is then divided by the sum of these two bands (Pettorelli, 2013b). This index can be calculated for any individual pixel and typically uses the red band as the visible component due to the high level of absorption of this band during photosynthesis. The NIR band is used as it is highly reflected by healthy plants, allowing a strong contrast with the red visible band. The blue band can be similarly used to the red band but is typically restricted to

low altitude data acquisitions due to the negative effect of Rayleigh scattering that can interfere with satellite measurements as light passes through the atmosphere. It is more commonly referred to as Blue-NDVI (BNDVI) and has been used successfully in other vegetation assessment studies (Beerli et al., 2007; Lu and He, 2017). NDVI sensitivity to phenological stages of the plants was assessed as they manifested relevant seasonal phenological changes. Initially, satellite data were obtained to determine the mean NDVI values correspondent to the 2014-18 period for the entire study area, and to establish seasonal trends (MOD13Q1 NDVI data extracted from the MODIS repository, Moderate Resolution Imaging Spectroradiometer, provided by NASA). Secondly, the Blue-NDVI was calculated from the acquired images for all the plants recorded within the study area. The highest resolution images were used for these comparisons: June low flight 3.5cm pixel and March low flight 3.5 cm pixel. Single-band raster images were analysed and vegetation indices calculated from the sUAS captured imagery. These data were used to identify differences in vegetation index values and pixel values across sampled species and previously determined family groups.

2.5. Diet composition

Faecal cuticle micro-histological analysis was used to confirm that previous studies completed on the Iberian Ibex diet are suitable for this study area. A micro-histological analysis was therefore performed on the field sampled data. This technique facilitated the identification of plant epidermal fragments in the 10 samples collected in December 2019. Samples were prepared following treatment described by Bartolomé et al. (1995), with minor modifications. Approximately 10 g from the milled sample were placed in test tubes with 5 ml of 65% concentrated HNO₃. The test tubes were then boiled in a water bath at 80° C for 2 min. After digestion in HNO₃,

the samples were diluted with 200 ml of water. This suspension was then passed through 1.00 mm and 0.125 mm filters. The 0.125–1.00 mm fraction was spread on glass microscope slides in a 50% aqueous glycerine solution and cover-slips were fixed with DPX micro-histological varnish. Three slides were prepared from each sample. The slides were examined under a microscope at 100-400x magnifications, conducting lengthwise traverses. Plant fragments were recorded and counted until 200 fragments of leaf epidermis were identified from each sample.

2.6. Classification Analysis and Statistics

A machine learning algorithm approach was used to classify and map plant species across the two study sites. Machine learning algorithms are effective at operating on large volume and multivariate datasets. They can have high accuracy, and they have been successfully used when regression models are not suitable (Li et al., 2019; Marrs and Ni-Meister, 2019; Van Ewijk et al., 2014). In particular, the Breiman's Random Forests Model (RFM, Breiman, 2001) has been shown to be effective in other species distribution studies (see Carvalho et al., 2018; Zhang et al., 2019). Digital values of the three recorded bands (Blue, Green, NIR) were used as predictor variables. The effect of pixel size (1.44, 1.52 and 3.5, flight height, the month of sampling, and the response variable (e.g., all species vs diet species only) was assessed.

Initially, all the species sampled in the area were included in the RFM classification. Seventy percent of the sampled individuals were used as training data, whilst the remaining 30% of sampled individuals were used as test data. The inclusion of the training data subset allowed independent assessment of the error in the classification method, using Out Of Bag (OOB) and Prediction Test Error (PTE). A confusion matrix was created, and the predictions evaluated against the independent ground-

truthing data. The final error matrix was then used to select the most suitable image acquisition approach and processing method.

Following the assessment of all species, a further analysis was conducted to discriminate between those sampled species recognised as Ibex diet species according to our micro-histological results. This step was conducted in two ways. Initially, species were grouped according to diet and a secondary “other” species group was included; and secondly, only species recognised as Ibex diet species were included within the model, and the “other” species group was omitted from the analysis. As a further investigation, and to understand the source of the error and the relevance of potential methodological issues, a linear model was generated that predicted the percentage of error according to the pool of species included in the classification and the study season when images were captured.

Finally, a Principal Components Analysis (PCA) was undertaken to further explore the relationship between individual species, species pools and the three bands recorded by the sensor (BG-NIR). In addition, PCA score values were assessed across dietary species and used to discern differences in mean scores through an ANOVA post-hoc analysis.

2.7. Foodscape mapping

To complete the study, a foodscape of the distribution of the main Iberian ibex resources in the study area was created. The original digital values of the already georeferenced pixels making up the orthomosaic were replaced by the predicted categories based on the RFM with the lowest test error. The procedure was done using the “rasterFromXYZ” function of the “Raster” package, version 3.07 (Hijmans, 2019).

3. Results

3.1. NDVI

The traditional red band NDVI obtained from MODIS for the study area for the 2014-2018 period presents a clear seasonal pattern. In fact, 43% of the observed NDVI variability was explained by the effect of months (Smooth term_{Month} = 21.5, p-value < 0.01, $R^2 = 43\%$, from a GAM). A peak in primary production was shown in winter (March) and a minimum in summer (June) (Figure 5.3A). March and June presented statistically significant differences between their NDVI values. The spatial resolution of the MODIS analysis provided a preliminary indicator of general NDVI trends in response to phenology which was then examined more specifically using the finer spatial resolution BG_NIR sensor.

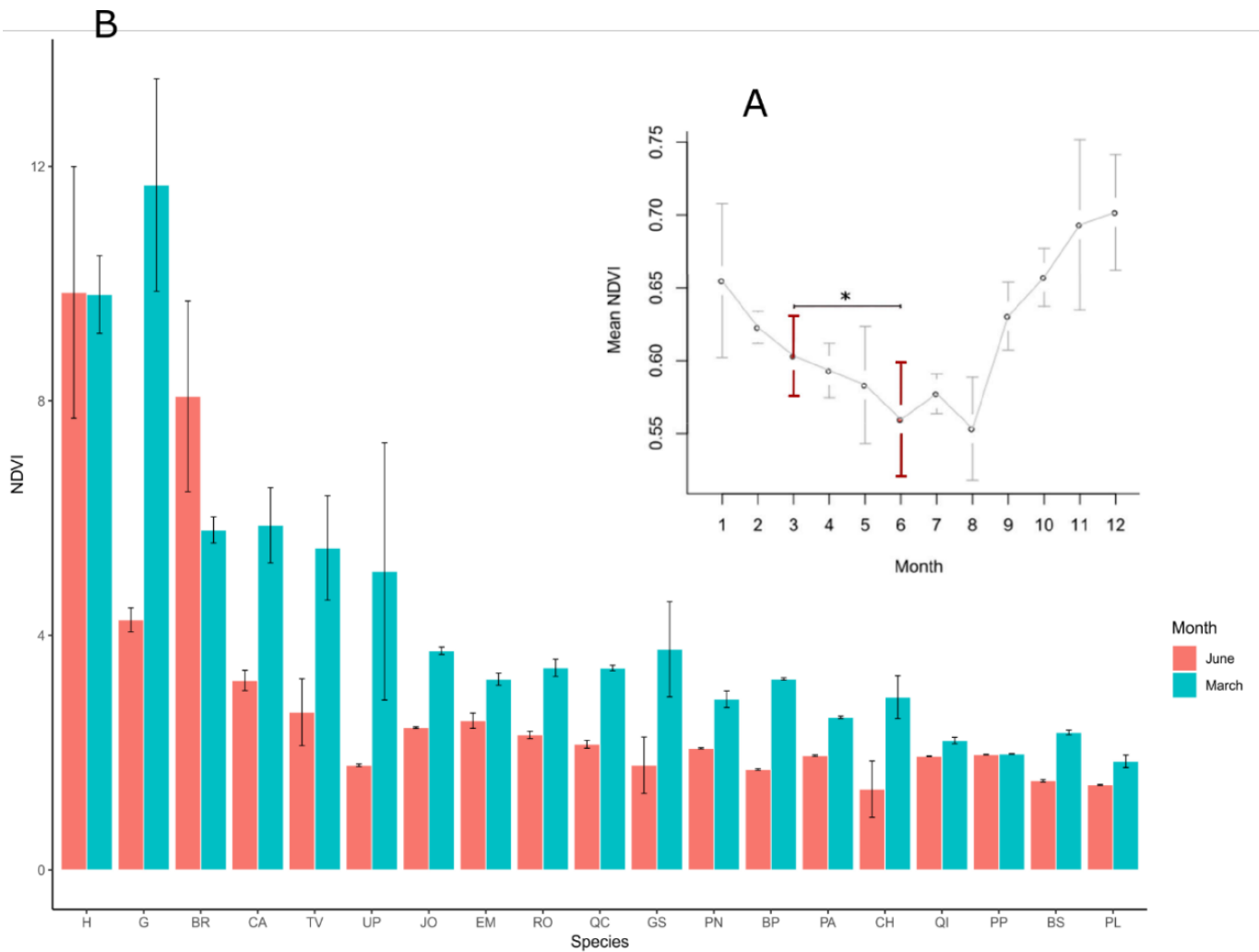


Figure 5. 3. A) Monthly variation of mean NDVI values recorded in the Iberian Ibx enclosure, in the NGRPTB. Mean NDVI values corresponding to the 2014–18 period. Clear seasonal pattern evident with peak primary production in winter and minimum in summer. The asterisk indicates statistically significant differences between march and June NDVI (red bars). B) Variation of mean Blue-NDVI in the plants recorded in the Ibx enclosure in March and June calculated from the images obtained by a BG-NIR camera. All species have statistical differences (t-test) except for those marked with asterisks. *Brachypodium retusum* (BR), *Helianthemum marifolium* (H), and *Pinus pinaster* (PP). All plant species abbreviations are depicted in Table 5. 2. (For interpretation of the references to colour in this figure legend, the reader is referred to the web version of this article).

In the absence of the red band, the BNDVI was used for the aerial data collection via the sUAS when analysing the NDVI values obtained for each recorded plant. Similar trends were obtained, across the two months studied using the sUAS mounted sensor, as found in the MODIS data. The differences between the values in both recorded

months are shown in Figure 5.3. Almost all species, 16 out of the 19 studied, have statistically significant differences in NDVI value between June and March (t-student test with $p\text{-value} < 0.05$), except *Brachypodium retusum* (BR, $p\text{-value}=0.1658$), *Helianthemum marifolium* (H, $p\text{-value}=0.9869$) and *Pinus pinaster* (PP, $p\text{-value}=0.1182$).

3.2. Faecal cuticle micro-histological analysis

Faecal cuticle micro-histological analyses clearly show that diet composition of Ibexes within the enclosure agrees with that in the base work (Martinez, 1994). Diet of Ibexes was mainly based on non-legume wood species (ONLW), *Erica multiflora* (EM), graminoids (G, such as *Brachypodium phoenicoides*, *B. retusum*), Labiatae-Asteraceae plants (L-A, e.g., *Rosmarinus officinalis*), and Fagaceae (e.g., *Quercus ilex*). No plant represented more than 14% of use (Figure. 5.4), indicating the generalist feeding behaviour of the species (Granados et al., 2001). As a result, species were classified into five broad family groups with the species consistent in the diet across all the year. The five groups were: *Quercus* spp. as the family Fagaceae (Group F), *Rosmarinus officinalis* and *Thymus vulgaris* as the family Labiatae (Group L), *Erica multiflora* (Group E), *Cistus albidus* (Group C), *Brachypodium phoenicoides*, *B. retusum*, and other grass-like plants as Graminoids (Group G). The remaining species were then placed into the category 'Others' that were excluded from the statistical analysis.

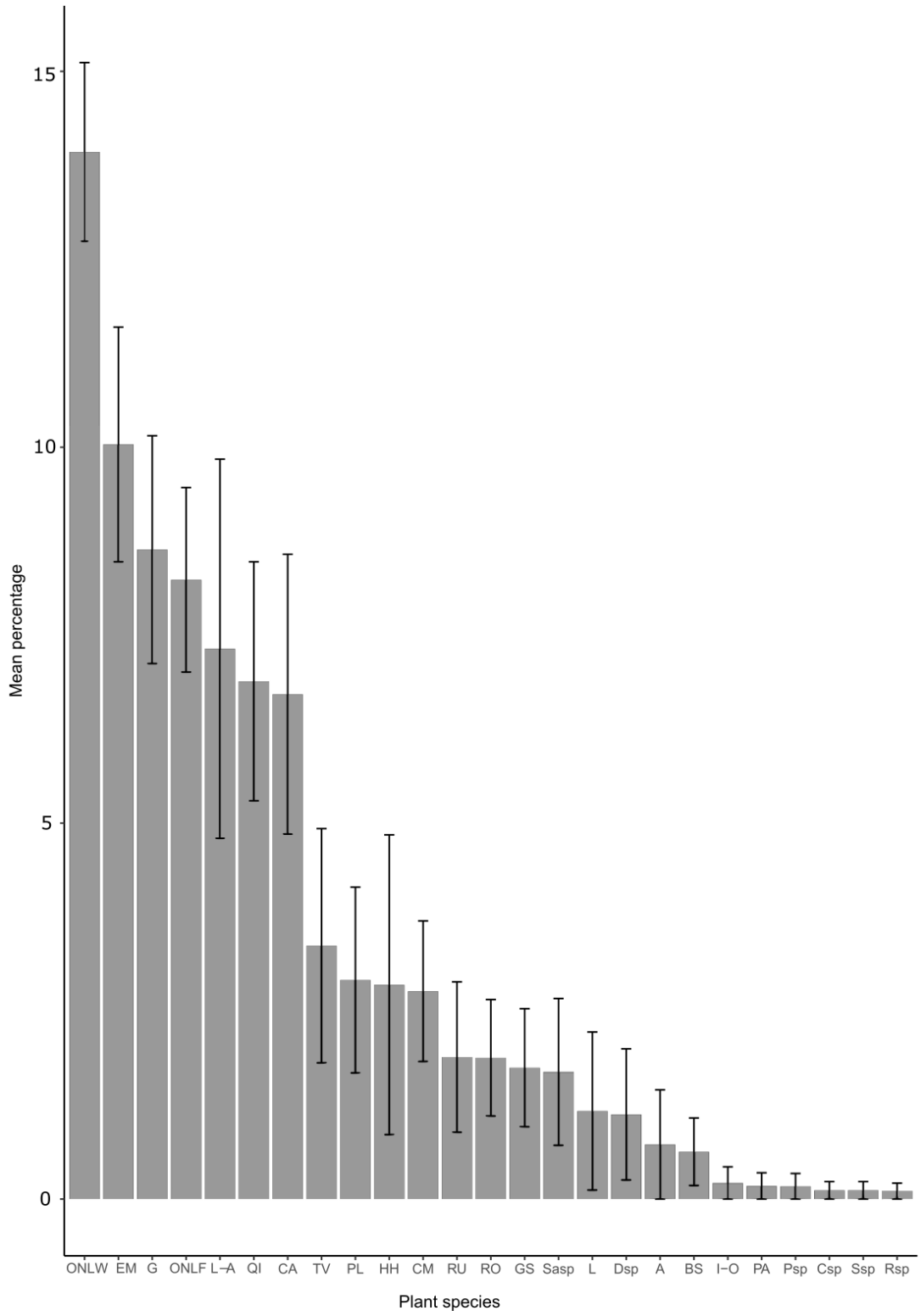


Figure 5. 4. Diet composition assessed by a faecal micro-histological analysis of 10 faecal samples collected in the Ibex enclosure in December 2019. Bars represent the mean of the proportion of each plant species in our faecal samples. ONLW (Other Non-Legume Wood species), EM (*Erica multiflora*), G (*Brachypodium phoenicoides*, *B. retusum* and other graminoids), ONLF (Other Non-Legume Forb species), L-A (Labiatae-Asteraceae), QI (*Quercus ilex*), CA (*Cistus albidus*), TV (*Thymus vulgaris*), PL (*Pistacia lentiscus*), HH (*Hedera helix*), CM (*Crataegus monogyna*), RU (*Rubus ulmifolius*), RO (*Rosmarinus officinalis*), GS (*Genista scorpius*), Sasp (*Smilax aspera*), L (Laminaceae), Dsp (Dorycnium sp.), A (Asteraceae), BS (*Buxus sempervirens*), I–O (Iridaceae- Orchidaceae), PA (*Phillyrea angustifolia*), Psp (Pinus sp.), Csp (Carex sp), Ssp (Satureja sp.), Rsp (Rosa sp.).

3.3. Image capture and processing

The results showed that the orthomosaic images were created and georeferenced with an error of between 3 cm and 28 cm (see table 5.2), and the resultant single-band raster images used to calculate vegetation indices.

3.4. Random Forest Modelling

The RFM was applied to all sUAS imagery collected in both July 2018 and March 2019 and assessed for classification error. The results from the RFM model indicate a consistent improvement in model performance using small pixel size (e.g., error reduction of 42.02% in predictions based on June flights at high height and 3.5 pixel per centimetre, see Table 5. 3). In all RFM groups, the 3.5 ppcm outperformed all other pixel size models. Moreover, it was found that as pixel size increased (up to 30 ppcm) model performance progressively deteriorated (Table 5.3). In addition, when the model was reapplied with spatially resampled data, the model performance deteriorated with an OOB error increase of 37.7% (60m flight, June 2018 3.5–30 ppcm).

Table 5. 3. Plant species classification from random forest models using digital values of the three bands recorded by a BG-NIR camera (NIR, Blue and Green). Data collected using a sUAS flying in July (2018) and March (2019) in the Iberian Ibex (*Capra pyrenaica*) enclosure in the NGRPTB. Images were recorded at two heights (30 and 60 m) and different resolutions (3.5, 5, 10 and 30 cm pixel size). OOB error is the classification error according to the random forest algorithm. Test error is the error obtained when comparing algorithm prediction results with test data not included in the model development. We performed two kinds of classification: for the most abundant plants in the enclosure (n=19, All species), and for plants preferred by Ibexes (Diet). In the Diet group, plants have been grouped in 4 types namely: *Cistus albidus*, *Erica multiflora*, Fagaceae (*Quercus coccifera* and *Q. ilex*) and Graminoids (e.g., *Brachypodium phoenicoides*, *B. retusum* and other graminoids).

Response variables	Flight	Month	Resolution (cm)	OOBerror (%)	Test error (%)
All species	low	March	30	70.89	70.66
	high	June	30	66.49	70.28
	low	March	10	69.14	68.56
	low	June	10	55.50	56.07
	low	June	5	53.24	52.73
	low	March	5	50.89	50.43
	high	June	10	50.03	49.19
	low	March	3.5	48.38	48.57
	high	June	5	43.54	43.77
	low	June	3.5	35.39	35.64
	low	June	30	68.99	29.78
	high	June	3.5	28.77	25.26
Diet	low	March	3.5	27.94	28.26
	low	June	3.5	23.51	23.87
	high	June	3.5	18.38	18.70

Conversely, when flight height (60m and 30m) was compared (for similar pixel resolution), the RF model performance increased when the sUAS imagery was captured at a higher flight height. Although, comparatively speaking, the effect of this

was not as substantial as the effect of pixel size on model performance (60 m flight vs 30 m flight; 3.5 ppcm; 6.6% increase in OOB error).

Further differences in model performance were observed when comparisons were made between survey seasons (June vs March). The model performance was better in June 2018 than in March 2019. The June 30 m flight outperformed the March 30m flight, with a 13% reduction in OOB error rates (see Table 5.3).

Finally, the best performance by the RF model was observed when the response variable was changed to focus on specific Ibex diet species. Simplification of the analysis to include only a 'diet species' group showed that the RF model's OOB error rate dropped to only 18.4%, meaning a correct prediction of plants in 81.6% of instances. This pattern of error reduction was apparent in all flights using the diet response variables.

The above analysis is supported by the linear modelling undertaken. The analysis showed that both pools of species (e.g., all species and diet) and month (season) were significant variables. Interestingly, and in support once again, the species pool was shown to be the variable that most affects the error (p -value = 0.001 for the pool, and p -value = 0.03 for month). However, it is worth noting that the error calculated for the March 2019 surveys is higher in all pool scenarios than for June 2018.

3.5. Principal Component Analysis

Principal Component Analysis (PCA) was performed on the image data that provided the best classification results (June 2018, high flight, 3.5 ppcm). PCA was used to understand the behaviour of bands and vegetation indices, and to identify the different band responses for each species and their natural groupings. Evaluating the responses of the three recorded bands for all the recorded species provided the following results.

The PCA axis 1 and 2 accounted for 97.9% of the variation in the dataset for the three spectral bands (Blue, Green, and Near Infrared). Axis 1 accounted for 82% of this variation with an associated elevated eigenvalue of 2.46. Axis 2 explained a further 15.9% (eigenvalue = 0.48) of the variation (Figure SM 5. 1, supplementary material). In addition, the score values of each species were calculated (Figure 5.5) and demonstrated that axis 1 scores showed the greatest potential to represent the variation of the spectral responses to the three bands. ANOVA test and corresponding post-hoc analyses showed statistically significant differences between the reflectance values of all plant species. However, it is worth noting that, this could be a false discovery rate due to effect size; as there were many sampled individuals (246) and therefore many pixels (up to 66264, in the data set of 3.5 ppcm, high flight, and June). To further understand the variability within species the above analysis was repeated accounting for solely the dietary species.

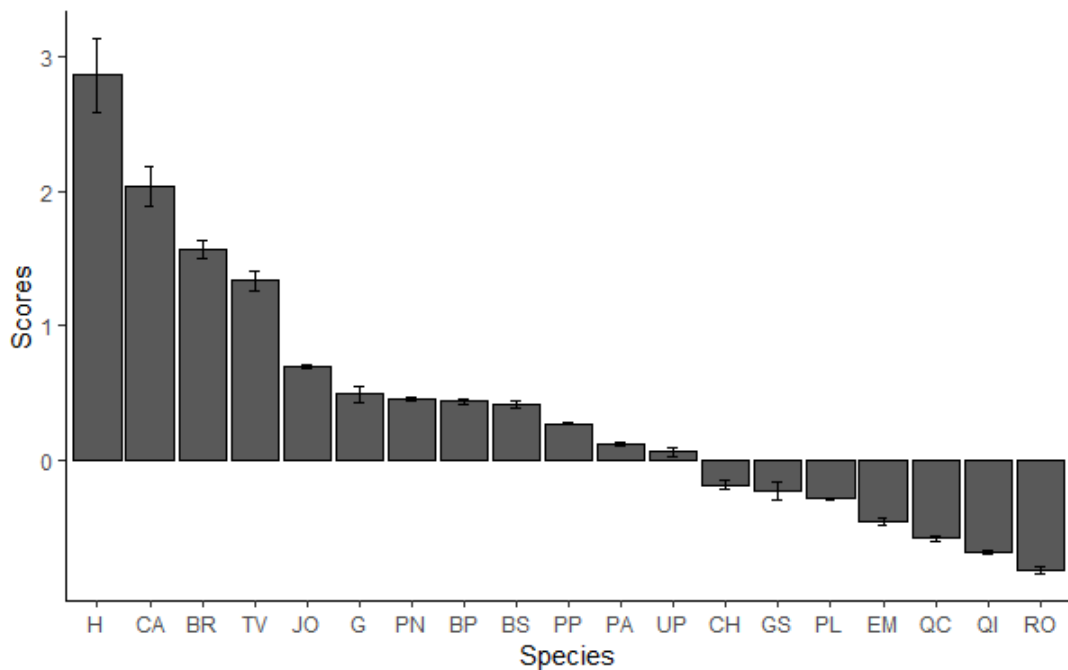


Figure 5. 5. Mean scores from the first PCA dimension performed with NIR, Green and Blue band recordings on 19 plant species sampled in the NGRPTB vegetation study. All plant species abbreviations are depicted in Table 5.2. (For interpretation of the references to colour in this figure legend, the reader is referred to the web version of this article.)

Evaluating the spectral response of each individual to the three recorded bands provided the following results. The PCA axis 1 and 2 accounted for the same proportion (97.9%) of the variation observed in the spectral responses across all individuals. Axis 1 accounted for 82% of the variation (eigenvalue = 2.50), and axis 2 explained a further 15% (eigenvalue = 0.44) of the variation (Figure SM 5. 2, supplementary material). In addition, the score values of each plant group were calculated to illustrate the differences. Post-hoc analysis revealed significant differences between all dietary groups except for the pair *Labiatae* and *Erica multiflora* (p-value = 0.0628, Figure 5.6).

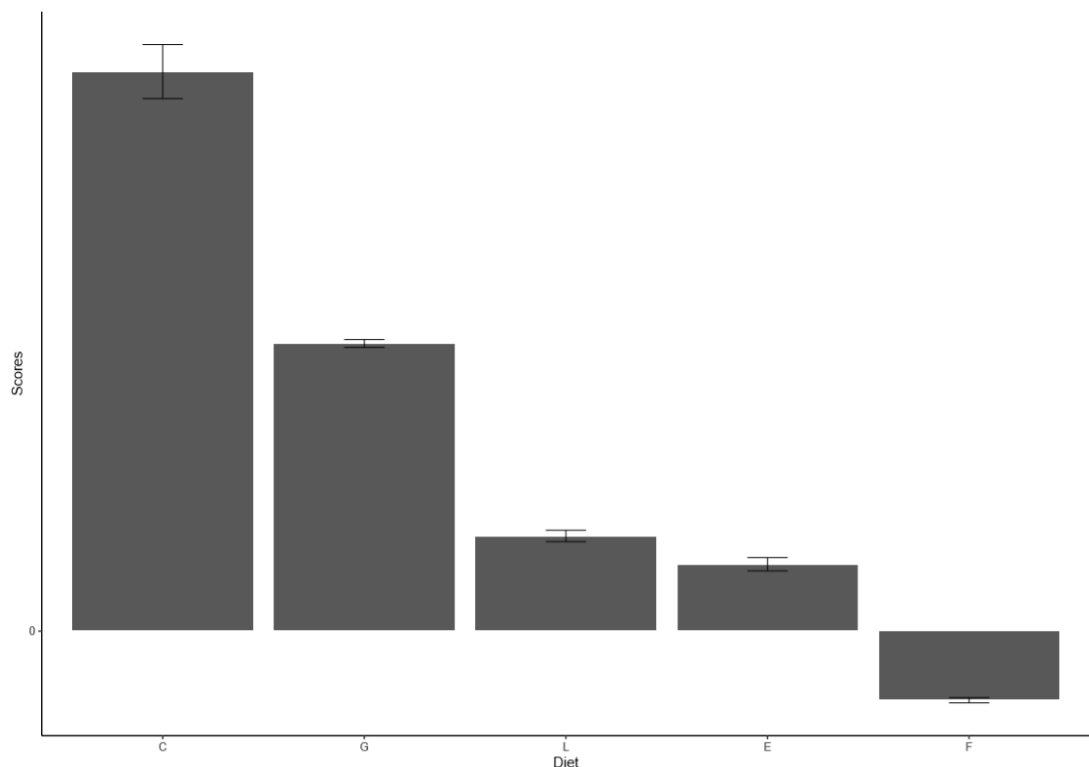


Figure 5. 6. Mean scores from the first PCA dimension performed with NIR, Green and Blue band recordings on 5 plant categories consumed by Iberian ibexes in the NGRPTB. ‘C’: *Cistus albidus*; ‘G’: *Brachypodium phoenicoides*, *B. retusum*, and other grass-like plants as Graminoids. ‘L’: *Rosmarinus officinalis* and *Thymus vulgaris* as the family Labiatae; ‘E’: *Erica multiflora*; ‘F’: *Quercus* spp. as the family Fagaceae. (For interpretation of the references to colour in this figure legend, the reader is referred to the web version of this article.)

3.6. Foodscape mapping

The foodscape map in Figure. 5.7 predicts that 13.04% of the study area is covered by Fagaceae plants (Group F), 4.08% by graminoids (Group G), 2.23% by Labiateae (e.g., *Rosmarinus* and *Thymus*, Group L), 1.77% by *Erica multiflora* (Group E) and 0.02% by *Cistus albidus* (Group C). Most of the area (78.06%), however, included other plants not found in the Ibex diet, bare soil and rocks.

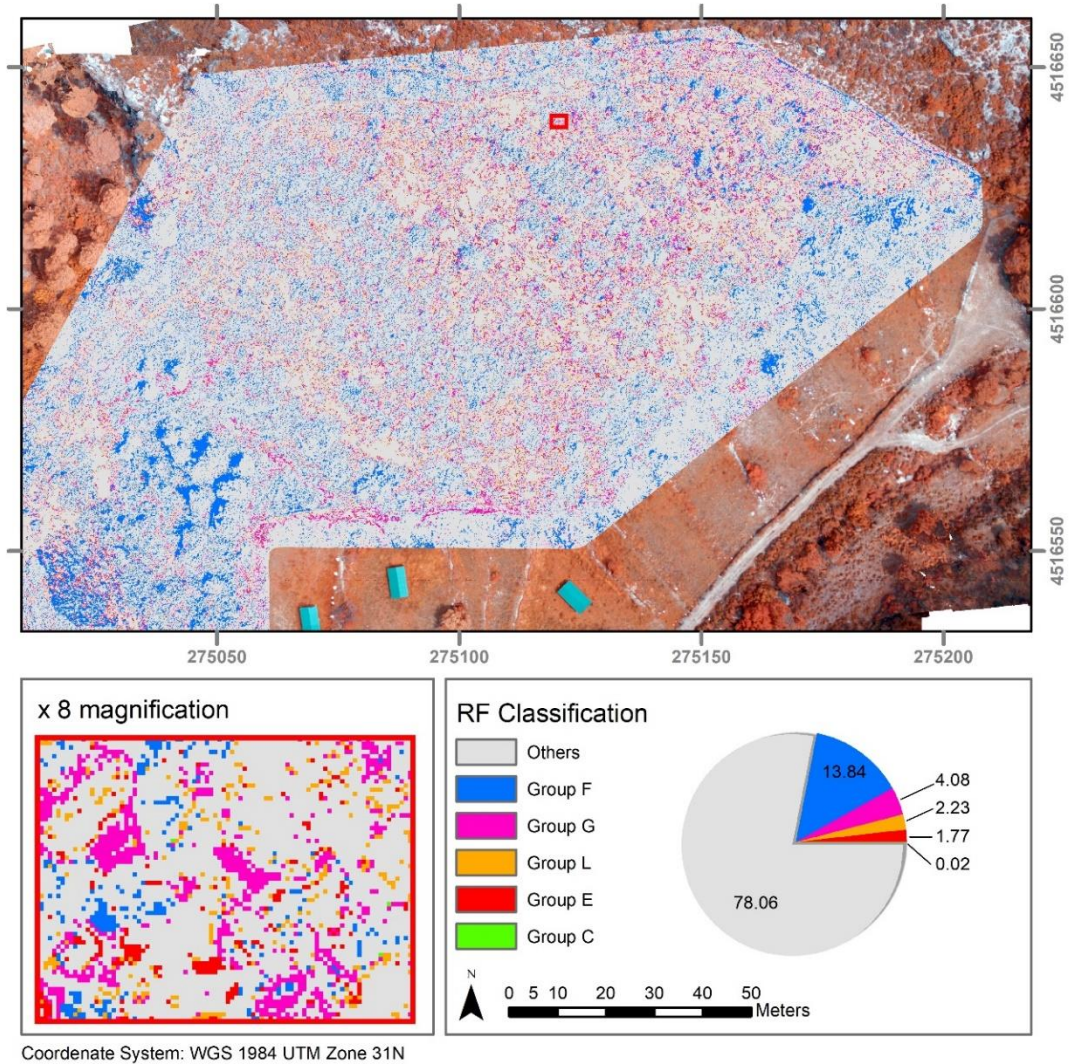


Figure 5. 7. Food scape map overlaid with the infrared false-colour orthomosaic of the study area. Predicted categories are based on RFMI with an OOB error of 18.4%. A pie chart illustrates the proportion of the 6 dietary categories: ‘F’: *Quercus* spp. as the family Fagaceae; ‘L’: *Rosmarinus officinalis* and *Thymus vulgaris* as the family Labiatae; ‘E’: *Erica multiflora*; ‘C’: *Cistus albidus*; ‘G’: *Brachypodium phoenicoides*, *B. retusum*, and other grass-like plants as Graminoids. ‘Others’ category includes plants without dietary interest, bare soil and rock.

4. Discussion

This study has successfully explored the application of a modified BG-NIR sensor, mounted on a low cost sUAS, to create foodscapes for a mixed feeder in a Mediterranean scrubland, rich in woody species with very different physiognomies.

Analysis has shown successful discrimination of species within a species rich and physiognomically heterogeneous Mediterranean scrubland. Plant prediction was correct in 81.6% of instances (prediction error 18.4%) when using a training data set of 173 individuals (73 in the test dataset) representing all the most abundant species at the two closely located sites. Plant prediction improved further to 88.2% when focussing on the Ibex diet species alone (prediction error 11.8%) using a training data set of 97 individuals (and a test dataset of 41). Such errors are similar or, in some case, lower than those obtained by using hyperspectral methodologies in complex ecosystems (e.g., Clark et al., 2005; Ferreira et al. 2016; including Mediterranean ones (e.g., Manevski et al., 2012).

Our classification results, along with those of the PCA analysis, show a wide range of spectral responses across the species investigated, but also a useable level of homogeneity within species groups; when considering both ‘all species’ and only those ‘within the Ibex diet’. These results indicate that successful classification is possible. The success of using only 3 spectral bands to identify significantly different spectral responses across species and similarities within species groups, coupled with the high level accuracy of classification, outlines the feasibility and potential for such a low-cost application to develop foodscapes and facilitate their long-term management.

The success in discriminating Ibex diet species remotely provides a strong foundation from which to discuss the technical issues in the classification process. Initially, the results indicate that small pixel size provides better classification results; as previously reported in other studies (Hsieh et al., 2001; Hu et al., 2019), which discuss the relevance of pixel size in classification performance and the effect of variations in plant size and ground coverage. However, for the same pixel size, higher flights have

shown to perform better than lower flights, which is similar to other methodological studies (e.g., Mesas-Carrascosa et al., 2015). The study by Mesas-Carrascosa et al. (2015) indicated that there was greater discrimination between species at higher flights. In addition, higher altitudes typically have less perspective distortion as the ratio of the topographic change to flying altitude is smaller; therefore accuracy of the orthophoto can be higher; as is reflected in the work of Nesbit and Hugenholtz, (2019). Therefore when choosing the ideal flight parameters (as pixel size is determined by both sensor type and flight height) a balance between both must be found; taking into account the area to evaluate, the flight platform employed, and the financial and time costs.

This study has also shown that season is a relevant factor when working with plant species in temperate regions since they manifest different physiological status and even morphologies throughout the year (see also Sperlich et al., 2014; Vogt and Gul, 1994). Our results show that the most suitable season to perform the classification study at this site is June (vs March), when most of the Mediterranean woody taxa end their growth and flowering. Thus, plants have a large part of their vegetative structure (not woody) renewed, with its characteristic morphology. At a tissue and chemical level, the Mediterranean woody plants are fully constituted to be able to withstand the water deficit and the severe heat stroke of the summer that starts in June (Fernandez-Marín et al., 2017). All these characteristics, along with net inter-species differences in water content (related to drought adaptations), determine the optical properties of the plants (Manevski et al., 2012). Due to its influence on the classification results the importance of prior knowledge of the phenological pattern of the area and the present plant species could be crucial to applying this methodology over a wider area and for it to not be restricted by site specific conditions.

In our study, the classification results improved when focusing on the target diet species (Prediction error reduced to 11.8%). The result showed that the pool of training species influenced classification success with an accuracy reported of 88.2%. This clearly indicates that an informed knowledge of the target diet species for the study area is of great value to maximise classification accuracy. Our results show that the classification accuracy can be improved by over 6%. Moreover, the importance of the micro-histological analysis or other related diet studies is evident in this process. However, caution is needed here, given the associated reduction in both test and training data samples. The micro-histological analysis has served as an effective tool, focusing and reducing the pool of input species identified as diet species and subsequently improving the relevance and overall classification performance. Reducing the number of diet species classes by combining similar species, for example, logically grouping *Pinus pinaster* and *P. nigra* as Pines, and *Brachypodium phoenicoides* and *B. restusum* as Graminoids offered further improvement in classification accuracy but was limited to an increase of 0.5-2%, with no significant improvement given the reduced specificity of the classification.

Regarding the obtained error, it is also relevant to consider the size (and biotype) of the plants. This seems to be case of *Helianthemum marifolium*, a representative taxon of typical prostrated chamaephytic communities on Mediterranean bedrocks. These small prostrated plants, with diameters around the calibration error (*circa* 20 cm) and loose branching on bare soils, appeared to yield higher errors in classification compared to those of bigger and thicker plants. These finding are similar to other recent, and related, studies in rangeland ecosystems where small shrub/subshrub species with low abundance, were found to have reduced classification success (Sankey et al., 2019)

However, with the relative successes of our study, when focussing on target diet species, areas for improvement are largely focused on the sensor rather than on the methodology adopted. Improvements are most likely to be achieved by increasing the sensitivity of spectral responses to plant species variation, and taking advantage of the increased spectral resolution of more expensive cameras. Although the low-cost aspect of this study is a unique selling point, upgrading to a more expensive hyperspectral camera could offer greater flexibility, and potentially accuracy, during the classification process (Manevski et al., 2012; Sankey et al., 2019). Known as hyperspectral sensors, these cameras can offer a greater quantity of spectral bands but also bands of finer spectral resolution and have been used advantageously in several other works (Beeri et al., 2007; Lone et al., 2014). However, with this consideration, one of the relevant achievements of this work should not be compromised. This being the creation of an accessible and affordable tool for land managers and researchers to be applied in heterogeneous landscapes and on animals with species-specific diet accounting for the general ecosystem characteristics, including plant species composition.

5. Conclusion

This feasibility study outlines the possibility of describing food location for a mixed herbivore in a heterogeneous environment. A modified BG-NIR camera, mounted on a low cost sUAS, has been shown to be successful in classifying plant species and describing the foodscapes of ungulates such as Ibex. The benefits of this study, the methodology presented, and the potential for further development apply to studies of wild and domestic herbivore distribution and welfare, predator distribution,

vegetation changes, and habitat biodiversity internationally (Boulanger et al., 2018; Moore et al., 2010; Oates et al., 2019; Peters et al., 2019; Searle et al., 2007)

Further studies with hyperspectral cameras are necessary to assess the improvements hypothesised, and the potential enhancement of efficiency and accuracy offered by an increased quantity and refined nature of spectral information. Additionally, it would be interesting to increase the number of sampling months to fully study plant availability throughout the year. Further research should be done to evaluate diet quality by improving and refining the affordable, accessible and non-time consuming methods that would be beneficial to land managers. Although previous studies have not determined that feeding quality can be separated according to individual species, we should improve our understanding of how feeders adapt their feeding habits throughout the year. The classification results obtained in this study provide a strong foundation on which to develop such diet quality studies.

6. References

- Alados, C.L., Escos, J., 1987. Relationships between movement rate, agonistic displacements and forage availability in Spanish ibexes (*Capra pyrenica*). *Biol. Behav.* 12, 245–255.
- Anderson, K., Gaston, K.J., 2013. Lightweight unmanned aerial vehicles will revolutionize spatial ecology. *Front. Ecol. Environ.* 11, 138–146.
<https://doi.org/10.1890/120150>
- Beeri, O., Phillips, R., Hendrickson, J., Frank, A.B., Kronberg, S., 2007. Estimating forage quantity and quality using aerial hyperspectral imagery for northern mixed-grass prairie. *Remote Sens. Environ.* 110, 216–225.
<https://doi.org/10.1016/j.rse.2007.02.027>

- Bergqvist, G., Wallgren, M., Jernelid, H., Bergström, R., 2018. Forage availability and moose winter browsing in forest landscapes. *For. Ecol. Manage.* 419–420, 170–178. <https://doi.org/10.1016/j.foreco.2018.03.049>
- Boulanger, V., Dupouey, J.L., Archaux, F., Badeau, V., Baltzinger, C., Chevalier, R., Corcket, E., Dumas, Y., Forgeard, F., Mårell, A., Montpied, P., Paillet, Y., Picard, J.F., Saïd, S., Ulrich, E., 2018. Ungulates increase forest plant species richness to the benefit of non-forest specialists. *Glob. Chang. Biol.* 24, e485–e495. <https://doi.org/10.1111/gcb.13899>
- Breiman, L., 2001. ST4_Method_Random_Forest. *Mach. Learn.* 45, 5–32. <https://doi.org/10.1017/CBO9781107415324.004>
- Carvalho, J., Santos, J.P.V., Torres, R.T., Santarém, F., Fonseca, C., 2018. Tree-based methods: Concepts, uses and limitations under the framework of resource selection models. *J. Environ. Informatics* 32, 112–124. <https://doi.org/10.3808/jei.201600352>
- Del, M., España, N.D.E., Martínez, T., 1994. DIETA ESTACIONAL DE LA CABRA MONTES (*Capra pyrenaica*) 373–380.
- Duparc, A., Garel, M., Marchand, P., Dubray, D., Maillard, D., Loison, A., 2019. Through the taste buds of a large herbivore: foodscape modeling contributes to an understanding of forage selection processes. *Oikos*. <https://doi.org/10.1111/oik.06386>
- Espunyes, J., Bartolomé, J., Garel, M., Gálvez-Cerón, A., Aguilar, X.F., Colom-Cadena, A., Calleja, J.A., Gassó, D., Jarque, L., Lavín, S., Marco, I., Serrano, E., 2019. Seasonal diet composition of Pyrenean chamois is mainly shaped by

primary production waves. PLoS One 14, 1–23.
<https://doi.org/10.1371/journal.pone.0210819>

Garbulsky, M.F., Peñuelas, J., Ogaya, R., Filella, I., 2013. Leaf and stand-level carbon uptake of a Mediterranean forest estimated using the satellite-derived reflectance indices EVI and PRI. *Int. J. Remote Sens.* 34, 1282–1296.
<https://doi.org/10.1080/01431161.2012.718457>

Golodets, C., Kigel, J., Sternberg, M., 2011. Plant diversity partitioning in grazed Mediterranean grassland at multiple spatial and temporal scales. *J. Appl. Ecol.* 48, 1260–1268. <https://doi.org/10.1111/j.1365-2664.2011.02031.x>

Granados, J.E., Pérez, J.M., Márquez, F.J., Serrano, E., Soriguer, R.C., Fandos, P., 2001. LA CABRA MONTÉS (*Capra. Galemys* 13, 3–37.

Hesketh, M., Sánchez-azofeifa, G.A., 2012. Remote Sensing of Environment The effect of seasonal spectral variation on species classification in the Panamanian tropical forest. *Remote Sens. Environ.* 118, 73–82.
<https://doi.org/10.1016/j.rse.2011.11.005>

Hijmans, R.J., 2019. Introduction to the 'raster' package (version 3.0-7) 1–250.

Insua, J.R., Utsumi, S.A., Basso, B., 2019. Estimation of spatial and temporal variability of pasture growth and digestibility in grazing rotations coupling unmanned aerial vehicle (UAV) with crop simulation models. *PLoS One* 14, 1–13. <https://doi.org/10.1371/journal.pone.0212773>

Karl, J.W., Colson, K., Swartz, H., 2011. Rangeland Assessment and Monitoring Methods Guide: An interactive tool for selecting methods for assessment and monitoring. *Rangelands* 33, 48–54. <https://doi.org/10.2111/1551-501X-33.4.48>

- Li, Z., Zan, Q., Yang, Q., Zhu, D., Chen, Y., Yu, S., 2019. Remote Estimation of Mangrove Aboveground Carbon Stock at the Species Level Using a Low-Cost Unmanned Aerial Vehicle System. *Remote Sens.* 11, 1018. <https://doi.org/10.3390/rs11091018>
- Lone, K., Van Beest, F.M., Mysterud, A., Gobakken, T., Milner, J.M., Ruud, H.P., Loe, L.E., 2014. Improving broad scale forage mapping and habitat selection analyses with airborne laser scanning: The case of moose. *Ecosphere* 5, 1–22. <https://doi.org/10.1890/ES14-00156.1>
- Lu, B., He, Y., 2017. Species classification using Unmanned Aerial Vehicle (UAV)-acquired high spatial resolution imagery in a heterogeneous grassland. *ISPRS J. Photogramm. Remote Sens.* 128, 73–85. <https://doi.org/10.1016/j.isprsjprs.2017.03.011>
- Manousidis, T., Kyriazopoulos, A.P., Parissi, Z.M., Abraham, E.M., Korakis, G., Abas, Z., 2016. Grazing behavior, forage selection and diet composition of goats in a Mediterranean woody rangeland. *Small Rumin. Res.* <https://doi.org/10.1016/j.smallrumres.2016.11.007>
- Marrs, J., Ni-Meister, W., 2019. Machine Learning Techniques for Tree Species Classification Using Co-Registered LiDAR and Hyperspectral Data. *Remote Sens.* 11, 819. <https://doi.org/10.3390/rs11070819>
- Martinez, T., 2014. Diet selection by Spanish ibex in early summer in Sierra Nevada. *Acta Theriol. (Warsz)*. 45, 335–346. <https://doi.org/10.4098/at.arch.00-33>
- Martinez, T., Martinez, E., 1987. in spring and summer at the Sierra de Credos, Spain.

- Martinez, T., Martinez, E., Fandos, P., 1985. Composition of the food of the Spanish Wild Goat in Sierras de Cazorla and Segura, Spain. *Acta Theriol. (Warsz)*. 30, 461–494. <https://doi.org/10.4098/at.arch.85-31>
- Moore, B.D., Lawler, I.R., Wallis, I.R., Beale, C.M., Foley, W.J., 2010. Palatability mapping: A koala's eye view of spatial variation in habitat quality. *Ecology* 91, 3165–3176. <https://doi.org/10.1890/09-1714.1>
- Oates, B.A., Merkle, J.A., Kauffman, M.J., Dewey, S.R., Jimenez, M.D., Vartanian, J.M., Becker, S.A., Goheen, J.R., 2019. Antipredator response diminishes during periods of resource deficit for a large herbivore. *Ecology* 100, 1–8. <https://doi.org/10.1002/ecy.2618>
- Ogaya, R., Barbeta, A., Başnou, C., Peñuelas, J., 2015. Satellite data as indicators of tree biomass growth and forest dieback in a Mediterranean holm oak forest. *Ann. For. Sci.* 72, 135–144. <https://doi.org/10.1007/s13595-014-0408-y>
- Pekkonen, M., Laakso, J.T., 2012. Temporal changes in species interactions in simple aquatic bacterial communities. *BMC Ecol.* 12, 18. <https://doi.org/10.1186/1472-6785-12-18>
- Peters, W., Hebblewhite, M., Mysterud, A., Eacker, D., Hewison, A.J.M., Linnell, J.D.C., Focardi, S., Urbano, F., De Groeve, J., Gehr, B., Heurich, M., Jarnemo, A., Kjellander, P., Kröschel, M., Morellet, N., Pedrotti, L., Reinecke, H., Sandfort, R., Sönnichsen, L., Sunde, P., Cagnacci, F., 2019. Large herbivore migration plasticity along environmental gradients in Europe: life-history traits modulate forage effects. *Oikos* 128, 416–429. <https://doi.org/10.1111/oik.05588>
- Petersen, C.A., Villalba, J.J., Provenza, F.D., Petersen, C.A., Villalba, J.J., Provenza, F.D., 2014. Influence of Experience on Browsing Sagebrush by Cattle and Its

Impacts on Plant Community Structure Influence of Experience on Browsing Sagebrush by Cattle and Its Impacts on Plant Community Structure 67, 78–87. <https://doi.org/10.2111/REM-D-13-00038.1>

Pullanagari, R.R., Kereszturi, G., Yule, I., 2018. Integrating airborne hyperspectral, topographic, and soil data for estimating pasture quality using recursive feature elimination with random forest regression. *Remote Sens.* 10. <https://doi.org/10.3390/rs10071117>

Rooney, T., 2015. Integrating Ungulate Herbivory into Forest Landscape Restoration.

Royo, A.A., Kramer, D.W., Miller, K. V., Nibbelink, N.P., Stout, S.L., 2017. Spatio-temporal variation in foodscapes modifies deer browsing impact on vegetation. *Landsc. Ecol.* 32, 2281–2295. <https://doi.org/10.1007/s10980-017-0568-x>

Schweiger, A.K., Risch, A.C., Damm, A., Kneubühler, M., Haller, R., Schaepman, M.E., Schütz, M., 2015a. Using imaging spectroscopy to predict above-ground plant biomass in alpine grasslands grazed by large ungulates. *J. Veg. Sci.* 26, 175–190. <https://doi.org/10.1111/jvs.12214>

Schweiger, A.K., Schütz, M., Anderwald, P., Schaepman, M.E., Kneubühler, M., Haller, R., Risch, A.C., 2015b. Foraging ecology of three sympatric ungulate species - behavioural and resource maps indicate differences between chamois, ibex and red deer. *Mov. Ecol.* 3, 6. <https://doi.org/10.1186/s40462-015-0033-x>

Searle, K.R., Hobbs, N.T., Gordon, I.J., 2007. It's the "Foodscape", not the Landscape: Using Foraging Behavior to Make Functional Assessments of Landscape Condition. *Isr. J. Ecol. Evol.* 53, 297–316. <https://doi.org/10.1560/ijee.53.3.297>

- Skidmore, A.K., Ferwerda, J.G., Mutanga, O., Van Wieren, S.E., Peel, M., Grant, R.C., Prins, H.H.T., Balcik, F.B., Venus, V., 2010. Forage quality of savannas - Simultaneously mapping foliar protein and polyphenols for trees and grass using hyperspectral imagery. *Remote Sens. Environ.* 114, 64–72. <https://doi.org/10.1016/j.rse.2009.08.010>
- Stout, S.L., Kramer, D.W., Miller, K. V, Nibbelink, N.P., 2018. Spatio-temporal variation in foodscapes modifies deer browsing impact on vegetation Spatio-temporal variation in foodscapes modifies deer browsing impact on vegetation. *Landsc. Ecol.* <https://doi.org/10.1007/s10980-017-0568-x>
- Valle Júnior, R.F. do, Siqueira, H.E., Valera, C.A., Oliveira, C.F., Sanches Fernandes, L.F., Moura, J.P., Pacheco, F.A.L., 2019. Diagnosis of degraded pastures using an improved NDVI-based remote sensing approach: An application to the Environmental Protection Area of Uberaba River Basin (Minas Gerais, Brazil). *Remote Sens. Appl. Soc. Environ.* 14, 20–33. <https://doi.org/10.1016/J.RSASE.2019.02.001>
- Van Ewijk, K.Y., Randin, C.F., Treitz, P.M., Scott, N.A., 2014. Predicting fine-scale tree species abundance patterns using biotic variables derived from LiDAR and high spatial resolution imagery. *Remote Sens. Environ.* 150, 120–131. <https://doi.org/10.1016/j.rse.2014.04.026>
- Villamuelas, M., Fernández, N., Albanell, E., Gálvez-Cerón, A., Bartolomé, J., Mentaberre, G., López-Olvera, J.R., Fernández-Aguilar, X., Colom-Cadena, A., López-Martín, J.M., Pérez-Barbería, J., Garel, M., Marco, I., Serrano, E., 2016. The Enhanced Vegetation Index (EVI) as a proxy for diet quality and composition in a mountain ungulate. *Ecol. Indic.* 61, 658–666. <https://doi.org/10.1016/j.ecolind.2015.10.017>

- Wachendorf, M., Fricke, T., Möckel, T., 2017. Remote sensing as a tool to assess botanical composition, structure, quantity and quality of temperate grasslands. *Grass Forage Sci.* 73, 1–14. <https://doi.org/10.1111/gfs.12312>
- Weisberg, P.J., Coughenour, M.B., Bugmann, H., 2010. Modelling of large herbivore–vegetation interactions in a landscape context, in: *Large Herbivore Ecology, Ecosystem Dynamics and Conservation*. <https://doi.org/10.1017/cbo9780511617461.014>
- Youngentob, K.N., Renzullo, L.J., Held, A.A., Jia, X., Lindenmayer, D.B., Foley, W.J., 2012. Using imaging spectroscopy to estimate integrated measures of foliage nutritional quality. *Methods Ecol. Evol.* 3, 416–426. <https://doi.org/10.1111/j.2041-210X.2011.00149.x>
- Zhang, L., Huettmann, F., Liu, S., Sun, P., Yu, Z., Zhang, X., Mi, C., 2019. Classification and regression with random forests as a standard method for presence-only data SDMs: A future conservation example using China tree species. *Ecol. Inform.* 52, 46–56. <https://doi.org/10.1016/j.ecoinf.2019.05.003>

6. General discussion

Over thousands of years, the grazing and animal husbandry in Mediterranean mountains have contributed significantly to the formation of its natural and cultural landscapes. However, the so-called global change drives changes toward closed habitats through a process of forest encroachment in these landscapes after agricultural abandonment of the productive areas (Espunyes, 2019). At the same time, during the last decades, the populations of wild and feral ungulates graze and browse freely, increasing their populations conditioned by dietary preferences and the availability of resources (Espunyes et al., 2019; Manousidis et al., 2016). In this thesis, novel analyses of ecosystem service changes in Mediterranean mountain ecosystems are conducted to address the role of wild herbivores in these changes in the long term, managing the complexity of spatial heterogeneity.

The first and second chapters are studies set in the Mallorca Island mountains, which represent those cultural Mediterranean landscapes well. The mountains of Mallorca provide a mosaic of habitats, showing the heterogeneity of local topographies, soil types and microclimates related to altitude, rainfall and slope exposure.

Results from Chapter 1 suggest that environmental heterogeneity and microtopography may be more critical drivers of soil ecosystem properties than the effects of ungulate herbivory. Contrary to the significant effect of herbivores on the plant community analysed in this experimental system, it seems that soils change variability depends on the context in which herbivory occurs due to the high environmental heterogeneity even at local scales (Andriuzzi and Wall, 2018; Forbes et al., 2019; Vermeire et al., 2021). Chapter 1 addresses this heterogeneity across the

General discussion

paired plots while accounting for the dependence of ungulate exclusion effects within study sites via a well-controlled multilevel meta-analysis (Hedges et al., 1999). This analysis found great variability on a very small scale (< 10m), supporting the idea that the soil heterogeneity makes resolving clear patterns very challenging (Eldridge et al., 2019; Zhang et al., 2020). Although the lack of significance of the effect of herbivory on the physicochemical and biological characteristics of the soil, trends were observed, so ungulates could be contributing to increasing the variability found in the soil characteristics. To test this hypothesis, it is recommended to conduct studies of the soil's ecosystem against the effect of ungulates, taking dynamic measures of the soil's characteristics rather than static, thus addressing the high spatial heterogeneity. The findings of this research contribute to a deeper understanding of the role of ungulates in terrestrial ecosystems.

The study of soil characteristics shows that small-scale effects can mask large-scale effects when conditions are highly heterogeneous. However, chapter 1 showed clear effects on the vegetation, which shows a degree of heterogeneity in response to pressure by ungulates less than that of the soil. This allowed us to propose large-scale studies on the effect of herbivores on vegetation using technology that allows large-scale studies. This thesis shows strategies to assess herbivore-plant interaction overcoming the issues of, on the one hand, the spatial heterogeneity and, on the other hand, the static measures by using remote sensing tools and geographic information systems (GIS, Chapters 2 & 3).

In chapter 2, a remote sampling was carried out by a satellite-based survey. The sampling procedure described in this work considers environmental variables that contribute to the heterogeneity of the Mediterranean landscapes (e.g., altitude, slope, exposure, or land cover). It shows a reliable procedure for finding vegetated areas of

General discussion

similar greening or browning dynamics (i.e., long-term increase or decrease in vegetation) and comparing treatments across time. The Landsat record goes back decades, allowing us to examine the state of the ecosystem dynamics anywhere on the planet. Here it has been applied to evaluate the effect of eradicating the highest density of black rat population ever reported on a Mediterranean island (Mayol et al., 2012) and thus overcome the usual lack of information on the state of the ecosystem both before and after a herbivore eradication campaign. The unsupervised time series processing tool BFAST was able to identify abrupt and gradual changes in vegetation dynamics. Different vegetation dynamics occurring within Landsat grid cells (i.e., a grid of 30 m on each side) might restrict the ability to detect an emerging shift in the ecosystem (Pettorelli et al., 2014). The dates, magnitude, and trend of these changes could not be explicitly attributed to rat herbivory compared to the historical changes on the islet and the changes found to co-occur within the control zone. Unlike other studies assessing rodent eradications (Le Corre et al., 2015; Lohr et al., 2014), the effects of the 2011 rat eradication on the Sa Dragonera Islet's primary production dynamics were insignificant at the Landsat resolution scale. Since the vegetation in the study area has a long history of permanent pressure from natural and domestic animals, as well as recurrent natural and man-made fires (Alcover and Alcover, 2008; Seguí et al., 2005), it is suggested that the prolonged coexistence of dominant plant taxa with herbivores in the Balearic archipelago could explain the resistance of vegetation dynamics to herbivory. The effects of herbivory on vegetation structure are well reported in the literature; however, monitoring herbivore removal outcomes is limited (Bastille-Rousseau et al., 2017; Jones, 2010; Jones et al., 2016), and pre-management data is generally lacking (Townes et al., 1990). Thus, this satellite-based approach represents a dynamic and spatially consistent methodology, which is critical

for understanding ecosystems' ongoing and evolving dynamics after herbivore removal, distinguishing them from phenology-driven changes and water-related events, which are considered the major change factors of the Mediterranean system.

However, satellite images do not allow the monitoring of different plant species. Since herbivores show a preference for specific species based on their nutritional value, identifying and mapping the distribution of the plant species is fundamental for managing large herbivores (Espunyes et al., 2019). In landscapes as heterogeneous as those of the Mediterranean mountains, mapping vegetation at a higher spatial resolution with Unmanned Aerial Vehicles (UAV) systems is a timely field of research. However, this technology is not affordable for most environmental management administrations. It deals with several technical issues to be addressed to establish it as a feasible method to map plant resources for herbivores. Chapter 3 addresses both challenges, heterogeneous environmental assessment and mixed feeder diet classification, using a simple, low-cost three spectral band camera. The study creates a foodscape (food availability map) assessment in a heterogeneous Mediterranean scrubland for the Iberian Ibex. One of the study outcomes is the description of a reproducible UAV-based survey effective plan, considering the Machine Learning algorithm Random Forest. The field observations are extended over the entire study area with an error of 18.4% in their prediction. Moreover, the prediction improves up to 11.2% error by focusing on the most important species in the Ibex diet. Such errors are similar or, in some cases, lower than those obtained by using more expensive hyperspectral methodologies in complex ecosystems (e.g., Clark et al., 2005; Ferreira et al., 2016), including the Mediterranean (e.g., Manevski et al., 2012). Therefore, this study shows the importance of diet studies to improve resource availability estimations. The study also shows the importance of finding the

right balance between the sensor used, the flight height and the pixel size, which are major parameters to take into account when designing a UAV-based survey. A priori, a smaller pixel size achieved by low flights obtains greater species discrimination accuracy, as reported in other studies. (Hsieh et al., 2001; Hu et al., 2019). However, in this study, the generalisation of the pixel obtained in higher flight performs better than the same pixel size obtained at low altitude, which is similar to other methodological studies (e.g., Mesas-Carrascosa et al., 2015). That could be due to a more minor perspective distortion as the ratio of the topographic change to flying altitude is also smaller; hence, the accuracy of the recorded data can be higher; as is reflected in the work of (Nesbit and Hugenholtz, 2019). The methodology presented in chapter 3 has direct applicability to studies of the distribution and welfare of wild and domestic herbivores. This UAV-based survey is less time-consuming than traditional ones, mainly in mountainous forest areas, which are often difficult to access. Conducting this remote sensing procedure across seasons could yield useful information on changes in vegetation and habitat. Therefore, it might represent a strong foundation for predicting the feeding behaviour of wild ungulates in the Mediterranean mountains.

This thesis shows analytical methods to assess the role of herbivory in Mediterranean mountain forests, which also happens to be one of the most rapidly shifting ecosystems in the face of climate change. Herbivory is a key player in Mediterranean ecosystems that environmental managers can manage to keep these landscapes' functional diversity and heterogeneity. However, this heterogeneity occurs at very small scales, as shown in the experimental system analysed in chapter 1, making it difficult to assess the effectiveness of herbivore management in the context of global change where when effects occur on a small scale in highly heterogeneous systems

such as mountain soil. Traditionally, ecosystem management has lacked an evaluation system that makes it possible to determine its long-term effectiveness beyond suggestions or anecdotal observations. In chapters 2 and 3, remote sensing-based sampling looks at the data, showing a low-cost and accurate alternative to traditional field sampling. These novel surveys allow measurements at different scales to inform the effectiveness and impact of herbivore management on vegetation.

The different approaches shown in this thesis demonstrate the high complexity of Mediterranean mountain systems and their high resilience against disturbances. The results of these works allow the implementation of three novel study techniques at different scales that will solve important questions about herbivores' management in these complex systems.

References

- Alcover, Josep Antoni, Alcover, J A, 2008. The First Mallorcans: Prehistoric Colonization in the Western Mediterranean. *J. World Prehistory* 2008 211 21, 19–84.
- Andriuzzi, W.S., Wall, D.H., 2018. Soil biological responses to, and feedbacks on, trophic rewilding. *Philos. Trans. R. Soc. B Biol. Sci.*
- Bastille-Rousseau, G., Gibbs, J.P., Campbell, K., Yackulic, C.B., Blake, S., 2017. Ecosystem implications of conserving endemic versus eradicating introduced large herbivores in the Galapagos Archipelago. *Biol. Conserv.* 209, 1–10.
- Clark, M.L., Roberts, D.A., Clark, D.B., 2005. Hyperspectral discrimination of tropical rain forest tree species at leaf to crown scales. *Remote Sens. Environ.* 96.

- Eldridge, D.J., Travers, S.K., Val, J., Wang, J.T., Liu, H., Singh, B.K., Delgado-Baquerizo, M., 2019. Grazing Regulates the Spatial Heterogeneity of Soil Microbial Communities Within Ecological Networks. *Ecosystems*.
- Espunyes, J., Bartolomé, J., Garel, M., Gálvez-Cerón, A., Aguilar, X.F., Colom-Cadena, A., Calleja, J.A., Gassó, D., Jarque, L., Lavín, S., Marco, I., Serrano, E., 2019. Seasonal diet composition of Pyrenean chamois is mainly shaped by primary production waves. *PLoS One* 14.
- Espunyes, N., 2019. Effects of global change on the diet of a mountain ungulate: The Pyrenean chamois. *Universitat Autònoma de Barcelona*.
- Ferreira, M.P., Zortea, M., Zanotta, D.C., Shimabukuro, Y.E., de Souza Filho, C.R., 2016. Mapping tree species in tropical seasonal semi-deciduous forests with hyperspectral and multispectral data. *Remote Sens. Environ.* 179.
- Forbes, E.S., Cushman, J.H., Young, T.P., Klope, M., Young, H.S., 2019. Synthesizing the effects of large, wild herbivore exclusion on ecosystem function 1597–1610.
- Hedges, L. V, Gurevitch, J., Curtis, P.S., 1999. THE META-ANALYSIS OF RESPONSE RATIOS IN EXPERIMENTAL ECOLOGY, Special Feature *Ecology*.
- Hsieh, P.F., Lee, L.C., Chen, N.Y., 2001. Effect of spatial resolution on classification errors of pure and mixed pixels in remote sensing. *IEEE Trans. Geosci. Remote Sens.* 39.
- Hu, P., Guo, W., Chapman, S.C., Guo, Y., Zheng, B., 2019. Pixel size of aerial imagery constrains the applications of unmanned aerial vehicle in crop breeding. *ISPRS J. Photogramm. Remote Sens.* 154.

- Jones, H.P., 2010. Prognosis for ecosystem recovery following rodent eradication and seabird restoration in an island archipelago. *Ecol. Appl.* 20, 1204–1216.
- Jones, H.P., Holmes, N.D., Butchart, S.H.M., Tershy, B.R., Kappes, P.J., Corkery, I., Aguirre-Muñoz, A., Armstrong, D.P., Bonnaud, E., Burbidge, A.A., Campbell, K., Courchamp, F., Cowan, P.E., Cuthbert, R.J., Ebbert, S., Genovesi, P., Howald, G.R., Keitt, B.S., Kress, S.W., Miskelly, C.M., Opper, S., Poncet, S., Rauzon, M.J., Rocamora, G., Russell, J.C., Samaniego-Herrera, A., Seddon, P.J., Spatz, D.R., Towns, D.R., Croll, D.A., 2016. Invasive mammal eradication on islands results in substantial conservation gains. *Proc. Natl. Acad. Sci. U. S. A.* 113, 4033–4038.
- Le Corre, M., Danckwerts, D.K., Ringler, D., Bastien, M., Orłowski, S., Morey Rubio, C., Pinaud, D., Micol, T., 2015. Seabird recovery and vegetation dynamics after Norway rat eradication at Tromelin Island, western Indian Ocean. *Biol. Conserv.* 185, 85–94.
- Lohr, C., Van Dongen, R., Huntley, B., Gibson, L., Morris, K., 2014. Remotely monitoring change in vegetation cover on the Montebello Islands, Western Australia, in response to introduced rodent eradication. *PLoS One* 9, 1–15.
- Manevski, K., Manakos, I., Petropoulos, G.P., Kalaitzidis, C., 2012. Spectral discrimination of mediterranean maquis and phrygana vegetation: Results from a case study in Greece. *IEEE J. Sel. Top. Appl. Earth Obs. Remote Sens.* 5.
- Manousidis, T., Kyriazopoulos, A.P., Parissi, Z.M., Abraham, E.M., Korakis, G., Abas, Z., 2016. Grazing behavior, forage selection and diet composition of goats in a Mediterranean woody rangeland. *Small Rumin. Res.*
- Mayol, J., Mayol, M., Domenech, O., Oliver, J., McMinn, M., Rodríguez, A., 2012.

General discussion

Aerial broadcast of rodenticide on the island of Sa Dragonera (Balearic Islands, Spain). A promising rodent eradication experience on a Mediterranean island. *Aliens Invasive Species Bull.* 32, 29–32.

Mesas-Carrascosa, F.J., Torres-Sánchez, J., Clavero-Rumbao, I., García-Ferrer, A., Peña, J.M., Borra-Serrano, I., López-Granados, F., 2015. Assessing optimal flight parameters for generating accurate multispectral orthomosaics by uav to support site-specific crop management. *Remote Sens.* 7.

Nesbit, P.R., Hugenholtz, C.H., 2019. Enhancing UAV-SfM 3D model accuracy in high-relief landscapes by incorporating oblique images. *Remote Sens.* 11.

Pettorelli, N., Safi, K., Turner, W., 2014. Satellite remote sensing, biodiversity research and conservation of the future. *Philos. Trans. R. Soc. B Biol. Sci.* 369.

Seguí, B., Payeras, L., Ramis, D., Martínez, A., Delgado, J.V., Quiroz, J., 2005. La cabra salvaje mallorquina: Origen, genética, morfología, notas ecológicas e implicaciones taxonómicas. *Bolletí la Soc. d'Historia Nat. les Balear.* 48, 121–151.

Towns, D.R., Atkinson, I.A.E., Daugherty, C.H., 1990. *Reconstructing the ambiguous: can island ecosystems be restored*, doc.govt.nz. Wellington.

Vermeire, M.L., Thoresen, J., Lennard, K., Vikram, S., Kirkman, K., Swemmer, A.M., Te Beest, M., Siebert, F., Gordijn, P., Venter, Z., Brunel, C., Wolfaard, G., Krumins, J.A., Cramer, M.D., Hawkins, H.J., 2021. Fire and herbivory drive fungal and bacterial communities through distinct above- and belowground mechanisms. *Sci. Total Environ.* 785, 147189.

Zhang, M., Li, G., Liu, B., Liu, J., Wang, L., Wang, D., 2020. Effects of herbivore assemblage on the spatial heterogeneity of soil nitrogen in eastern Eurasian

steppe. *J. Appl. Ecol.* 57, 1551–1560.

7. Conclusions

1. Soil characteristics are heterogeneous at very low spatial scales in Mediterranean mountains, which explains the not consistent effects of herbivores.
2. The meta-analysis allows the detection of large-scale effects under heterogeneous conditions.
3. The analysis of the vegetation dynamics through long time series of greenness indicators obtained from satellite observations is a suitable tool to assess the long-term impact of herbivores on vegetation.
4. Modified BG-NIR cameras onboard low-cost UAVs are appropriated for classifying vegetation in heterogeneous landscapes. The classification process upgrades when focusing on the dietary resources for ungulates such as the Iberian ibex.
5. Vegetation surveys based on remote sensing allow the collection of accurate sampling data in a dynamic and low-cost manner, making them critical tools for assessing vegetation in highly heterogeneous and difficult-to-access areas.

8. Supplementary material

Supplementary material chapter 1

Table MS 3. 1. Effect of the continuous covariates (elevation, NPP, temperature, and soil texture), and the categorical covariate habitat on the effect size $\ln(RR)$ of ungulate exclusion on soil characteristics, soil microbial activities (measured as AWCD) and functional diversity (measured as a H considering observances of by Biolog EcoPlates™) and organic material Stabilization factor (S) and Decomposed rate (k) (measured with the “Tea Bag index” method). The p-value associated with the test of moderators Q_M indicates statistical significance at $\alpha = 0.95$ NPP Net Primary Productivity, texture corresponds to the first PC of a PCA made with all percentages of the soil texture classes.

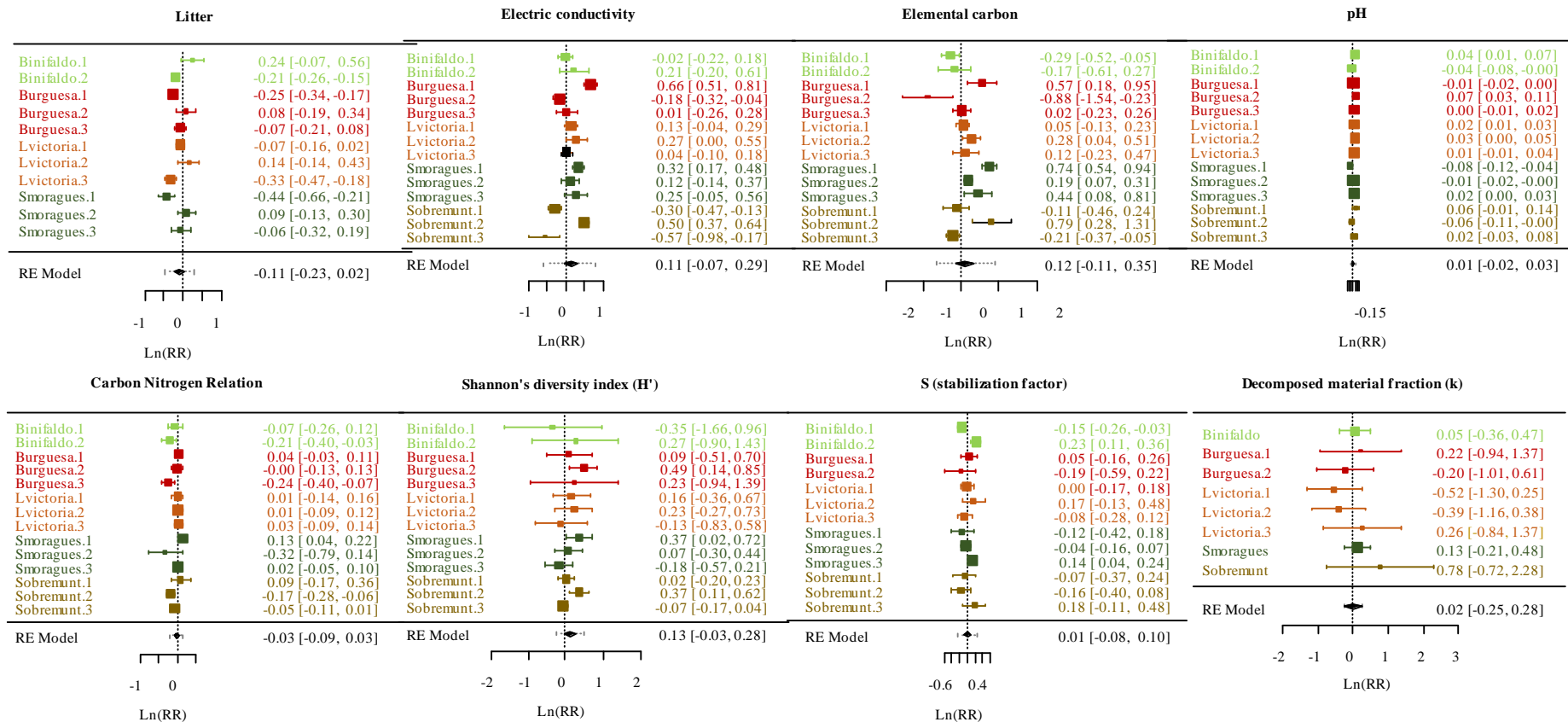
Variable	Elevation(m)		NPP		Temperature		Texture		Habitat		
	Estimate (95% CI)	Q_M p-value	Estimate (95% CI)	Q_M p-value	Estimate (95% CI)	Q_M p-value	Estimate (95% CI)	Q_M p-value	Forest	Shrubland	Q_M p-value
									Estimate (95% CI)	Estimate (95% CI)	
Bulk Density	0.000 (-0.001 0.001)	0.016 0.901	0.054 (-1.628 1.737)	0.004 0.950	-0.000 (-0.008 0.007)	0.015 0.902	-0.009 (-0.101 0.082)	0.041 0.839	-0.098 (-0.280 0.084)	-0.106 (-0.264 0.052)	2.855 0.240
Litter	-0.000 (-0.000 0.000)	0.809 0.368	-0.187 (-0.462 0.084)	1.850 0.174	0.001 (-0.000 0.002)	1.427 0.232	0.006 (-0.008 0.019)	0.607 0.436	-0.007 (-0.032 0.019)	0.018 (-0.008 0.044)	2.090 0.352
Electrical Conductivity	-0.000 (-0.001 0.001)	0.105 0.746	0.368 (-2.933 2.196)	0.079 0.779	0.003 (-0.008 0.015)	0.346 0.557	0.012 (-0.106 0.130)	0.041 0.839	0.081 (-0.076 0.239)	0.238 (-0.018 0.493)	4.347 0.114
Elemental Carbon	0.000 (-0.000 0.000)	0.001 0.977	0.172 (-1.074 1.419)	0.074 0.786	0.000 (-0.006 0.005)	0.012 0.913	-0.023 (-0.039 0.084)	0.530 0.467	0.013 (-0.092 0.118)	0.001 (-0.148 0.151)	0.061 0.970

Supplementary material Chapter 1

Organic Matter	0.000 (-0.001 0.001)	0.010 0.922	1.465 (-2.449 5.379)	0.538 0.463	-0.003 (-0.022 0.016)	0.103 0.749	-0.119 (-0.295 0.058)	1.737 0.187	0.207 (-0.142 0.556)	0.036 (-0.361 0.434)	1.382 0.501
Elemental Nitrogen	-0.000 (-0.002 0.002)	0.201 0.654	-0.835 (-6.872 5.201)	0.074 0.786	-0.011 (-0.014 0.036)	0.713 0.398	0.016 (-0.253 0.246)	0.019 0.890	0.025 (-0.301 0.351)	0.550 (0.126 0.974)	6.483 0.039
C/N	-0.000 (-0.000 0.000)	1.146 0.284	-0.109 (-0.159 0.941)	0.041 0.839	0.002 (-0.003 0.006)	0.609 0.435	0.046 (-0.002 0.094)	3.548 0.060	-0.043 (-0.132 0.047)	0.026 (-0.112 0.086)	0.941 0.625
AWCD	0.000 (-0.001 0.001)	0.223 0.637	0.431 (-0.519 1.382)	0.792 0.374	-0.002 (-0.010 0.014)	0.107 0.743	-0.015 (-0.140 0.110)	0.057 0.812	0.079 (-0.147 0.306)	0.155 (-0.097 0.407)	1.919 0.383
Shannon (H)	0.000 (-0.000 0.000)	0.001 0.973	1.014 -2.185 4.213)	0.386 0.534	-0.002 (-0.016 0.013)	0.043 0.836	-0.107 (-0.271 0.056)	1.654 0.198	0.201 (-0.082 0.483)	0.099 (-0.221 0.420)	2.300 0.317
Stabilization factor (S)	-0.000 (-0.000 0.001)	0.499 0.480	-0.017 (-2.790 2.756)	0.000 0.991	-0.003 (-0.015 0.008)	0.345 0.557	-0.078 (-0.196 0.040)	1.661 0.197	0.297 (0.091 0.074)	-0.011 (-0.201 0.179)	9.959 0.007
Decomposed rate (k)	-0.000 (-0.001 0.001)	0.063 0.802	0.420 (-3.283 4.124)	0.050 0.824	0.001 (0.016 0.018)	0.007 0.934	-0.065 (-0.226 0.095)	0.637 0.425	0.143 (-0.172 0.457)	0.077 (-0.296 0.451)	0.958 0.619

Supplementary material Chapter 1

Figure SM 3. 1. Forest plot of the effect of the herbivory on additional response variables (Litter, Electrical Conductivity, Organic Carbon, pH, C/N, H', S, k). In each plot, the names on the left identify the individual plots in each of the five study areas. The boxes represent the Ln(RR) of the individual studies, and the horizontal lines are their 95% confidence intervals. The size of the boxes expresses the weight (see methods) of each study in the total effect, which is represented by a diamond. Response rates less than zero (vertical dotted line) indicate a negative exclusion effect, while values greater than zero indicate a positive effect. If the diamond does not cross the zero line, the overall effect is significant.



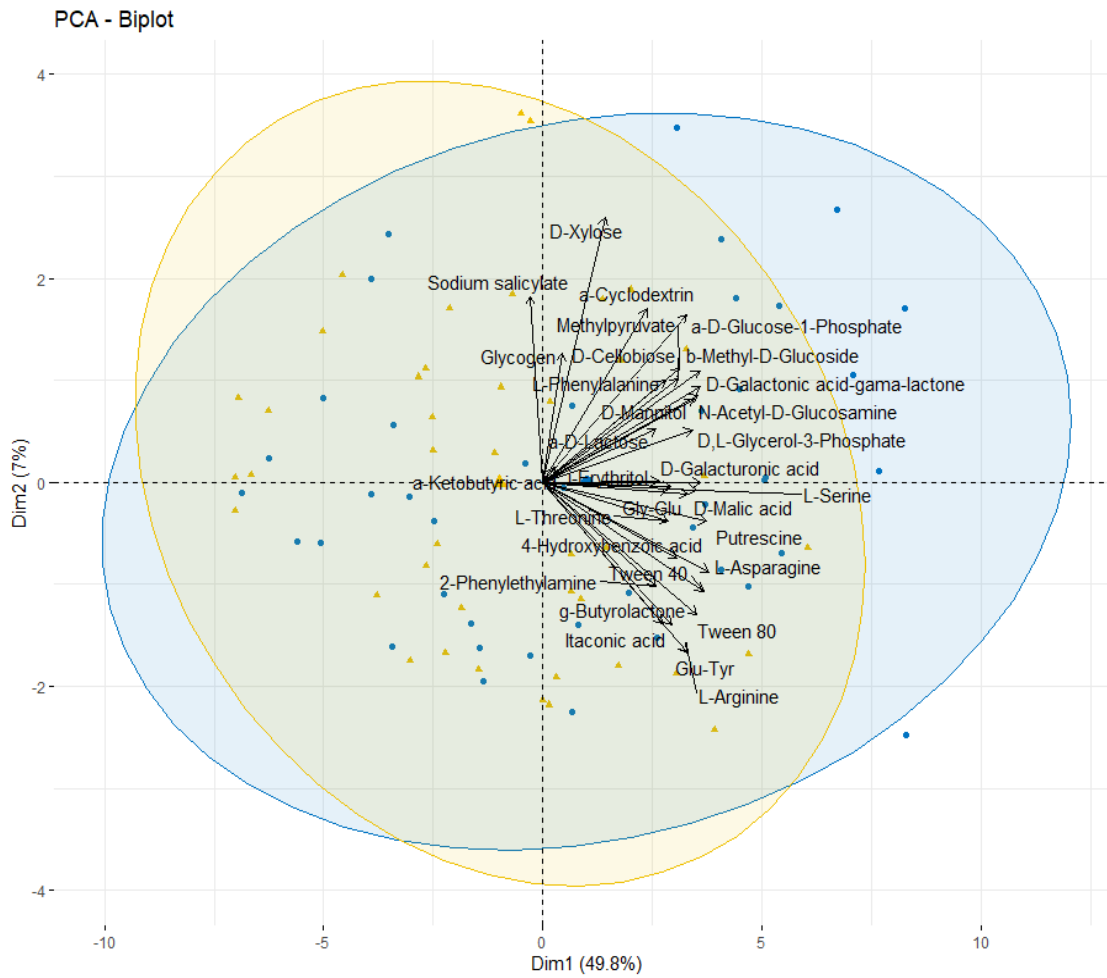


Figure SM 3. 2. Principal Component Analyses (PCA) of the absorbance of the 31 substrates analysed by Biolog EcoPlates™ after 96 h of incubation. Clusters represent the excluded (Blue) and grazing (Yellow) points.

Supplementary material chapter 2

R CODE: SATELLITE-BASED MONITORING OF PRIMARY PRODUCTION IN A MEDITERRANEAN ISLET POST BLACK RAT ERADICATION

- 01 NDVI time series construction
 - Load spectral bands and NDVI raster layers creation
 - TM and ETM+ imagery
 - OLI imagery
 - Extract NDVI values
- 02 Gap-filling
 - Preparing dataset for gap-filling:
 - Complete the time series where dates are missing
 - gap-filling with linear interpolation between neighbouring values
- 03 Savitzky-Golay smoothing
- 04 Historical time series analysis
 - Preparing Time-Series objects
 - Seasonal Decomposition of Time Series by Loess
 - BFAST
- 05 Hydrological Drought Index (HDI) data

Load libraries

```
suppressPackageStartupMessages(library(sp))
suppressPackageStartupMessages(library(raster))
suppressPackageStartupMessages(library(tidyverse))
```

01 NDVI time series construction

323 Landsat SR images were obtained from January 1999 to December 2019 from the Landsat 5 TM, Landsat 7 ETM + and Landsat 8 OLI sensors. The images were provided by the USGS (United States Geological Survey) and are accessed through the website <https://earthexplorer.usgs.gov/>.

The images were stored on an external disk and proceeded to load them. As the naming of the bands is different for OLI sensor than those for TM and ETM +, It is done separately

Load spectral bands and NDVI raster layers creation

TM and ETM+ imagery

```

timeStart<- proc.time()

# Calling all the required TM & ETM+ bands to create the NDVI raster layers
list_dirs<- list.dirs(path = "D:/landsat_data/Dragonera/TM_ETM/", recursive = F)
names(list_dirs)<- basename(list_dirs)

# Red bands
Red.list <- lapply(list_dirs, function(dir){
  stack(list.files(dir, pattern = glob2rx("*band3*.tif$"), full.names = T, recursive = T))
})

# NIR bands
NIR.list <- lapply(list_dirs, function(dir){
  stack(list.files(dir, pattern = glob2rx("*band4*.tif$"), full.names = T, recursive = T))
})

e<- extent(439926, 446541, 4378735, 4384556)# Reducing the extent of Landsat scenes to the study area. For this, its size is defined by (xmin, xmax; ymin, ymax)

for (i in 1:length(Red.list)) {
  Red_crop <- crop(Red.list[[i]],e)
  NIR_crop <- crop(NIR.list[[i]],e)

  ndvi <- overlay(x = Red_crop, y = NIR_crop, fun = function(x,y) (y-x)/(y+x))

  n<-names(list_dirs)[[i]]
  acquisition_date<- substring(n,11,18)

  sep<- "_"

  sensor<- substring(n,1,4)

  output_name_NDVI<- paste0('outputs_loops/',acquisition_date,sep,sensor,sep,'NDVI','.tif')
  writeRaster(ndvi,output_name_NDVI,overwrite=TRUE)
}
proc.time() - timeStart

```



```
## user system elapsed
## 83.25 3.47 150.32
```

OLI imagery

```
timeStart<- proc.time()

# Calling all the required OLI bands to create the NDVI raster layers
list_dirs<- list.dirs(path = "D:/landsat_data/Dragonera/OLI/", recursive = F)
names(list_dirs)<- basename(list_dirs)

# Red bands
Red.list <- lapply(list_dirs, function(dir){
  stack(list.files(dir, pattern = glob2rx("*band4*.tif$"), full.names = T, recursive = T))
})

# NIR bands
NIR.list <- lapply(list_dirs, function(dir){
  stack(list.files(dir, pattern = glob2rx("*band5*.tif$"), full.names = T, recursive = T))
})

e<- extent(439926, 446541, 4378735, 4384556)# Reducing the extent of Landsat scenes to the study area. For this, its size is defined by (xmin, xmax; ymin, ymax)

for (i in 1:length(Red.list)) {
  Red_crop <- crop(Red.list[[i]],e)
  NIR_crop <- crop(NIR.list[[i]],e)
  ndvi <- overlay(x = Red_crop, y = NIR_crop, fun = function(x,y) (y-x)/(y+x))

  # The folders where the Landsat spectral bands are housed follow a naming convention from which it can extract the acquisition date and the sensor used. This information is used to name the generated NDVI layers.

  n<-names(list_dirs)[[i]]
  acquisition_date<- substring(n,11,18)
  sep<- "_"
```

```

sensor<- substring(n,1,4)

output_name_NDVI<- paste0('outputs_loops/',acquisition_date,sep,s
ensor,sep,'NDVI','.tif')
writeRaster(ndvi,output_name_NDVI,overwrite=TRUE)
}
proc.time() - timeStart

## user system elapsed
## 36.80 1.62 82.08

```

Extracting NDVI values

Combine all the NDVI raster layers created in the previous step

```

indices_list<- list.files(path = "outputs_loops/", pattern = "tif",
full.names = TRUE)# creates a vector containing NDVI Layer names
indices<- stack(indices_list)# stack them in a Large RasterStack ob
ject

#Plotting some random NDVI Layers
plot(indices[[c(71:82)]], col=rev(terrain.colors(10)), zlim=c(0.2,0
.8), axes=FALSE)

```

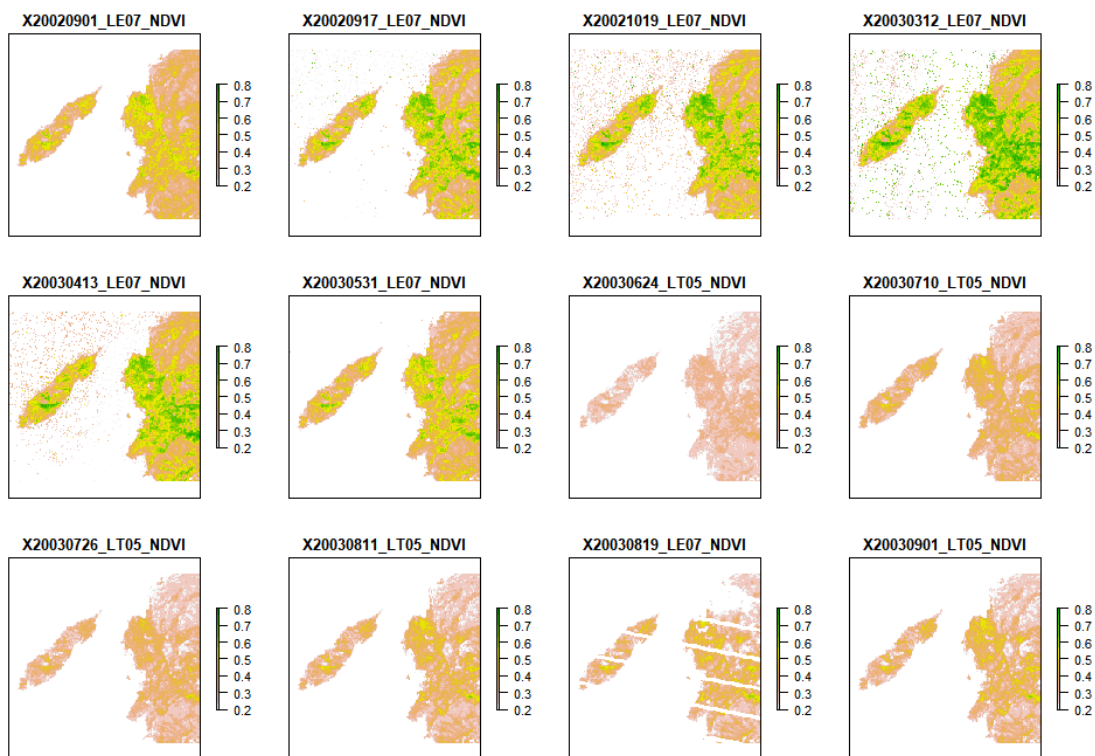


Figure 4.2. Temporal distribution of Landsat Collection 1 Surface Reflectance (SR) imagery. More images were used (when available) where clouds obstructed data collection or where SLC off-Data error in Landsat 7 was detected over study zones

```

raster_data <- list.files(path = "outputs_loops/", all.files=T, ful
l.names=F)
raster_data<- raster_data[-c(1:2)]

```

```

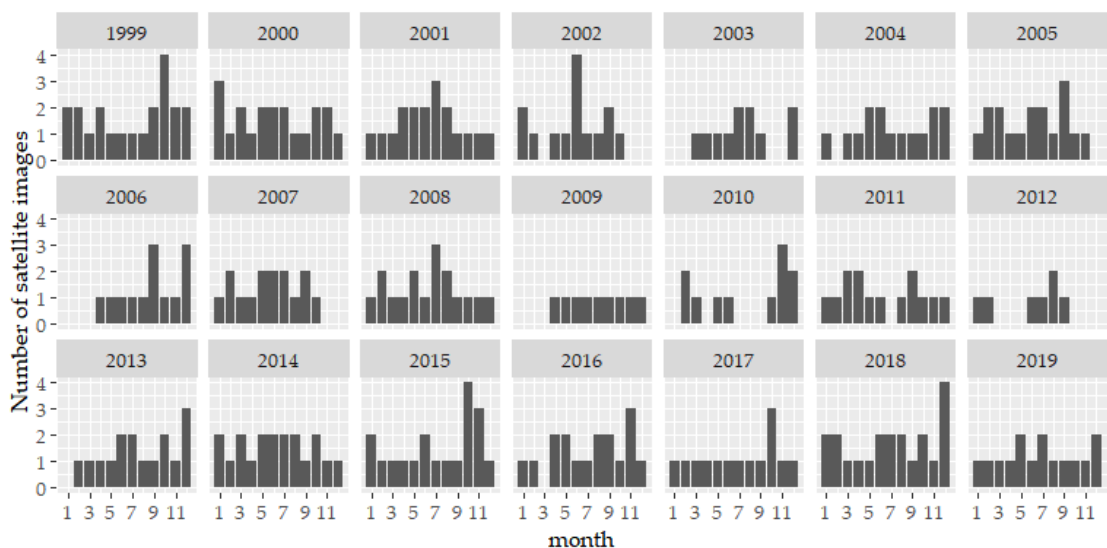
year<- substring(raster_data, 1,4)
month<-substring(raster_data,5,6)
sensor<-substring(raster_data,10,13)

lista<- cbind(year,month,sensor)
lista<- as.data.frame(lista)
lista$month<-as.integer(lista$month)
lista<- lista %>% dplyr::filter(year>1998, year<2020)

library(extrafont)# applying Palatino Linotype required in Remote S
ensing Journal
#loadfonts(device = "win")

ggplot(data = lista) +
  geom_bar(aes(x = month),stat = "count") +
  ylab("Number of satellite images")+
  facet_wrap(~ year, ncol = 7)+
  scale_x_continuous(breaks=c(1,3,5,7,9,11))+
  theme(text = element_text(size = 12, family= "Palatino Linotype")
)

```



The material and methods section of chapter 2 describes the workflow to locate the sampling plots. This process was done in ArcGIS. Here CSV document is read with the UTM coordinates of the sampling plots

```

pointCoordinates<- read.csv(file = "plots_coordinates.csv", sep=";"
, dec = ".")
pointCoordinates<- pointCoordinates
coordinates(pointCoordinates)= ~ easting+ northing

```

Extract NDVI values for sampling plot locations

```

# Terra package is considerably faster than the Raster. For this re
ason, both the raster and vector objects are transformed to the for
mat recognisable by this package.
library(terra)

```

```
r <- rast(indices)
rasValue<- terra::extract(r, vect(pointCoordinates))

combinePointValue<- cbind(pointCoordinates,rasValue)
datos<- as.data.frame(combinePointValue)
```

NDVI dataset preparing and cleaning

```
datos <- datos %>% select(-c(ID,easting,northing)) %>% #Removing un
necessary information in the NDVI database (coordinates and extra i
dentifier)
  mutate(FID= as.factor(FID)) %>%
  pivot_longer(cols = starts_with("X"),names_to = "Date", values_
to = "NDVI") %>% # Sets dates in rows rather than in columns.
  separate(Date, c("Date", "Sensor"), sep = "_", remove = TRUE) %
>% # dates and the sensor in different columns.
  separate(Date, c(NA, "Date"), sep = "X", remove = TRUE) %>% # j
ust cleaning
  dplyr::filter(NDVI>0.2) %>% dplyr::filter(NDVI<1) %>% arrange(
by= treatment) # Removing NDVI values outside the range of the targ
et vegetation index range, (1>NDVI>0.2)
head(datos)

## # A tibble: 6 x 5
##   FID   treatment Date       Sensor  NDVI
##   <fct> <chr>      <chr>    <chr>  <dbl>
## 1 0      Control   19990104 LT05    0.510
## 2 0      Control   19990120 LT05    0.478
## 3 0      Control   19990205 LT05    0.485
## 4 0      Control   19990221 LT05    0.474
## 5 0      Control   19990325 LT05    0.412
## 6 0      Control   19990410 LT05    0.401
```

02 Gap-filling

Due to the absence of satellite images in some months and the elimination of some records during data cleaning, the time series is incomplete. Our time series is 21 years. Therefore there should be $21 \times 12 = 252$ NDVI records.

Empty slots are first created in the time series. In a later step, they are filled by interpolating the adjacent data.

Preparing dataset for gap-filling:

```
datos$Date<- as.POSIXct(datos$Date, format= "%Y%m%d", tz = "UTC") #
Convert Date field in Date-time format
datos$Date<- trunc.POSIXt(datos$Date, "months")# Truncate the date
field to manipulate it on a monthly basis
datos<- separate(datos,Date, c("year","month"), sep = "-", remove =
FALSE)

datos<- datos %>%
  group_by(FID,treatment,Date,month) %>%
  summarise(NDVI= max(NDVI)) %>% # The NDVI values were then selec
ted according to the maximum-value composite (MVC) criterion
```

```

    group_by(Date, treatment) %>%
    summarise(NDVI= median(NDVI))# calculates median to avoid the effect of outliers

## `summarise()` has grouped output by 'FID', 'treatment', 'Date'.
You can override using the `.groups` argument.

## `summarise()` has grouped output by 'Date'. You can override using the `.groups` argument.

```

Take a look at the percentage of gaps in each time series. Each series should be 21 years X 12 months = 252 observations.

```

gaps<- datos %>%
  group_by(treatment) %>%
  summarise(observ= n()) %>%
  mutate(gaps= 100- (observ/(21*12)*100)) %>%
  print()

## # A tibble: 2 x 3
##   treatment observe gaps
##   <chr>         <int> <dbl>
## 1 Control         221  12.3
## 2 Dragonera      220  12.7

```

Completing the time series where dates are missing

Starting with the treatment zone

```

indices_treatment<- datos %>% # Select treatment zone observations
  dplyr::filter(treatment== "Dragonera")

```

```

data.length<- length(indices_treatment$Date)
time.min<- indices_treatment$Date[1]
time.max<- indices_treatment$Date[data.length]
all.Dates <- seq(time.min, time.max, by="month")
all.Dates.frame<- data.frame(list(Date = all.Dates))
merge.data_D<- right_join(indices_treatment, all.Dates.frame)

```

```
## Joining, by = "Date"
```

```
merge.data_D<- merge.data_D %>% arrange(merge.data_D)
```

Same for the control zone

```

indices_control<- datos %>%
  dplyr::filter(treatment== "Control")

```

```

data.length<- length(indices_control$Date)
time.min<- indices_control$Date[1]
time.max<- indices_control$Date[data.length]
all.Dates <- seq(time.min, time.max, by="month")
all.Dates.frame<- data.frame(list(Date = all.Dates))
merge.data_C<- right_join(indices_control, all.Dates.frame)

```

```
## Joining, by = "Date"
merge.data_C<- merge.data_C %>% arrange(merge.data_C)

library(signal)# package that applies a Savitzky-Golay smoothing filter
library(zoo) # package that orders observations
```

Transform the Date field into a zoo-recognizable format

```
control<- merge.data_C
control$Date<- as.Date(control$Date)
dragonera<- merge.data_D
dragonera$Date<- as.Date(dragonera$Date)
```

gap-filling with linear interpolation between neighbouring values

```
zooValues_Control <- zoo(control[3],control$Date)# Order observations
approxValues_control <- na.approx(zooValues_Control)# Replace NA by interpolation
approxValues_control<-fortify.zoo(approxValues_control)# converts zoo object into a data frame
approxValues_control$Treatment<- "Control" # reintroduces the treatment field
```

Same for the treatment zone

```
zooValues_dragonera <- zoo(dragonera[3],dragonera$Date)
approxValues_dragonera <- na.approx(zooValues_dragonera)
approxValues_dragonera<-fortify.zoo(approxValues_dragonera)
approxValues_dragonera$Treatment<- "Dragonera"
```

03 Savitzky-Golay smoothing

Control zone

```
NDVI_Control<- approxValues_control[[2]]

NDVI.ts2 = ts(NDVI_Control, start=1, end=252)
NDVI_SG=sgolayfilt(NDVI.ts2, p=3, n=13, ts=1)

NDVI_SG<- cbind(NDVI_SG)
approxValues_control<- approxValues_control %>% dplyr:: select(c(1, 3))
approxValues_control<- cbind(approxValues_control,NDVI_SG)
```

Same for the treatment zone

```
NDVI_Treatment<- approxValues_dragonera[[2]]

NDVI.ts2 = ts(NDVI_Treatment, start=1, end=252)
NDVI_SG=sgolayfilt(NDVI.ts2, p=2, n=13, ts=1)

NDVI_SG<- cbind(NDVI_SG)
```

```

approxValues_dragonera<- approxValues_dragonera %>% dplyr:: select(
c(1,3))
approxValues_dragonera<- cbind(approxValues_dragonera,NDVI_SG)

```

Finally, the databases of both treatments are combined

```

final_dataset<- rbind(approxValues_control, approxValues_dragonera)
names(final_dataset)[1]<- "Date"

```

```

final_dataset<- final_dataset %>%
  separate(Date, c("year", "month"), sep = "-", remove = FALSE) %>%
  rename(NDVI= NDVI_SG)

```

```

final_dataset$Date<- as.Date(final_dataset$Date)
final_dataset$year<- as.Date(final_dataset$Date)

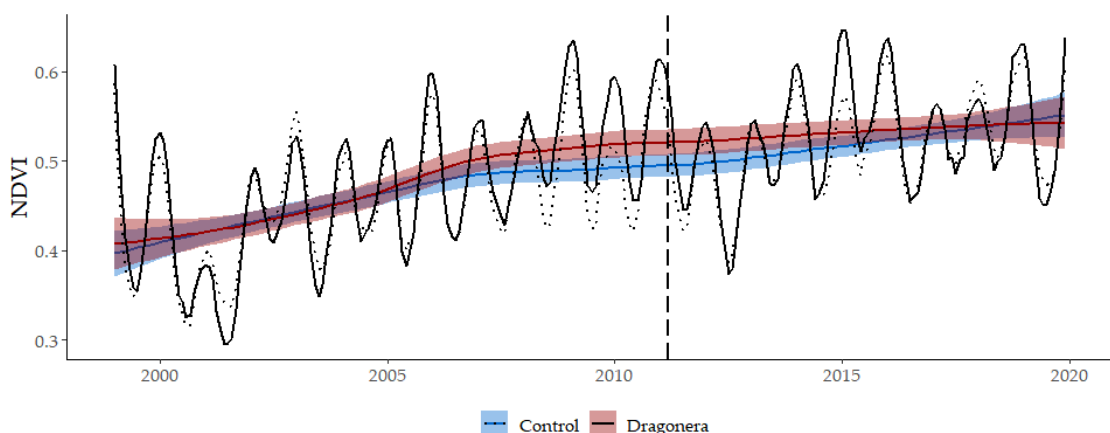
```

Figure 4.5. The monthly NDVI time series show the average NDVI of the sampling plots for each zone. The coloured lines (Red = Treatment zone; Blue = Control zone) represent the trend throughout the study period, with a LOESS smoothing and standard deviation shown with the corresponding colours. The black lines represent the real data for each treatment (Solid = Sa Dragonera; Dotted= Control zone), in which the seasonal variation can be observed. The dashed vertical line dates the rodent eradication campaign (February 2011).

```

ggplot(final_dataset, aes(x=year, y=NDVI)) + geom_smooth(aes(color
= Treatment, fill= Treatment), method= "loess")+
  geom_line(aes(linetype = Treatment), size=1)+
  scale_linetype_manual(values=c("dotted", "solid"))+
  scale_color_manual(values=c("#0066CC", "#990000"))+
  scale_fill_manual(values=c("#0066CC", "#990000"))+
  labs(x=" ", y = "NDVI")+
  theme_classic()+
  theme(legend.position = "bottom", legend.title = element_blank(),
axis.title.x=element_blank(), text = element_text(size = 14, family
= "Palatino Linotype"))+
  geom_vline(aes(xintercept=final_dataset[["Date"]][147]),linetype=
"longdash", size=0.8)

```



04 Historical time series analysis

Preparing Time-Series objects

```

suppressPackageStartupMessages(library(strucchange))
suppressPackageStartupMessages(library(bfast))

db<- final_dataset %>% select(c(1,4,5)) # Select just necessary data
# for the historical analysis of the time series

create two Time Series objects (one for each treatment)

# Treatment zone
db_Treatment<- db %>% dplyr::filter(Treatment=="Dragonera") %>% select(-c(1,2)) # eliminates the first two columns since the time series object has to be dimension-one.
Treatment_TS<- ts(db_Treatment, frequency = 12, start = c(1999,1), end = c(2019,12))# Time-Series Object
dim(Treatment_TS)<- NULL

# Control zone
db_Control<- db %>% dplyr::filter(Treatment=="Control") %>% select(-c(1,2))
Control_TS<- ts(db_Control, frequency = 12, start = c(1999,1), end = c(2019,12))
dim(Control_TS)<- NULL

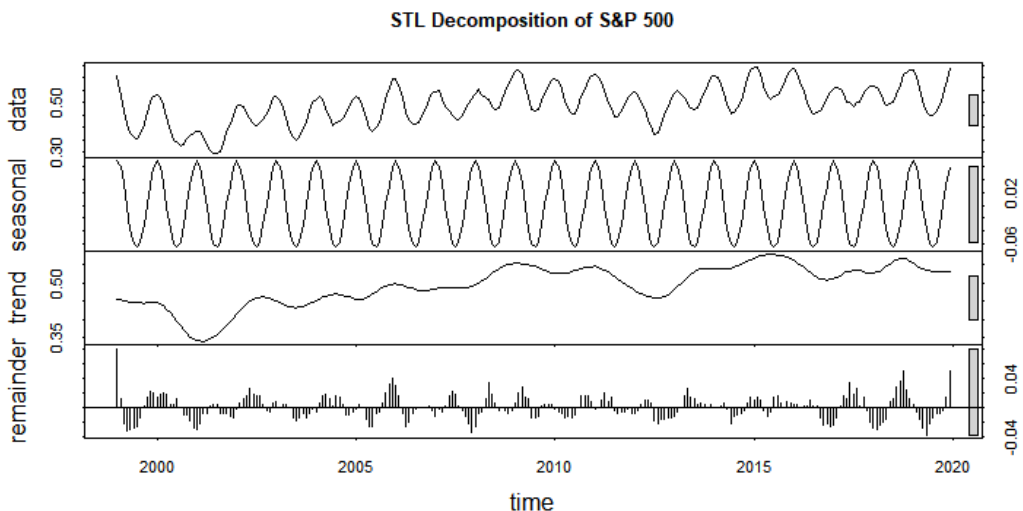
```

Seasonal Decomposition of Time Series by Loess

```

dragonera.stl <- stl(Treatment_TS,s.window="periodic")
plot(dragonera.stl,main="STL Decomposition of S&P 500")

```



```

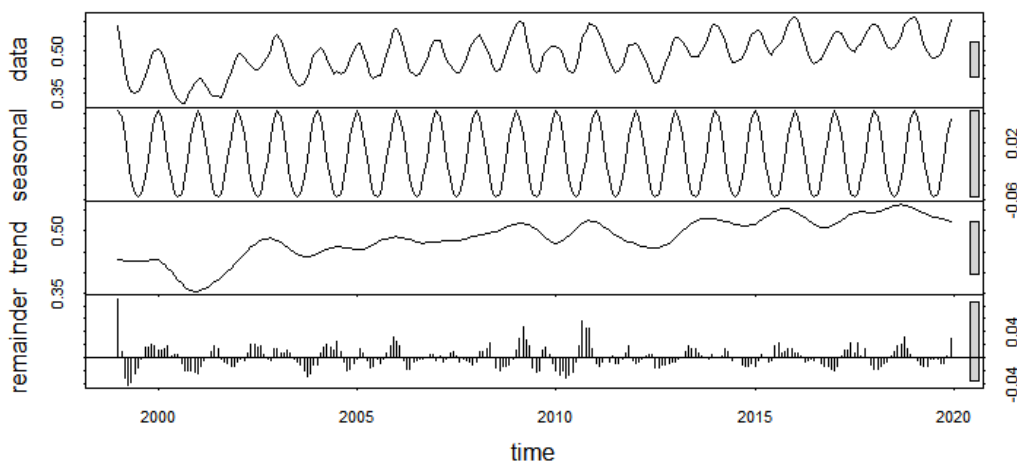
P1<-autoplot(stl(Treatment_TS,s.window="periodic"))+ theme(text = element_text(size = 20,family = "Palatino Linotype"))+ labs(title = "Sa Dragonera")+theme_bw()

```

```

Control.stl <- stl(Control_TS,s.window="periodic")
timeSeries:: plot(Control.stl)

```

```
summary(Control.stl)
```

```
## Call:
## stl(x = Control_TS, s.window = "periodic")
##
## Time series components:
##      seasonal          trend          remainder
## Min.   :-0.05781040   Min.   :0.3557966   Min.   :-0.04329992
## 1st Qu.: -0.03777987   1st Qu.:0.4601134   1st Qu.: -0.00975747
## Median :-0.00254524   Median :0.4840139   Median :-0.00184645
## Mean   : 0.00000000   Mean   :0.4846907   Mean   : 0.00000727
## 3rd Qu.: 0.03648236   3rd Qu.:0.5205968   3rd Qu.: 0.00902292
## Max.   : 0.06497654   Max.   :0.5626864   Max.   : 0.09125563
## IQR:
##      STL.seasonal STL.trend STLremainder data
##      0.07426      0.06048  0.01878  0.09566
## % 77.6          63.2      19.6     100.0
##
## Weights: all == 1
##
## Other components: List of 5
## $ win  : Named num [1:3] 2521 19 13
## $ deg  : Named int [1:3] 0 1 1
## $ jump : Named num [1:3] 253 2 2
## $ inner: int 2
## $ outer: int 0
```

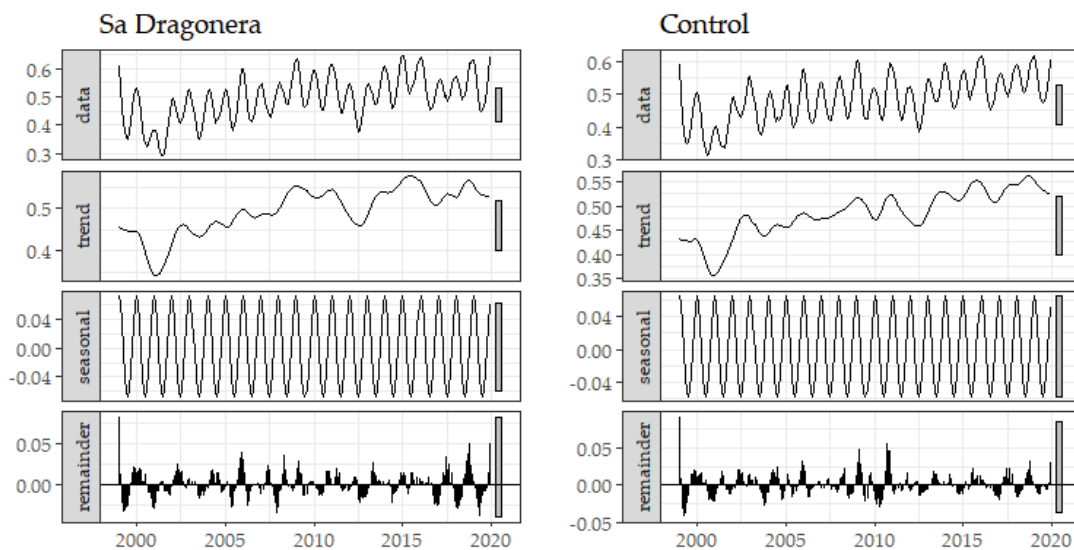
```
P2<-autoplot(stl(Control_TS,s.window="periodic"))+ theme(text = element_text(size = 20,family = "Palatino Linotype"))+ labs(title = "Control")+theme_bw()
```

Figure 4.6. The STL decomposition of the monthly NDVI time series of Sa Dragonera and control zone (Mallorca Island) into seasonal, trend, and remainder components. In each plot NDVI units are plotted against time. The seasonal component is estimated by taking the mean of all seasonal sub-series (e.g. for a monthly time series the first sub-series contains the January values). The sum of the seasonal, trend, and remainder components equals the data series. The solid bars on the right-

hand side of the plots act as a **reference** to show the same data range and aid comparison

```
library(gridExtra)
library(grid)

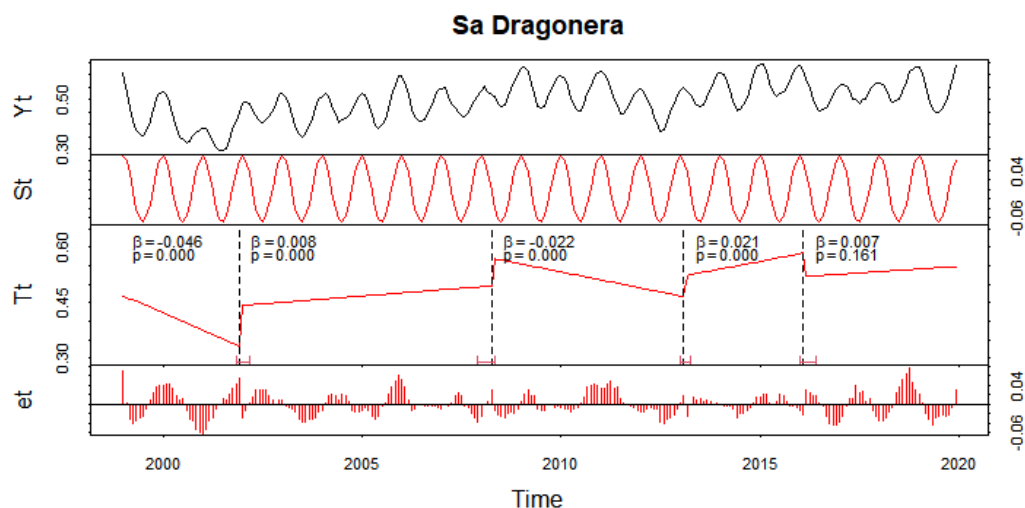
p <- grid.arrange(P1 + theme(legend.position = "none", axis.title.x = element_blank(), text = element_text(size = 12, family = "Palatino Linotype")), P2 + theme(legend.position = "none", axis.title.x = element_blank(), text = element_text(size = 12, family = "Palatino Linotype")), nrow = 1)
```



BFAST

Tuning BFAST for Treatment zone

```
rdist <- 1/7
dim(Treatment_TS) <- NULL
fit_dragonera <- bfast(Treatment_TS, h=rdist,
  season="harmonic", max.iter=10, breaks = 20) # Give an
  exaggeratedly high number of breaks (20), although the highest number
  of breaks, according to the value of h, will be 7
plot(fit_dragonera, main="Sa Dragonera", ANOVA=TRUE)
```



```
## NULL

fit_dragonera

##
## TREND BREAKPOINTS
## Confidence intervals for breakpoints
## of optimal 5-segment partition:
##
## Call:
## confint.breakpointsfull(object = bp.Vt, het.err = FALSE)
##
## Breakpoints at observation number:
## 2.5 % breakpoints 97.5 %
## 1 35 36 39
## 2 108 112 113
## 3 169 170 172
## 4 205 206 210
##
## Corresponding to break dates:
## 2.5 % breakpoints 97.5 %
## 1 2001(11) 2001(12) 2002(3)
## 2 2007(12) 2008(4) 2008(5)
## 3 2013(1) 2013(2) 2013(4)
## 4 2016(1) 2016(2) 2016(6)
##
## SEASONAL BREAKPOINTS: None

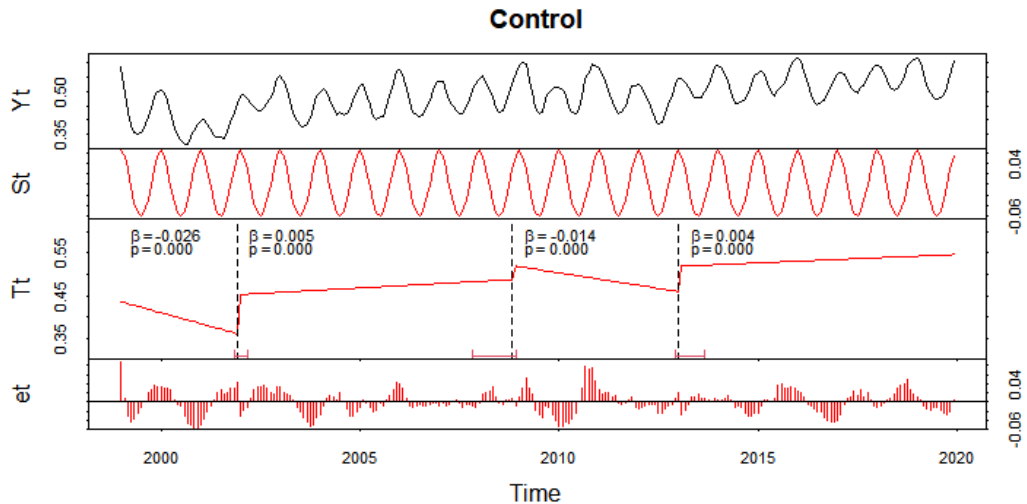
fit_dragonera[5]#magnitudes

## $Mags
## [,1] [,2] [,3]
## [1,] 0.3336526 0.4425164 0.10886387
## [2,] 0.4951428 0.5690493 0.07390651
## [3,] 0.4665653 0.5234401 0.05687479
## [4,] 0.5833825 0.5205444 -0.06283806
```

Tuning BFAST for Control zone

Supplementary material Chapter 2

```
rdist <- 1/7
dim(Control_TS)<-NULL
fit_Control <- bfast(Control_TS, h=rdist,
                     season="harmonic", max.iter=10, breaks = 20)
plot(fit_Control, main="Control", ANOVA= TRUE)
```



```
## NULL

fit_Control

##
## TREND BREAKPOINTS
## Confidence intervals for breakpoints
## of optimal 4-segment partition:
##
## Call:
## confint.breakpointsfull(object = bp.Vt, het.err = FALSE)
##
## Breakpoints at observation number:
## 2.5 % breakpoints 97.5 %
## 1 35 36 39
## 2 107 119 120
## 3 168 169 177
##
## Corresponding to break dates:
## 2.5 % breakpoints 97.5 %
## 1 2001(11) 2001(12) 2002(3)
## 2 2007(11) 2008(11) 2008(12)
## 3 2012(12) 2013(1) 2013(9)
##
## SEASONAL BREAKPOINTS: None

fit_Control[5]#magnitudes

## $Mags
## [,1] [,2] [,3]
## [1,] 0.3617281 0.4529810 0.09125284
```

```
## [2,] 0.4879550 0.5194116 0.03145665
## [3,] 0.4604973 0.5194034 0.05890604
```

05 Hydrological Drought Index (HDI) data

Comparing the BFAST results with the hydrological drought index (HDI). This is reported by the General Directorate of Water Resources (DGRH) of the government of the Balear Islands in the Hydrological Demand Unit (HDU) of Sierra Tramuntana Sur. https://www.caib.es/sites/aigua/es/index_de_sequia/

```
HDI <- read.table(file = "HDI_data.txt", header = TRUE, sep = "\t",
stringsAsFactors = TRUE)
HDI$Data<- as.POSIXct(HDI$Data, format= "%d/%m/%Y", tz = "UTC")
head(HDI)# note that its value is always = 1 and is used to create
the graph bars
```

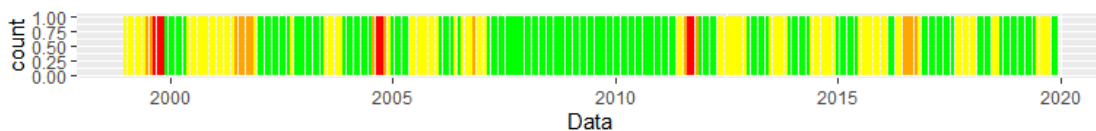
```
##      Data      state value
## 1 1999-01-01 pre-alert     1
## 2 1999-02-01 pre-alert     1
## 3 1999-03-01 pre-alert     1
## 4 1999-04-01 pre-alert     1
## 5 1999-05-01 pre-alert     1
## 6 1999-06-01 pre-alert     1
```

```
sort(table(HDI$state))
```

```
##
## emergency      alert pre-alert normality
##           7         16         87         142
```


```
my_palet <- c('orange',
              'red',
              'green',
              'yellow')
```

```
ggplot(data = HDI)+
  geom_bar(mapping= aes(x= Data, fill= state))+
  scale_fill_manual(values = my_palet)+
  scale_colour_hue()+
  theme(legend.position = "none")
```



Supplementary material chapter 3

This scientific publication declares an equal contribution of the first two authors. The declaration signed by Laura Alonso-Martínez guarantees the right to use this article as a chapter of this thesis.



DECLARACIÓN

Yo LAURA ALONSO MARTÍNEZ nacida el 03/07/1996 con DNI 36175300A declaro que el trabajo con título “Remote mapping of foodscapes using sUAS and a low cost BG-NIR sensor” no va a ser utilizado para el manuscrito final de mi tesis doctoral.

Pontevedra, 25 de Mayo de 2022.

ALONSO
MARTINEZ
LAURA -
36175300A

Firmado digitalmente por ALONSO MARTINEZ LAURA - 36175300A
Fecha: 2022.05.25 16:52:58 +02'00'

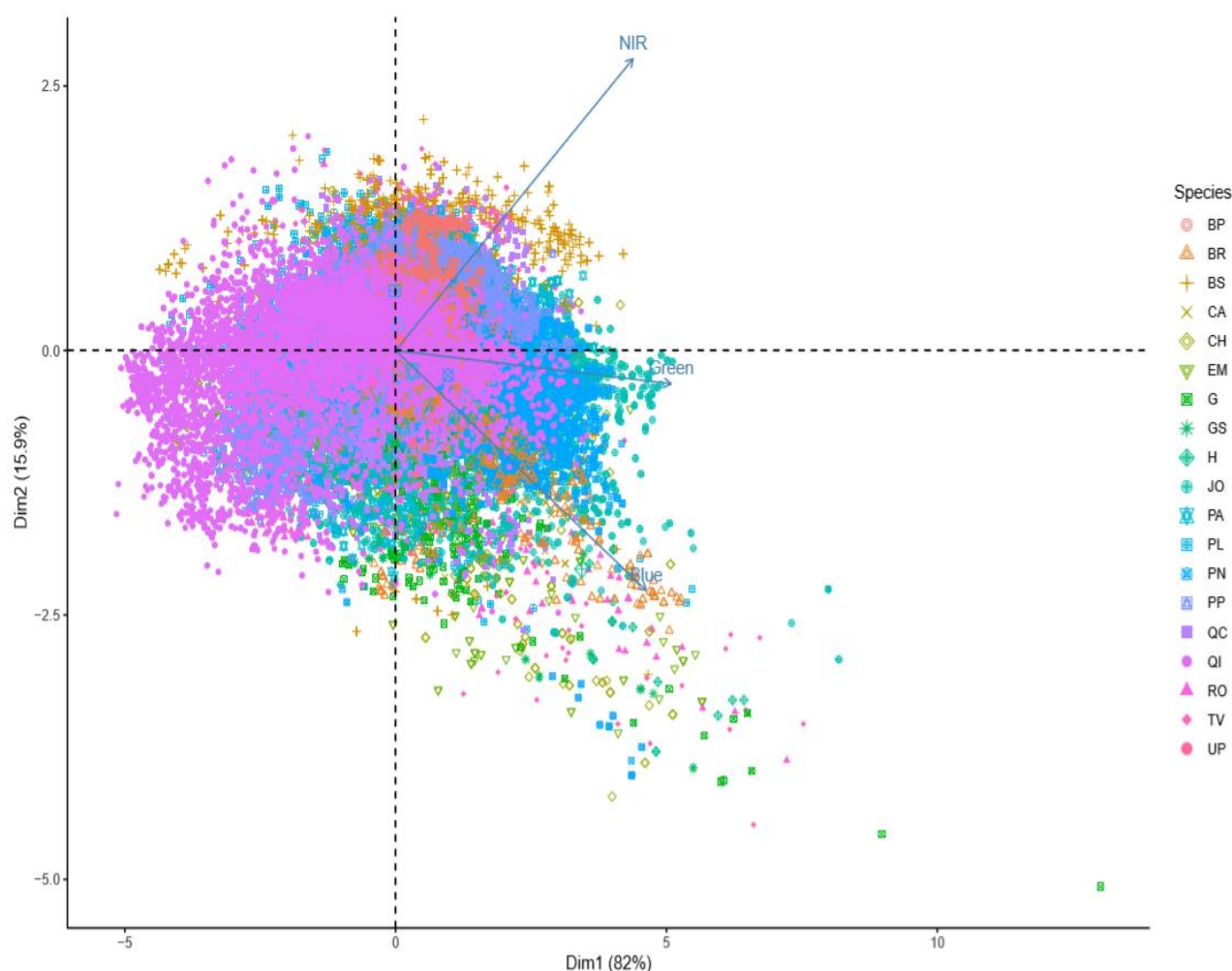


Figure SM 5. 1. PCA calculated from the digital values of the images obtained in the National Game Reserve “Ports de Tortosa i Beseit” in Catalonia, northeast Spain (40°46’08” N, 0°20’04” E, 450 m. a. s. l.). Lines represent the recorded bands (variables) and points represent the sampled pixels coloured by species (individuals). Up to 20 individuals of these plant species were marked with a dGPS. *Brachypodium phoenicoides* (BP), *Brachypodium retusum* (BR), *Buxus sempervirens* (BS), *Cistus albidus* (CA), *Chamaerops humilis* (CH), *Erica multiflora* (EM), Graminoids (G), *Genista scorpius* (GS), *Helianthemum marifolium* (H), *Juniperus oxycedrus* (JO), *Phillyrea angustifolia* (PA), *Pistacia lentiscus* (PL), *Pinus nigra* (PN), *Pinus pinaster* (PP), *Quercus coccifera* (QC), *Quercus ilex* (QI), *Rosmarinus officinalis* (RO), *Thymus vulgaris* (TV), *Ulex parviflorus* (UP).

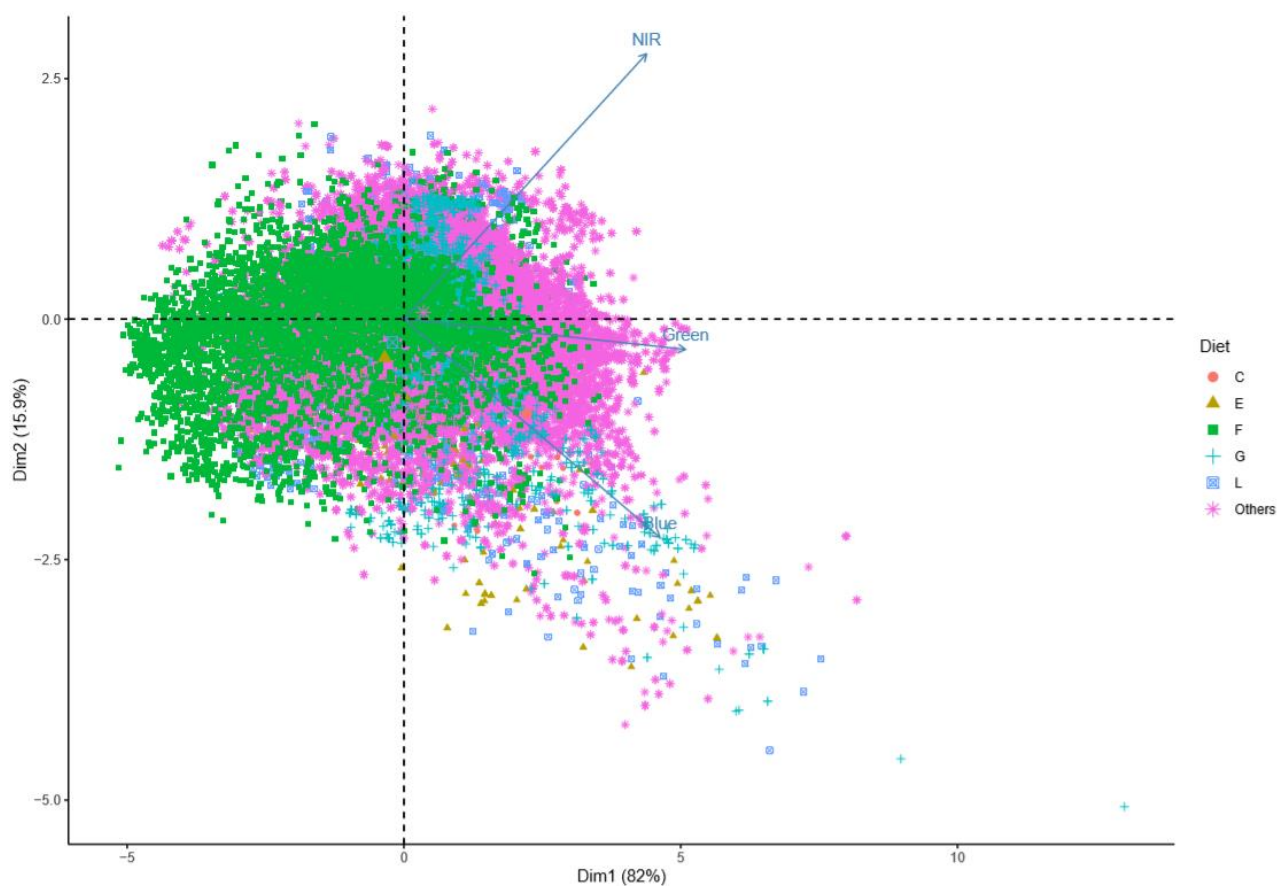


Figure SM 5. 2. PCA calculated from the digital values of the images obtained in NGRPTB. Lines represent the recorded bands (variables) and points represent groups of plant species consumed by a flock of ibexes (*Capra pyrenaica*) in the National Game Reserve “Ports de Tortosa i Beseit” in Catalonia, northeast Spain (40°46’08” N, 0°20’04” E, 450 m. a. s. l.). Plant groups are the following: *Quercus* spp. as the family Fagaceae (Group F), *Rosmarinus officinalis* and *Thymus vulgaris* as the family Labiatae (Group L), *Erica multiflora* (Group E), *Cistus albidus* (Group C), *Brachypodium phoenicoides*, *B. retusum*, and other grass-like plants as Graminoids (Group G).

